AD_____

Award Number: DAMD17-01-1-0029

TITLE: Comprehensive Development Program of Hunter-Killer Peptides for Prostate Cancer

PRINCIPAL INVESTIGATOR: Howard M. Ellerby, Ph.D.

CONTRACTING ORGANIZATION: Buck Institute for Age Research
Novato, CA 94948

REPORT DATE: May 2005

TYPE OF REPORT: Final

PREPARED FOR: U.S. Army Medical Research and Materiel Command
Fort Detrick, Maryland 21702-5012

REPORT DOCUMENTATION PAGE

Form Approved
OMB No. 0704-0188

1. REPORT DATE	2. REPORT TYPE	3. DATES COVERED
1 May 2005	Final	1 May 2001 – 30 Apr 2005

4. TITLE AND SUBTITLE

Comprehensive Development Program of Hunter-Killer Peptides for Prostate Cancer

5a. CONTRACT NUMBER

5b. GRANT NUMBER
DAMD17-01-1-0029

5c. PROGRAM ELEMENT NUMBER

6. AUTHOR(S)

Howard M. Ellerby, Ph.D.

E-Mail: mellerby@touro.edu

5d. PROJECT NUMBER

5e. TASK NUMBER

5f. WORK UNIT NUMBER

7. PERFORMING ORGANIZATION NAME(S) AND ADDRESS(ES)

Buck Institute for Age Research
Novato, CA 94948

8. PERFORMING ORGANIZATION REPORT NUMBER

9. SPONSORING / MONITORING AGENCY NAME(S) AND ADDRESS(ES)
U.S. Army Medical Research and Materiel Command
Fort Detrick, Maryland 21702-5012

10. SPONSOR/MONITOR'S ACRONYM(S)

11. SPONSOR/MONITOR'S REPORT NUMBER(S)

12. DISTRIBUTION / AVAILABILITY STATEMENT
Approved for Public Release; Distribution Unlimited

13. SUPPLEMENTARY NOTES

14. ABSTRACT
Previously we invented Hunter Killer Peptides (HKP) for cancer therapy. In this comprehensive program to develop HKPs for **prostate cancer** we accomplished the following: 1) evaluated an original HKP in the TRAMP mouse model of **prostate cancer**, showing that we could inhibit metastasis and demonstrating a trend toward extension of survival; 2) designed new peptides (both targeting and cell killing) and determined using *in vitro* assays that some of these new designs were superior (had improved therapeutic indices) to the original designs; 3) evaluated one of our most unique peptides (KP-5) in a PC-3 xenograft mouse model of **prostate cancer**, showing that we could limit primary tumor growth and increase survival; 4) determined that the dimeric form of one of our targeting peptides (HP-3) not only bound to aminopeptidase N (facilitating the internalization of HKPs into the cytosol of targeted endothelial cells to exert their anti-angiogenic effect), but also inhibited the enzymatic activity of aminopeptidase N, (also an anti-angiogenic effect) thus providing a synergetic anti-cancer effect; 5) determined that the dimeric form of one of our original HKPs (HKP-3) was more efficacious than the monomeric HKP-1; 6) determined the LD50 of original HKPs.

15. SUBJECT TERMS
prostate cancer, Hunter-Killer Pepides, angiogenesis, aminopepddidase N, TRAMP mice, PC-3 prostate cells, tumor, xenograft, mitochondria, HKP-3, HKP-1, HP-3, LD50, dimeric, momomeric

16. SECURITY CLASSIFICATION OF:			17. LIMITATION OF ABSTRACT	18. NUMBER OF PAGES	19a. NAME OF RESPONSIBLE PERSON
a. REPORT	b. ABSTRACT	c. THIS PAGE			USAMRMC
U	U	U	UU	105	19b. TELEPHONE NUMBER *(include area code)*

Table of Contents

Introduction

The subject of our research is prostate cancer. The purpose of this research is the development of a more effective and less toxic treatment for prostate cancer. The currently used chemotherapeutic agents are drugs with the narrowest therapeutic index in all of medicine. Therefore, effective doses of a wide variety of anti-cancer agents are restricted by their non-selective, highly toxic effect on normal tissues. In response to this, we designed short peptides composed of two functional domains, one a tumor blood vessel 'homing' sequence and the other a programmed cell death-inducing sequence, and synthesized them by basic peptide chemistry. The 'homing' domain was designed to guide the peptide to targeted cells and permit its internalization. The pro-apoptotic domain was designed to be non-toxic outside all cells, but toxic when internalized into just the targeted cells by the disruption of mitochondrial membranes. Thus our approach was to create non-toxic anticancer peptides, which we named **Hunter- Killer Peptides** (**HKP**), designed to only destroy tumor blood vessels while leaving normal blood vessels unharmed. We succeeded in the development of HKPs, demonstrating that although our 2 prototypes contained only 21 and 26 amino acid residues, they were selectively toxic to angiogenic endothelial cells and had strong anti-cancer activity in an *in vivo* mouse model of human breast carcinoma (human tumor xenografts) (Ellerby *et al.*, 1999). The research under DAMD17-01-1-0029 was designed to extend our approach to **prostate** cancer. In extending this work to prostate cancer, there were 5 Specific Aims under the current award. These aims were addressed over a period of 4 years, due to a one-year no-cost extension (for medical reasons), which is discussed below, at the beginning of the **Body** section of this report (at the request of the previous review). **Task 1** (**Specific Aim 1): Optimize the dose of current HKPs in the Tramp C model** was addressed in year 4 of the award. **Task 2** (**Specific Aim 2): Design HKPs with improved therapeutic indices** was addressed in years 1, 2 and 3. **Task 3** (**Specific Aim 3): Evaluate in vitro efficacy and toxicity of new HKPs** was addressed in years 1, 2 and 3. **Task 4** (**Specific Aim 4): Evaluate the in vivo efficacy of new HKPs in the TRAMP model of prostate cancer** was addressed in year 2. **Task 5** (**Specific Aim 5): Determine the in vivo pharmacokinetics of HKPs in the TRAMP C model of prostate cancer** could not be completed as we ran out of time while debugging a problem with our "gold standard"

peptide, HKP-1 (see Table 1 below for all peptide sequences), and so we substituted an analysis the properties of a newly designed (under this award) targeting peptide (HP-3) and its corresponding hunter-killer peptide (HKP-3). This relevant and derivative substitution allowed the discovery of a new approach to the design of our peptides (dimers), probably solved the problems associated with HKP-1, and showed that HP-3 acted not only as an internalization peptide, but also as an inhibitor of the enzymatic activity of the receptor aminopeptidase N which in itself is anti-angiogenic. Thus we discovered that HP-1 has a dual function anti-angiogenic activity, which we discuss in detail in the **Body** of this report. We believe that these studies were central to our understanding of HKPs, and to their continued application to prostate cancer.

Body

Explanation of No-cost Extension

The review of our previous Final Report indicated that we had not explained how the extra year of this award, the no cost extension 2004-2005 (year 4), had been beneficial to the work, and what exactly had been accomplished in year 4, and requested that we provide this information.

The purpose of the original request for a no-cost extension was that the PI had undergone 3 separate spinal fusion operations in a period from late 2001 to early 2004 (and at present is now scheduled for more). Thus, not all of the funds had been spent, as research had proceeded at a less than optimal pace. At that time, the grant manager for this award, DAMD17-01-1-0029, immediately appreciated the seriousness of this medical complication, and therefore a no-cost extension of one year was granted. In addition to this problem, we also encountered a problem with our "gold standard" peptide, HKP-1, and the required and critical debugging, or the working of this problem, also consumed much extra time. Rather than simply pushing forward with Specific Aims 1, 4 and 5 (Specific Aims 2 and 3 were completed), having unanswered questions about HKP-1 (discussed below), we conserved our funds and took our time to conscientiously address the peptide problem, while at the same time looking for logical workarounds/alternatives consistent with the stated Specific Aims.

Specifically, the year of no-cost extension allowed us to complete the following work:

1. Address **Specific Aim 1**.
2. Continue work on debugging the problem with HKP-1.
3. While in the process discussed in 2, substituted a consistent alternative for **Specific Aim 5**, with the discovery and investigation of the novel and exciting properties of HKP-3 (a dimer of HKP-1) that had been designed and evaluated *in vitro* in year 3 of this award as part of **Specific Aims 2 and 3**.

In light of the no-cost extension, we provide here a discussion of the timeline for the research funded under this award, so that it will be evident when and how each Specific Aim was addressed.

Timeline of Research

Period of Award: May 2001 to May 2005:

Year 1: 5/2001-5/2002

Year 2: 5/2002-5/2003

Year 3: 5/2003-5/2004

Year 4: 5/2004-5/2005 (year of no cost extension)

Task 1

Specific Aim 1: Optimize the dose of current HKPs in the Tramp C model.

Rationale.

In the second year of this award, 2002-2003, while we were preparing to work on Task 1, delayed for the reasons outlined in **Explanation for No-cost Extension**, we discovered a problem with our original peptide HKP-1. In preparation for the Task 1 study of a first-generation (HKP-1 or 2) in the TRAMP C model, we conducted an animal study of our original HKP-1 in a xenograft model of breast carcinoma (435 human **breast** carcinoma cells). The rational for this study was that while our laboratory had performed *in vivo* studies with KP-5 including **prostate** (PC-3 derived) xenografts (See Task 3), we had no previous experience with HKP-1 or HKP-2 in xenograft models, let alone in the TRAMP C model. Our previous expertise had been in peptide design and *in vitro* evaluation of

those designs. Dr. Renata Pasqualini had performed all previous *in vivo* studies (Ellerby *et al.*, 1999). Thus, our newly hired animal technicians, while having experience with xenograft models, had no previous experience with HKPs or with the TRAMP model. So the results of this first animal study (HKP-1 in 435 breast carcinoma xenografts) then were to be compared with the results of Dr. Pasqualini form the 1999 publication to verify that we had a good foundation on which to build (to then perform the HKP study in TRAMP C mice). When this first animal study was completed it was evident that we could not reproduce her work with HKP-1 on 435 breast carcinoma xenografts.

At this time, we decided that we needed to determine exactly why the study of HKP-1 had failed rather than moving into the TRAMP C model. Responding to this problem, we put together a task force of about 6-8 Buck Institute scientists to brainstorm on a regular basis about how we might best proceed. The option of switching to HKP-2 was temporarily tabled because of the increased cost associated with the production of HKP-2 (2 disulfide bonds in specific locations). **However, as working the problem with HKP-1 extended from months to years, we did as a group decide to evaluate HKP-2 in the TRAMP model, addressing Task 1 (Specific Aim 1), in year 4 of this award.** We now discuss the results of this research.

Methods.

Transgenic Adenocarcinoma of the Mouse Prostate (TRAMP) Mice. TRAMP mice (Gingrich *et al.*, 1996; Hsu *et al.*, 1998), were bred at our Animal Facility in accordance with previously established methods (Gingrich *et al.*,1996; Hsu *et al.*, 1998; Arap *et al.*, 2002) and the breeding and animal experimentation was reviewed and approved by the Institute's Animal Research Committee (IACUC).

Treatment Groups

Treatment Groups (n=17 / group)	Dosing paradigm	Route	Times/ Wk	TX days
1. DMEM Vehicle	100 uls serum free DMEM 1x media	IP	1x	T
2. RGD	250 ug/100 uls	IV	1x	T
3. RGD	250 ug/100 uls	IP	1x	T
4. RGD	250 ugs/100 uls (total 500 ug/wk)	IP	2x	T&F

Peptide Protocol.

Group	# of animals	Total volume (100 uls x # of animals)	# of mgs of peptide
1. DMEM control	13+2=15	1500 uls of DMEM media	0
2. RGD 250 ug/100 uls	17 + 3=20	2000 uls of DMEM media	5
3. RGD 250 ug/ 100 uls	14 + 2=16	1600 uls of DMEM media	4
4. RGD 250 ug/ 100 uls	16 + 2=18	1800 uls of DMEM media	4.5

* Groups 2 ,3, and 4 can be combined into one tube for IV and IP injections since dose is the same for all groups (13.5 mgs in 5400 uls)

Monitoring Mice.

1. Mice are to be weighed once a week and weight recorded in RGD logbook (weight worksheet)
2. Mice are to be palpated in genital and entire abdominal area for tumors once a week and results recorded in RGD logbook as follows (palpation worksheet):
    a. NVNP = not visible, not palpable tumor
    b. NVP = not visible, but palpable tumor
    c. VP = visible and palpable tumor
3. Do not record testis as palpable tumor
4. Once injections are done for that week, check off box on back of cage card and initial next to box. Also record a yes or no injection status in RGD logbook (injection status worksheet)

Metastasis Assays (used for the RGD4C Study in TRAMP C mice). India Dye Technique: Lung perfusion with black dye for identifying lung tumors. **Materials:** India Dye from Hardy Diagnostics (cat. # Z64); 10 cc syringe with 21 gauge needle; saline or Ix PBS; hemostats; serrated forceps; thread; 20 ml glass scintillation filled with 4% pfa. **Perfusion Protocol.** Dilute India Dye 1:10 with saline or Ix PBS and fill a 10 cc syringe capped with 21 gauge needle; euthanize animal, cut through the chest cavity, exposing lungs and trachea; place a piece of thread around bottom part of trachea near thymus and aortic lymph nodes, tie a slipknot, but do not tighten; insert needle into ~(top) portion of trachea, being very careful to not puncture tracheal wall. Slowly move needle down trachea toward the lungs, stop just above the thymus and aortic lymph nodes. Using the serrated forceps, clamp around the needle to prevent backflow of the dye slowly perfuse with 2-3 mls of dilute India dye until lungs are fully inflated withdraw needle and quickly clamp the trachea with hemostats pull tight the slipknot, release the hemostats gently remove the lungs and attached lymph nodes and heart. Remove the heart, but leave the lymph nodes weigh lungs with attached lymph nodes (wet weight) and place into pfa 10. 24-48 hours later, wash lungs in Ix PBS, and store at 4°.

Counting Tumors. In a dissecting dish filled with Ix PBS, separate individual lobes of lungs and remove mass of lymph nodes and thymus blot tissue dry, but don't let tissue dry out weigh all lung lobes, then weigh lung and lymph nodes together (record as lung dry weight and lung& lymph node dry weight respectively) using a dissecting scope, count lung tumors. The tumors do not take up the dye so white spots are tumors and normal tissue is black.

Results.

In that we were experiencing the difficulty with HKP-1, we made the decision to address this specific aim, through the use of HKP-2 (see Table 1 below), our RGD-based peptide, ACDCRGDCFC-GG-KLAKLAKKLAKLAK (with D-amino acids and disulfide bonds between specific cysteines as defined in Table 3), first applied to human breast carcinoma xenografts (Ellerby *et al.*, 1999), now applied to treat **transgenic adenocarcinoma of the mouse prostate (TRAMP) mice**. In keeping with the state goals of this aim, of dose optimization and route optimization, we designed a study that consisted of 3 treatment groups and one control group (Table 1) involving 2 doses and 2 routes of administration.

Treatment Groups (n=17 / group)	Dosing paradigm	Route	Times/ Wk	TX days
1. DMEM Vehicle	100 uls serum free DMEM 1x media	IP	1x	T
2. RGD	250 ug/100 uls	IV	1x	T
3. RGD	250 ug/100 uls	IP	1x	T
4. RGD	250 ugs/100 uls (total 500 ug/wk)	IP	2x	T&F

Table 1.

While the plan called for 17 animals per group, the actual numbers varied somewhat (Table 2). Group 1 was the control group receiving DMEM. Group 2 received 250 μg of HKP-2 per week in a single IV injection. Group 3 received 250 μg of HKP-2 per week, given as an IP injection. Group 4 received 250 μg of HKP-2, twice a week, for a total of 500 μg per week, given as IP injections. The rationale for looking at the IP injection was that this route of administration had looked promising in a study involving 435 breast carcinoma xenografts using HKP-1 (data not shown).

Group	# of animals	Total volume (100 uls x # of animals)	# of mgs of peptide
1. DMEM control	13+2=15	1500 uls of DMEM media	0
2. RGD 250 ug/100 uls	17 + 3=20	2000 uls of DMEM media	5
3. RGD 250 ug/ 100 uls	14 + 2=16	1600 uls of DMEM media	4
4. RGD 250 ug/ 100 uls	16 + 2=18	1800 uls of DMEM media	4.5

* Groups 2 ,3, and 4 can be combined into one tube for IV and IP injections since dose is the same for all groups (13.5 mgs in 5400 uls)

Table 2.

Average Days of Survival. The difference in the **average** number of days that TRAMP mice treated with HKP-2 lived as compared with control mice was not statistically significant (Figures 1 and 2). Much of this was due to the great variation in survival in the control group, as seen in the combined plot of Figure 2. However, there was also large variability in the HKP treated groups as well. Individual groups showed p values ranging from 0.2-0.3, while in the combined plot showed a p value of 0.1. Yet there was a trend in all groups indicative of increased survival.

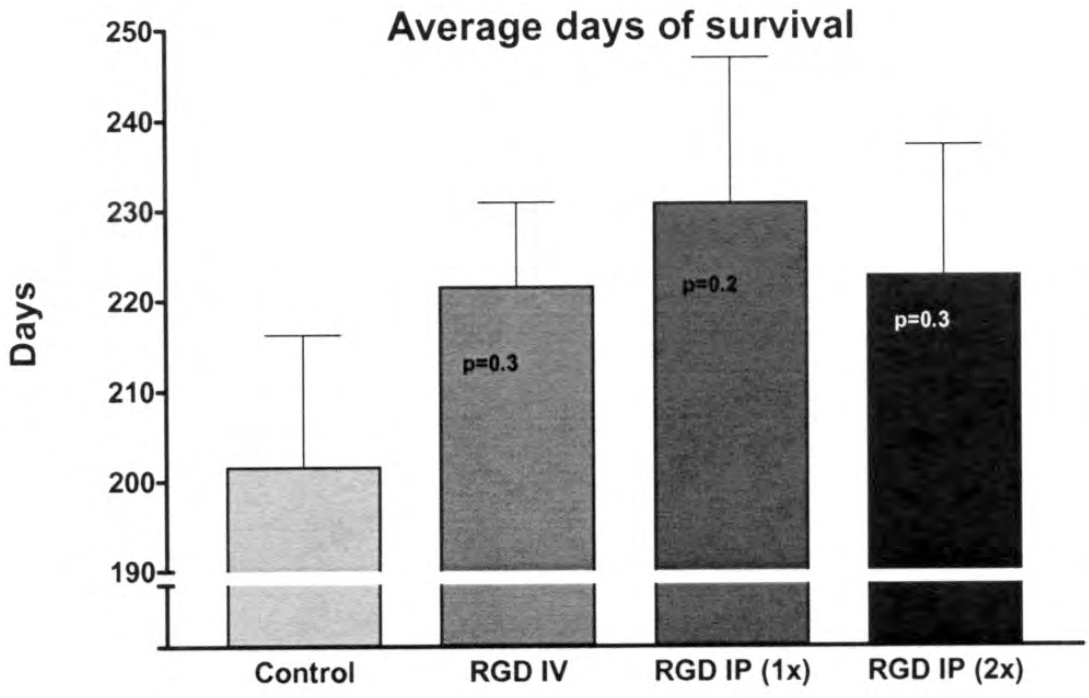

Figure 1. Average Days of Survival of Separate Groups as Compared with Control.

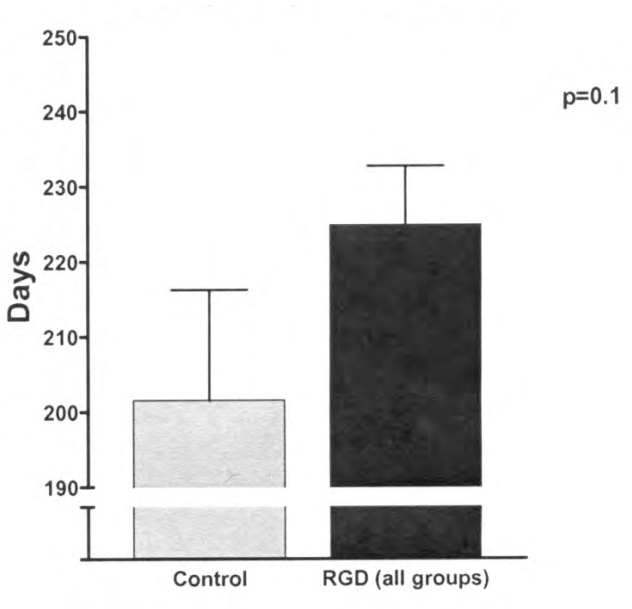

Figure 2. Average Survival Days of Combined RGD Groups Versus Control.

Survival Timelines. Based on the fact that there was a trend toward longer survival in the average survival data, we proceeded to examine the actual timeline of percent survival (Figs. 3, 4, 5, 6, 7, 8). Figure 3, 4, and 5 are shown without error bars for clarity.

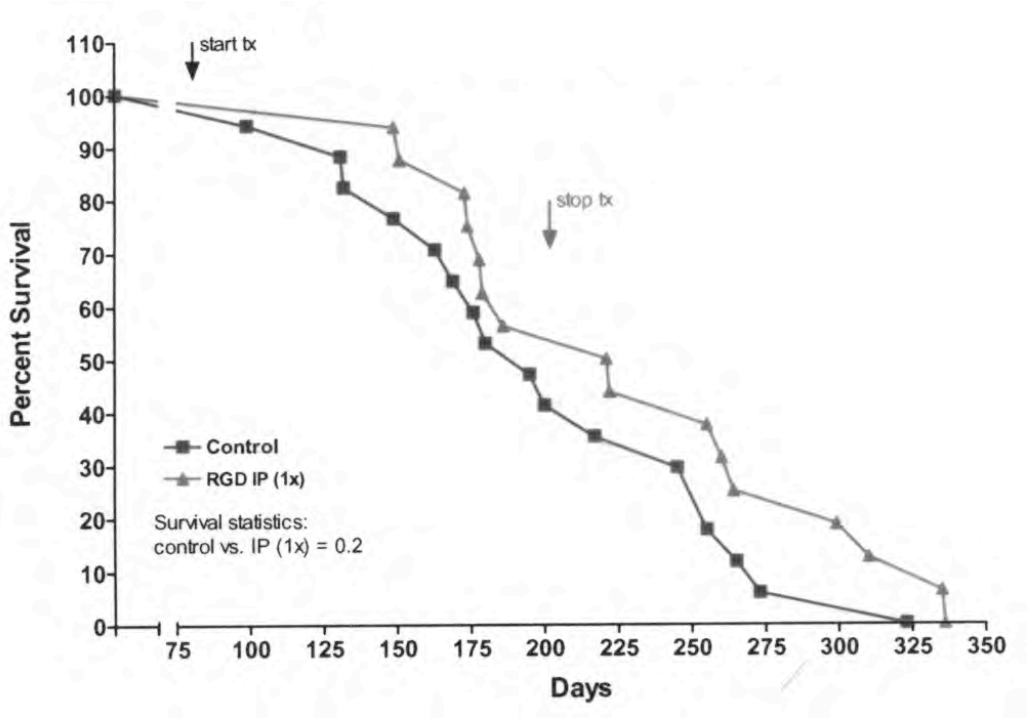

Figure 3. Percent Survival with Time for HKP-2 via IP Injection Route (1x/wk).

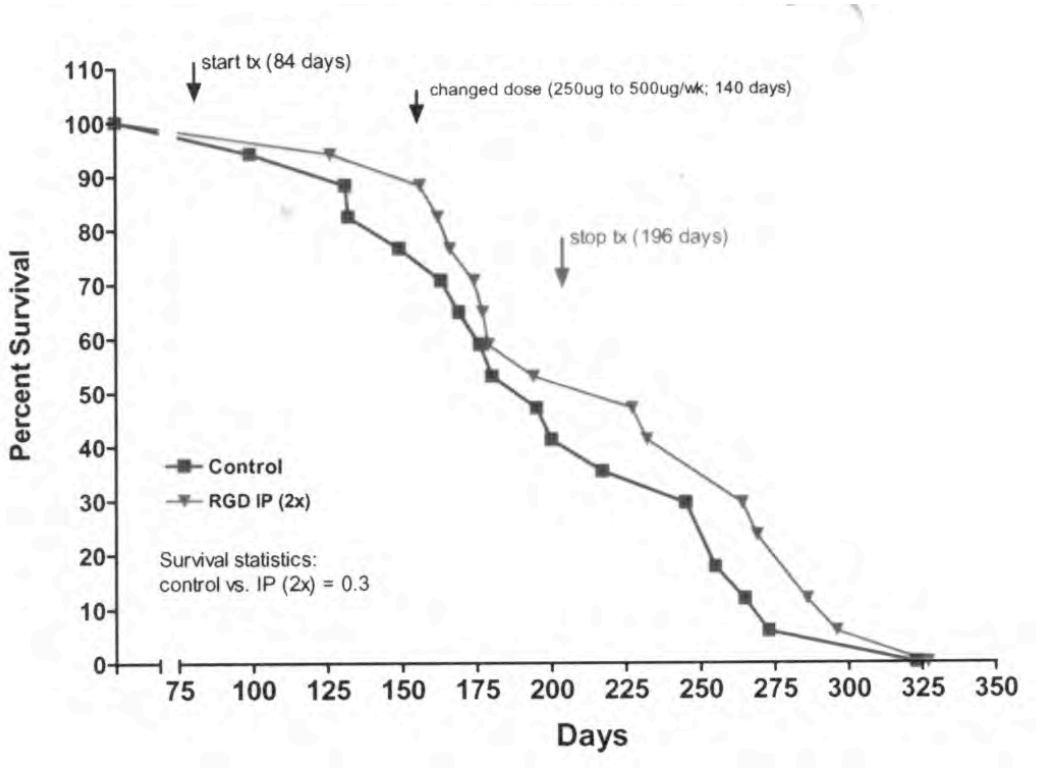

Figure 4. Percent Survival with Time for HKP-2 via IP Injection Route (2x/wk).

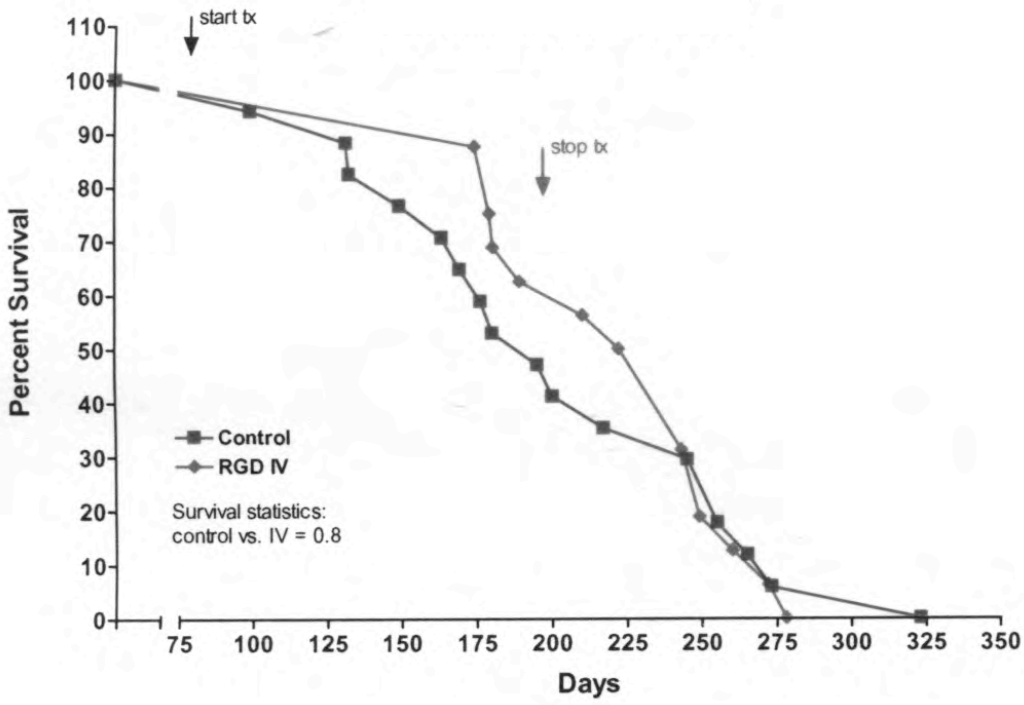

Figure 5. Percent Survival with Time for HKP-2 via IV Injection Route.

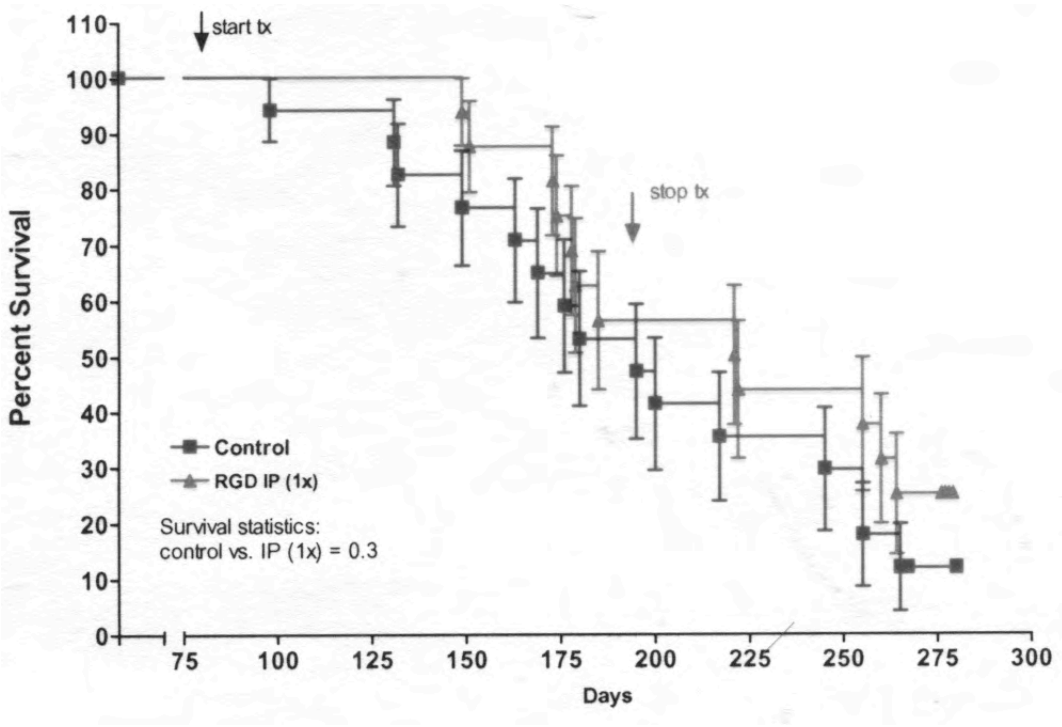

Figure 6. Percent Survival with Time for HKP-2 via IP Injection Route (1x/wk).

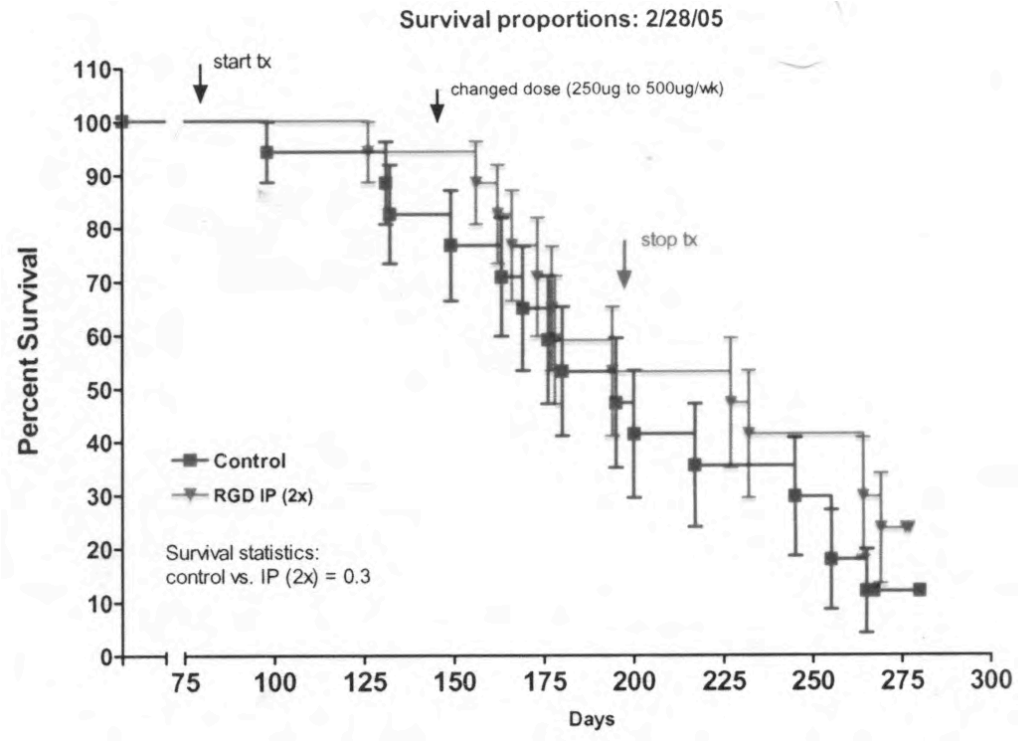

Figure 7. Percent Survival with Time for HKP-2 via IP Injection Route (2x/wk).

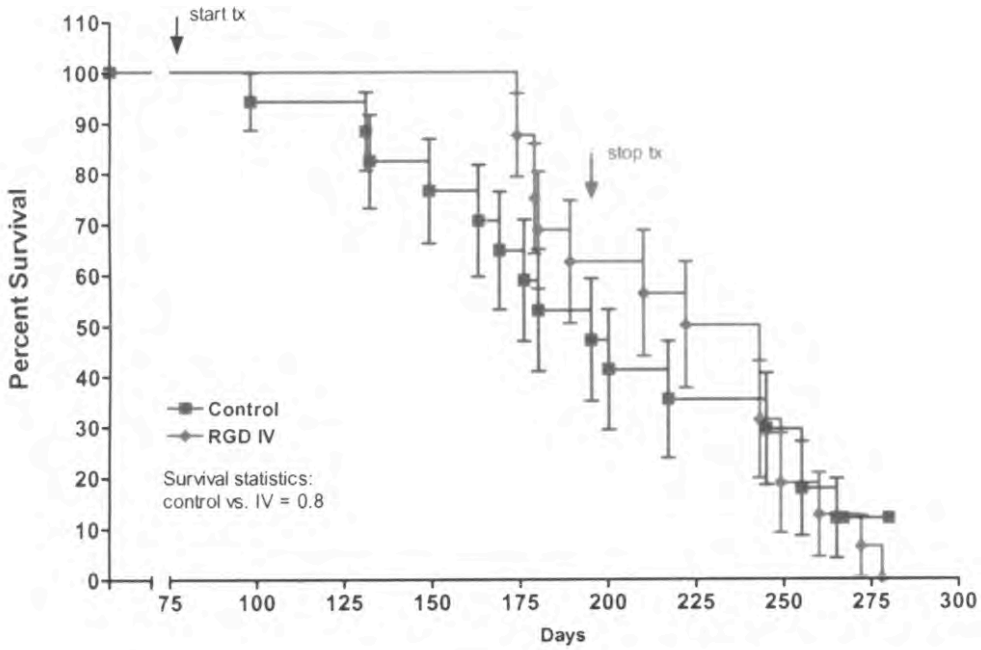

Figure 8. Percent Survival with Time for HKP-2 via IV Injection Route (1x/wk).

In addition to the individual survival plots we also considered composite plots, Figure 9 and 10.

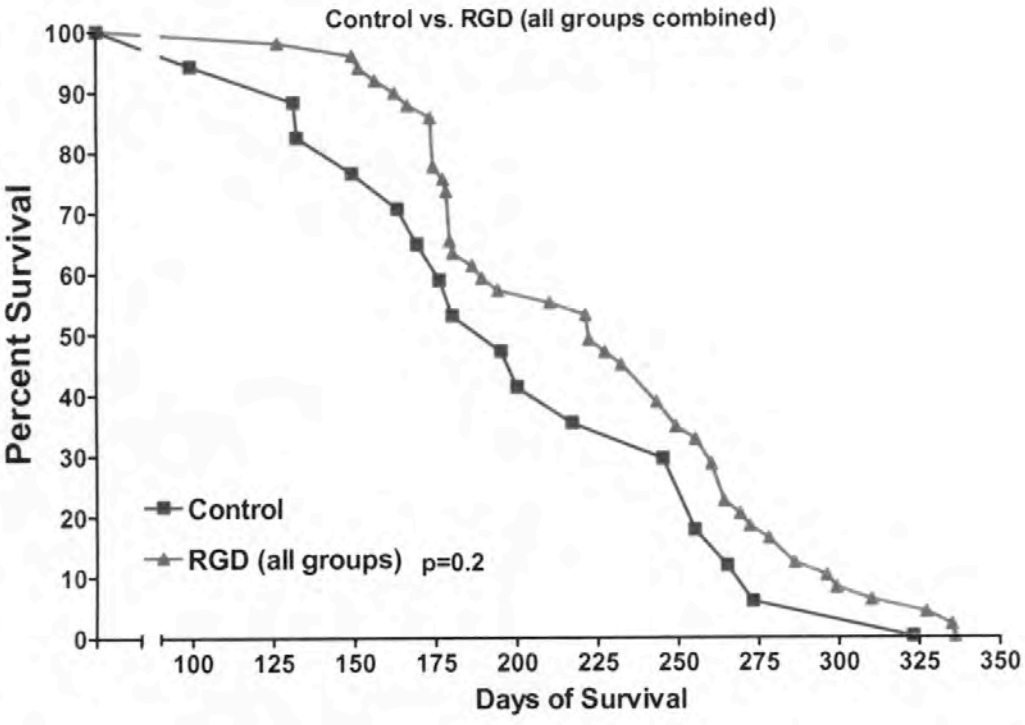

Figure 9. Percent Survival with Time for All HKP-2 Groups Versus Control.

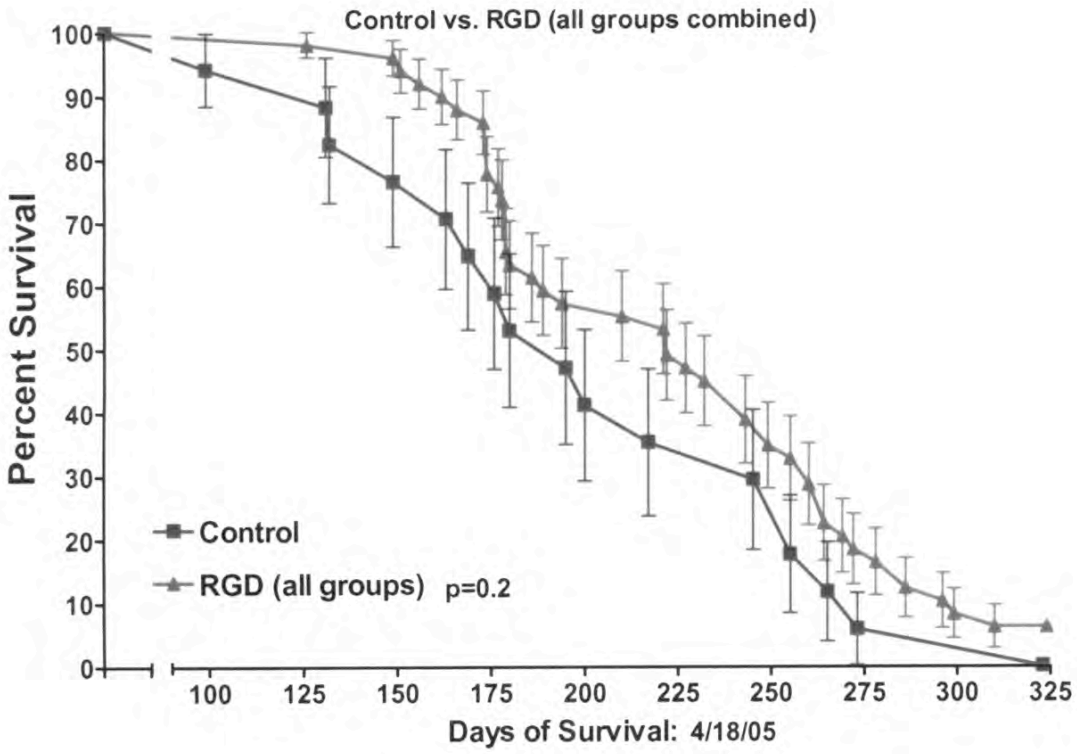

Figure 10. Percent Survival with Time for All HKP-2 Groups Versus Control.

Metastasis Study. The In addition to the investigation of survival, we also looked at the possibility that HKP-2 could inhibit metastasis. This was done by three complementary methods. First we looked at lung weights; second we counted individual lung tumors; and third we looked at lymph node weights, all according to standard established methods (See Methods). The results indicated that the group that received HKP-2 as an IP injection once a day versus the control group had differences in lung weight, number of lung metastases, and lymph node weight that were all statistically significant. The p value for the difference between control and HKP-2 (IP 1x) for lung weights was < 0.03; the p value for the difference between control and HKP-2 (IP 1x) for the number of lung metastases was < 0.05; and the p value for the difference between control and HKP-2 (IP 1x) for the number of lymph node metastases was < 0.03. The results also indicated that the group that received HKP-2 as an IV injection once a day versus the control group had differences in lung weights that were statistically significant. The p value for the difference between control and HKP-2 (IV 1x) for lung weights was < 0.05.

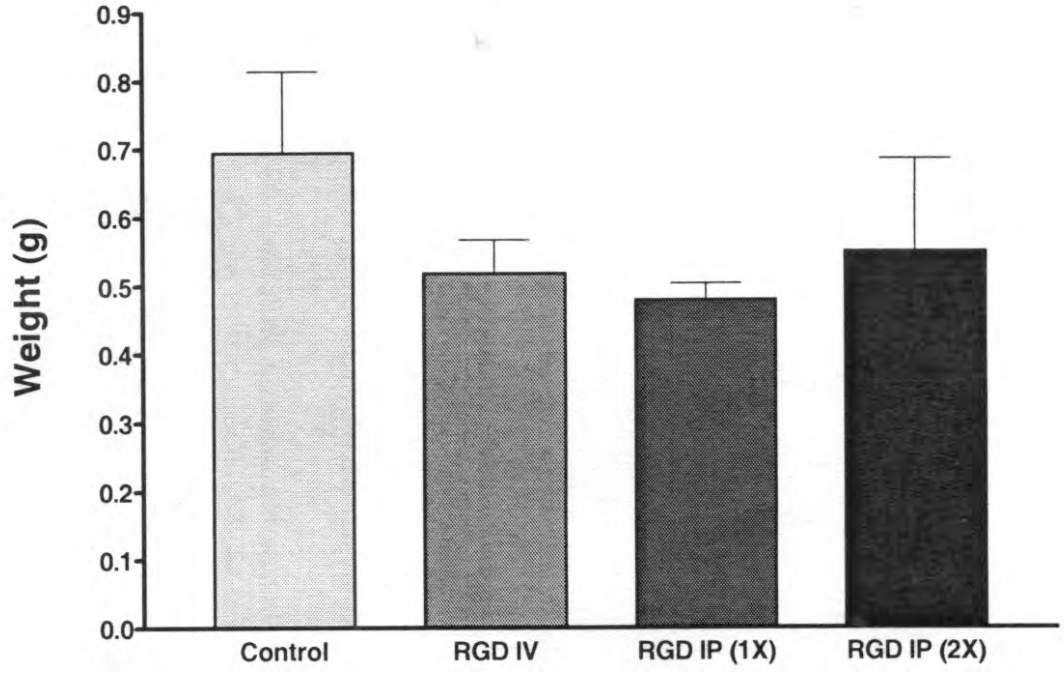

Figure 11. Lung Weights of TRAMP C Mice.

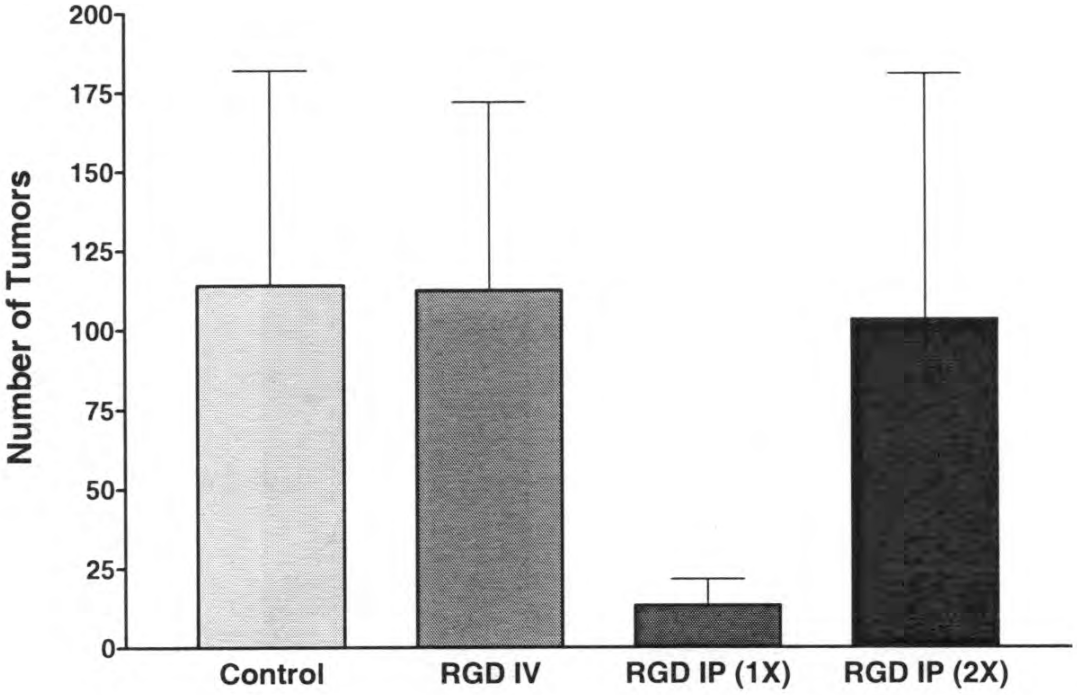

Figure 12. Number of Lung Tumors in TRAMP C Mice.

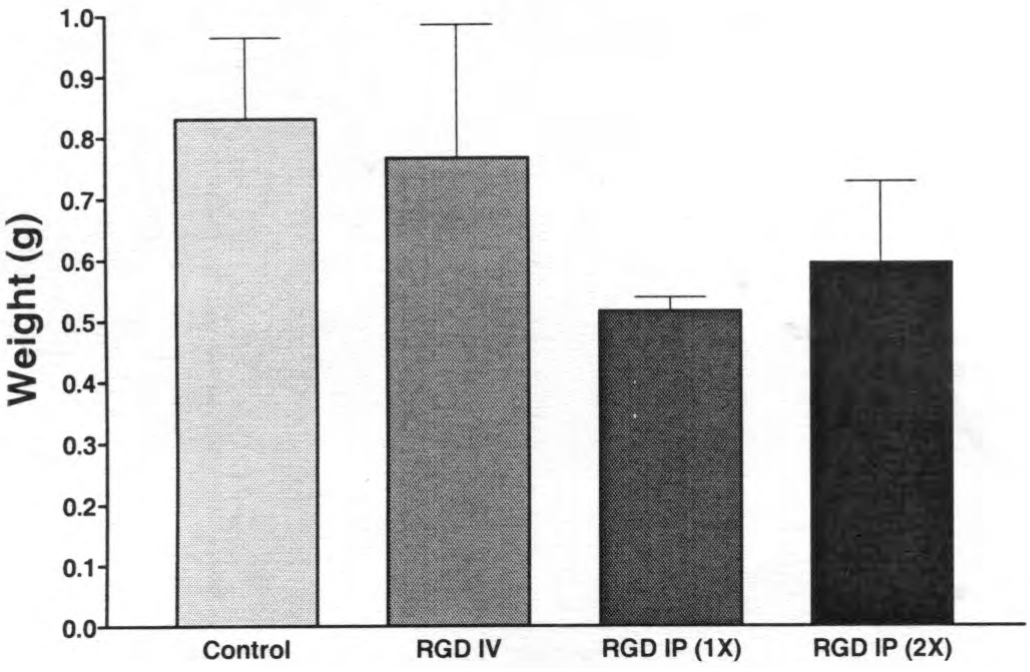

Figure 13. Lymph Node Weights in TRAMP C Mice.

Conclusion.

We made the decision to treat our TRAMP mice with HKP-2 rather than HKP-1 because we were still in the process of evaluating the inconsistent results that we obtained using it in a study of 435 breast carcinoma xenografts (study mentioned above in **Explanation of No Cost Extension**). We did not use HKP-3, the CNGRC dimer HKP (see Tasks 2, 3 and 5) because we were running our first study to evaluate the potential *in vivo* efficacy of HKP-3 in 435 breast carcinoma xenografts (the model we were most familiar with as described above) at the same time we were running HKP-2 in TRAMP mice (the study described here). Based on the success of that study, the next step after the study of HKP-2 in TRAMP mice would have been to evaluate HKP3 in TRAMP mice, but unfortunately this study requires further funding.

The results of this study show that HKP-2 is capable of inhibiting metastasis in the TRAMP model, even if it was not capable of increasing the survival in a statistically significant manner. However, the combined plots, Figures 9 and 10 do show a statistically significant increase in survival of HKP-2 treated mice over control mice from the beginning of the study up to around 175 days (or about 6 weeks into the study), more than half way through. Thus, perhaps with more animals in the study we might have seen

the emergence of a statistically significant result for HKP-2 (in light of course with the caveat that the HKP-2 groups were treated differently). It is also possible that the kinetics of cancer progression in the TRAMP model was accelerated over that of say the 435-breast carcinoma xenograft model. Indeed, HKP-2 was quite successful in increasing survival and inhibiting tumor volume in the 435-breast carcinoma xenograft model (Ellerby *et al.*, 1999). Nevertheless this study clearly demonstrated that HKP-2 was capable of inhibiting metastasis in the TRAMP model, and furthermore showed a positive trend toward increasing survival. The next steps in this research are a study of HKP-3 in the TRAMP model, and to publish the above results (manuscript in preparation). In addition to this work on Specific Aim 1, the PI of DAMD17-01-1-0029 was supported under this award for his contribution to other related work performed in collaboration with Dr. Wadih Arap evaluating the HKP, SMSIARL-GG-KLAKLAKKLAKLAK in the TRAMP model (Arap *et al.*, 2002).

Task 2

Specific Aim 2: Design HKPs with improved therapeutic indices.

Rationale.

We addressed Task 2 and Task 3 in years 1, 2 and 3 of this award (see Table 1). These Tasks were originally to be completed in year 1 and 2. While the vast majority of this work was completed in years 1 and 2, we extended the work into year 3 for the reasons outlined in **Explanation for No-cost Extension**.

Methods.

The method used was rational design based on our previous experience with the properties of amphipathic peptides (Ellerby *et al.*, 1999; Furuya *et al.*, 2003).

Results.

We designed 6 peptides over the course of the first 3 years of DAMD17-01-1-0029. These peptides are listed in the following table (Table 3), and we discuss them below:

Year	Abbr.	Peptide
3	HP-3	[CNGRC] **Dimer**
3	HKP-3	[CNGRC-GG-$_D$(KLAKLAK)$_2$] **Dimer**
1	HKP-4	$_D$(ALLLAIRRR-KKK)-GG-CNGRC
1	KP-4	$_D$(ALLLAIRRR-KKK)
2	KP-6	$_D$(KKK-KLLKLLLKLWLKLLKLLL)
2	HKP-6	CNGRC-GG-$_D$(KKK-KLLKLLLKLWLKLLKLLL)

Table 3.

In Table 3, the year that the peptides were designed appears in column 1, the abbreviation for the peptide appears in column 2, and the amino acid sequence of the peptide appears in column 3. The abbreviations however are not chronological and have never been used previously (except HKP-1 and HKP-2). They are used here in this report for convenience so that peptide sequences do not have to be explicitly written out and repeated. All of the peptides and their abbreviations discussed in this report can be seen in Table 4. In Tables 3 and 4 […]Dimer represents the dimer of the peptide in the brackets, where the dimer has been forme by disulfide bonds between the cysteines. $_D$(…) represents the fact that all the amino acids within the parentheses are D-amino acids (this was done to prevent proteolytic cleavage; Bessalle *et al.*, 1990; Wade *et al.*, 1990). The designation HP denotes "hunting peptide," as these moieties target to the tumor vasculature endothelial cells. The designation HKP denotes "hunter killer peptide." And in Table 4 below, KP denotes "killing peptide," as these moieties disrupt membranes.

KP-4 and HKP-4 (Year 1)

The designs of KP-4 and HKP-4 were based on an antibiotic peptide previously described, the synthetic 9-mer ALLLAIRRR, because it killed bacteria at concentrations 2000 times lower than those required to kill eukaryotic cells (fibroblasts) (Saido-Sakanaka *et al.*, 1999). The decision to use ALLLAIRRR as the basis of a killing domain was rational in that the trend we had always found was that antibacterial peptides also swelled mitochondria at about the same concentration that they killed bacteria. However, in preliminary studies our laboratory performed on ALLLAIRRR (the parent peptide of KP-4), it was determined that this peptide was too hydrophobic, and had solubility problems. We then re-designed the peptide as ALLLAIRRR-KKK to increase solubility.

Follow-up experiments on HK-4 involving mitochondrial swelling and cell culture experiments confirmed that HK-4 was now soluble, and that we had not lost anti-mitochondria swelling properties, and had in fact gained something in that ALLLAIRRR-KKK was somewhat less toxic on eukaryotic cells than ALLLAIRRR (data not shown). The choice then to create HKP-4, rather than say an RDG based design (e.g. ALLLAIRRR-KKK-GG-ACDCRGDCFC; see HKP-2, Table 4 and Ellerby *et al.*, 1999), was mostly an economic one, weighing the cost differential between CNGRC-GG (one disulfide bond) and GG-ACDCRGDCFC (two disulfide bonds in a complex pattern; a disulfide bond between the two inner cysteines (closest to RGD), and a disulfide between the two outer cysteines). We discuss the *in vitro* evaluation of KP-4 and HKP-4 in Task 3 (Specific Aim 3).

KP-6 and HKP-6 (Year 2)

The designs of KP-6 and HKP-6 were a logical extension of our work on the parent killing peptide, KLLKLLLKLWLKLLKLLL, also known as Hel13-5 (Lee *et al.*, 2001; Furuya *et al.*, 2003). We had determined that Hel13-5 had unique membrane disrupting properties in synthetic membrane systems and therefore we decided to create KP-6, and the corresponding HKP-6. Again we found the parent compound to be too hydrophobic/toxic for our application here, and so we added KKK to make the peptide less hydrophobic. We discuss the *in vitro* evaluation of KP-4 and HKP-4 in Task 3 (Specific Aim 3).

HP-3 and HKP-3 (Year 3)

The designs of HP-3 and HKP-3 were a result of our work to debug the problem we were experiencing with our original peptide design HKP-1. As described above in this report, in Task 1 (Specific Aim 1), in preparation for the Task 1 study of a first-generation (HKP-1 or 2) in the TRAMP C model, we conducted an animal study of our original HKP-1 in a xenograft model of breast carcinoma (435 human **breast** carcinoma cells). When this first animal study was completed it was evident that we could not reproduce previous work with HKP-1 on 435 breast carcinoma xenografts. At this time, we decided that we needed to determine exactly why the study of HKP-1 had failed rather than moving into the TRAMP C model, and in response formed a task force work the

problem. During the course of this work, we asked the question (based on information we received from several other scientists with years of experience with peptide therapeutics) if the active fraction in our peptide preparations might not be the dimer form of the HKP, there before this considered just an impurity. We therefore decided to look into this possibility, and created HP-3 and HKP-3, dimers of our original HP-1 and HKP-1. As it turned out this was a very fortuitous and important decision because it opened the door to a successful study of HKP-3 in 435 breast carcinoma xenografts, which while not part of DAMD17-01-1-0029 work, led to the study of the properties of HP-3, which was performed as part of DAMD17-01-1-0029, and which was quite successful in the discovery of a dual function role of HP-3, the internalization into the cytosol of cells by binding to aminopeptidase N, and the inhibition of aminopeptidase N enzymatic activity via a different site on the enzyme.

Conclusion. We addressed this specific aim through the creation of 6 new peptide designs, which we then evaluated in addressing in Task 3 (Specific Aim 3).

Task 3

Specific Aim 3: Evaluate in vitro efficacy and toxicity of new HKPs.

Rationale. We addressed Task 2 and Task 3 in years 1, 2 and 3 of this award (see Table 1). These Tasks were originally to be completed in year 1 and 2. While the vast majority of this work was completed in years 1 and 2, we extended the work into year 3 for the reasons outlined in **Explanation for No-cost Extension**.

Methods.

Reagents. N-acetyl-Asp-Glu-Val-Asp-pNA; (DEVD-pNA; BioMol, Plymouth Meeting, Pennsylvania). Peptides; AnaSpec (San Jose, California) and Bachem (Germany).

Cell Culture. Dermal microvessel endothelial cells (DMECs), KS1767, MDA-MB-435, and PC3 cells were cultured as described previously (Ellerby *et al.*, 1999; Ellerby *et al.*, 2003).

Morphological Quantification of Cellular Apoptosis. LC_{50}s (Table 1) were determined by apoptotic morphology, using previously described methods (1999). For the LC_{50} assay, cells were incubated with various concentrations, and the values listed in Table 1

reflect the LC_{50}. Cell culture medium was aspirated at various times from adherent cells, and the cells were gently washed once with PBS at 37°C. Then, a 20-fold dilution of the dye mixture (100 μg/ml acridine orange and 100 μg/ml ethidium bromide) in PBS was gently pi petted on the cells, which were viewed on an inverted microscope (Nikon TE 300). The cell death seen was apoptotic cell death and in some cases was confirmed by a caspase activation assay. Not all cells progressed through the stages of apoptosis at the same time. At the initial stages, a fraction of the cells were undergoing early apoptosis. At later stages, this initial fraction had progressed to late apoptosis and even to the necrotic-like stage associated with very late apoptosis (for example, loss of membrane integrity in apoptotic bodies). However, these cells were joined by a new fraction undergoing early apoptosis. Thus, cells with nuclei showing margination and condensation of the chromatin and/or nuclear fragmentation (early/mid-apoptosis; acridine orange-positive) or with compromised plasma membranes (late apoptosis; ethidium bromide-positive) were considered not viable. At least 500 cells per time point were assessed in each experiment. LC_{50s} were assessed at 24 h.

Mitochondrial swelling assays. Rat liver mitochondria were prepared as described (Ellerby *et al.*, 1997; Ellerby *et al.*, 1999). The concentrations used were as in Table 1, with a control of 200 μM Ca2+ (positive control). The peptides were added to mitochondria in a cuvette, and swelling was quantified by measuring the optical absorbance at 540 nm as described previously (Ellerby *et al.*, 1997; Ellerby *et al.*, 1999).

Caspase activity of cell lysates. Cell-free systems were reconstituted as described (1999). For the mitochondria-dependent reactions, rat liver mitochondria were suspended in normal (non-apoptotic) cytosolic extracts of human prostate carcinoma cells: PC-3s. The peptides were then added at the stated concentrations. After incubation for 2 h at 30°C or 37 °C, mitochondria were removed by centrifugation, and the supernatant was analyzed. The caspase activity of PC3 lysates was measured as described (Ellerby *et al.*, 1997; Ellerby *et al.*, 1999). Aliquots of cell lysates (1 μl lysate; 8-15 mg/ml) were added to 100 μM DEVD-pNA (100 μI; 100 mM HEPES, 10% sucrose, 0.1 % CHAPS and 1 mM on, pH 7.0). Hydrolysis of DEVD-pNA was monitored by spectrophotometry (400 nm) at 25°C.

Results.

The results of our evaluation of our peptides are summarized in Table 4 below. What follows that table is a discussion of the table beginning with a specific time line for when the experiments were completed and then following that a discussion of each result. All results shown in Table 4 were repeated in at least 3 separate experiments, at least 3 data points per experiment. All P values < 0.05, t-test. Bold **D** indicates dimer. Subscript D indicates D amino acids. $(\ldots)_2$ means repeat the sequence.

Year	Abbr.	Peptide	LC_{50} (μM)			Swelling (μM)
			DMEC	KS1767	PC-3	Mito
1 (PC-3)	KP-1	$_D$(KLAKLAK)$_2$	492*	387*	356	3*
1 (PC-3)	HKP-1	CNGRC-GG-$_D$(KLAKLAK)$_2$	481*	58*	94	-
3	HP-1	CNGRC	512	463	533	-
3	HP-3	[CNGRC] **D**	493	199	262	-
3	HKP-3	[CNGRC-GG-$_D$(KLAKLAK)$_2$] **D**	404	11	21	-
1 (PC-3)	HKP-2	(RGD-4C)-GG-$_D$(KLAKLAK)$_2$	492*	10*	452	-
1	HKP-4	ALLLAIRRR-KKK-CNGRC	533	23	325	-
1	KP-4	ALLLAIRRR-KKK	>5,000	>4,000	>4,000	3
1	KP-5	SGP	10	4	2.5	0.5
2	KP-6	KKK-KLLKLLLKLWLKLLKLLL	250	276	245	1
2	HKP-6	CNGRC-GG-KKK-KLLKLLLKLWLKLLKLLL	267	58	66	-

Table 4.

Discussion of Table 4:

Timetable:

Period of Award: May 2001 to May 2005

Year 1: 5/2001-5/2002

Year 2: 5/2002-5/2003

Year 3: 5/2003-5/2004

Year 4: 5/2004-5/2005 (year of no cost extension)

Previous to DAMD17-01-1-0029: data designated by * in Table 1, included for comparison only. All other data under DAMD17-01-1-0029, specifically:

PC-3 Cells (prostate specific cells):
Year 1: KP-1, HKP-1, HKP-2, KP-4, HKP-4, KP-5
Year 2: KP-6, HKP-6
Year 3: HP-1, HP-3, HKP-3

DMEC Cells (for comparison with PC-3 cells):
Year 1: KP-4, HKP-4, KP-5
Year 2: KP-6, HKP-6
Year 3: HP-1, HP-3, HKP-3

KS1767 Cells (for comparison with PC-3 cells)
Year 1: KP-4, HKP-4, KP-5
Year 2: KP-6, HKP-6
Year 3: HP-1, HP-3, HKP-3

Mitochondria (for comparison with cells to estimate a therapeutic index)
Year 1: KP-3, KP-4,
Year 2: KP-5

KP-1 and HKP-1.

The results under DAMD17-01-1-0029 involved the treatment of human prostate tumor cells. The trend involving LC_{50} was similar and consistent with the results on KS1767 Kaposi's sarcoma (human) cells, with the notable feature that the LC_{50} for PC-3 cells was higher than the LC_{50} of KS1767 cells, but lower than that of non-cancerous DMEC cells (human microdermal vascular cells). This can be explained in that KS1767 cells express a high level of aminopeptidase N while PC-3 cells express a low level of aminopeptidase N. Cells such as DMECs do not express aminopeptidase N (Ishii *et al.*, 2001).

HKP-2.

The results under DAMD17-01-1-0029 involved the treatment of human prostate tumor cells. Again the trend involving LC_{50} was similar and consistent with the results on KS1767 Kaposi's sarcoma (human) cells. This can be explained in that KS1767 cells and PC-3 cells both express alpha 5 beta 3 integrins, the receptor for RGD peptides that facilitates the internalization of HKP-2 (Duo-Qi Zheng *et al.*, 2000).

HP-3 and HKP-3.

The results under DAMD17-01-1-0029 involved the treatment of all cell types in Table 4. The results here show that the dimer HKP-3 had an improved therapeutic index over the monomer HKP-1 by about a factor of 5, and that HKP-3 was even slightly more effective than HKP-2. Thus the goal of designing a peptide with an improved therapeutic index was satisfied here. Interesting, some of this extra potency appears to have come from the targeting moiety HP-3, in that by itself, had a cytostatic or cytotoxic effect on the cells

(KS1767 and PC-3) that express aminopeptidase N, noting again that it was more effective on KS cells, no doubt owing to the higher expression of aminopeptidase N.

KP-4 and HKP-4.

The results under DAMD17-01-1-0029 involved the treatment of human prostate tumor cells. Clearly from Table 4, HKP-4 had an improved therapeutic index over HKP-1, HKP-2, and HKP-3, including PC-3 cells. The main effect was the lower toxicity of KP-4 on mammalian cells, while maintaining the toxicity on mitochondria. In light of the results for HKP-3, creating the dimer version of HKP-3 would have been the next step in the evolution of this work.

KP-5.

The results under DAMD17-01-1-0029 involved the treatment of human prostate tumor cells. The results of KP-5 on PC-3 cells are consistent with those found on KS1767 and DMEC cells. Interesting, KP-5 showed a preference for tumor cells over normal cells by a factor of about 2-4. Taken together with the results on mitochondria may indicate a slight preference for negatively charge membranes. Based on this, and other results, the treatment of PC-3 xenografts described in Task 4 (Specific Aim 4) was a logical extension of our work. And in fact, in agreement with the results on 435 breast carcinoma xenografts, KP-5 was quite potent as an antitumor agent in the PC-3 human prostate xenograft model (see Task 4).

KP-6 and HKP-6.

The results under DAMD17-01-1-0029 involved the treatment of all cell types in Table 4. The results for HKP-6 were somewhat disappointing, owing to the greater toxicity on mammalian cells over HKP-1, HKP-2, HKP-3 and HKP-4. However, further work may have allowed a re-design of this peptide. Possible solutions include the addition of more lysines, which in general has the tendency to lower toxicity on mammalian cells. Yet, the great results obtained for HKP-3 and HKP-4 would make further evaluation and improvement of this design unlikely.

Conclusion.

Together, the purpose of Task 2 (Specific Aim 2) and Task 3 (Specific Aim 3) was to create and to evaluate new peptide designs leading to designs with improved therapeutic indices. We accomplished this through the creation of HKP-3 and HKP-4. Had we not run out of time, and now with additional funding, the next step would have been to treat TRAMP mice with either HKP-3 or HKP-4, or to first consider *in vitro* evaluation of a dimer of HKP-4, and then to proceed with the best of these peptides.

Task 4

Specific Aim 4: Evaluate the in vivo efficacy of new HKPs in the TRAMP model of prostate cancer.

Rationale. As discussed above, in year 1 of this award, we had identified a problem with HKP-1, which precluded proceeding with any further animal studies using HKP-1 until we had determined exactly the nature of the problem. However, the aegis of this funded research was a **comprehensive** development of Hunter-Killer Peptides for prostate cancer (the title of the funded proposal was "Comprehensive Development Program of Hunter-Killer Peptides for Prostate Cancer"). Thus in keeping with this program we evaluated the Killer Peptide KP-5 in the PC-3 xenograft model of prostate cancer. We had determined that this peptide was effective as an anti-tumor agent, without the necessity of targeting through the direct lysing of tumor cells (Ellerby *et al.*, 2003). Our laboratory at the Buck Institute had performed successful studies using the novel peptide KP-5 on human lung carcinoma xenografts. We therefore made the logical and consistent decision to perform an *in vivo* study of KP-5 in human prostate (PC-3) xenografts. This 69-amino acid killing peptide (KP), known in our publication as Small Globular Protein (SGP), had a 2 to 4-fold preference for killing tumor cells, as compared with normal cells. However, we determined that its direct toxicity on normal human cells precluded its use in its current form. Yet, the fact that this peptide folded and thus had properties of a protein, allowed it to be directly injected into a tumor, without the need to be targeted. Thus the logical strategy became to exploit an anticancer effect due to direct tumor cell killing rather than the killing of tumor vasculature endothelial cells. The results of this study were quite successful, demonstrating that KP-5 could increase survival, and decrease tumor size, in a

model of human prostate cancer (PC-3 xenografts in nude mice). These results were included in the publication Ellerby *et al.* 2003. However, an inaccurate and unfortunate oversight resulted in the omission of DAMD17-01-1-0029 from the acknowledgements. The success of this research led us to the design of a targeted KP-5, consisting of HK-5 sequestered inside, with targeting peptides coating the outside, of nanospherical particles, targeted to tumor vasculature (with HP-3). However, we ran out of funding before this design could be evaluated *in vitro*, or *in vivo* in the TRAMP C model. In summary, we addressed Specific Aim 4 by evaluating one of our peptides, KP-5, in a model of human prostate carcinoma.

Methods.

Synthesis and Purification. KP-5 (SGP) was synthesized according to the Fmoc procedure starting from Fmoc-Leu-PEG (polyethylene glycol) resin using a Miligen automatic peptide synthesizer (Model 9050) to monitor the de-protection of the Fmoc group by UV absorbance. After cleavage from the resin by trifluoroacetic acid, the crude peptide obtained was purified by HPLC chromatography with an ODS column, 20 x 250 mm, with a gradient system of water/acetonitrile containing 0.1% trifluoroacetic acid. Amino acid analysis was performed after hydrolysis in 5.7 M HCl in a sealed tube at 110 °C for 24 h. Analytical data obtained were as follows: Gly, 6.2 (6); Ala, 9.5 (10); Leu, 26.5 (25); Asp, 3.0 (3); Pro, 2.9 (3); Tyr, 3.1 (3); Lys, 18.9 (18). Molecular weight was determined by fast atom bombardment mass spectroscopy using a JEOL JMX-HX100: base peak, 7555.1; calculated for C367H639O77N91 H+, 7554.8. Peptide concentrations were determined from the UV absorbance of Trp and three Tyr residues at 280 nm in buffer (e = 8000). Gel filtration HPLC chromatography was performed using Tris buffer (10 mM Tris, 150 mM NaCl, pH 5.0 or pH 7.4) on COSMOSIL 5DIOL-300 (Nakalai Tesk, Kyoto, Japan).

Human Tumor Xenografts. PC-3-derived human tumor xenografts were established in 2-month-old female or male (according to the tumor type), nude/nude Balb/c mice (Jackson Labs, Bar Harbor, ME) by administering 10^6 tumor cells per mouse in a 200 μl volume of serum-free Dulbecco's modified Eagle's medium into the mammary fat pad or

on the flank. The mice were anesthetized with Avertin as described (Ellerby *et al.*, 1999). SGP was administered directly into the center of the tumor mass at a concentration of 100 μM given slowly in 5 μl increments, for a total volume of 40 μl. Measurements of tumors were taken by caliper under anesthesia and used to calculate tumor volume. Animal experimentation was reviewed and approved by the Institutional Animal Care and Use Committee.

Results.

KP-5 Treatment of Nude Mice Bearing Human Prostate Cancer Xenografts. The data in Figure 14 are shown for human PC3-derived prostate carcinoma tumors. Tumor cells were implanted on the flank at the start of the experiments. Mice were divided in similar groups based on matched tumor volumes at the start of the experiment (open circles). KP-5 was administered directly into the center of the tumor mass at a concentration of 100 μM given slowly in 5 μl increments, for a total volume of 40 μl. Measurements of tumors were taken by caliper under anesthesia and used to calculate tumor volume. KP-5-treated PC-3 tumors are smaller than control PBS-treated tumors. Differences in tumor volumes at 10 weeks are shown (t test, $p = 0.05$). $n = 7$ for each experimental group. In one case a KP-5-treated tumor disappeared.

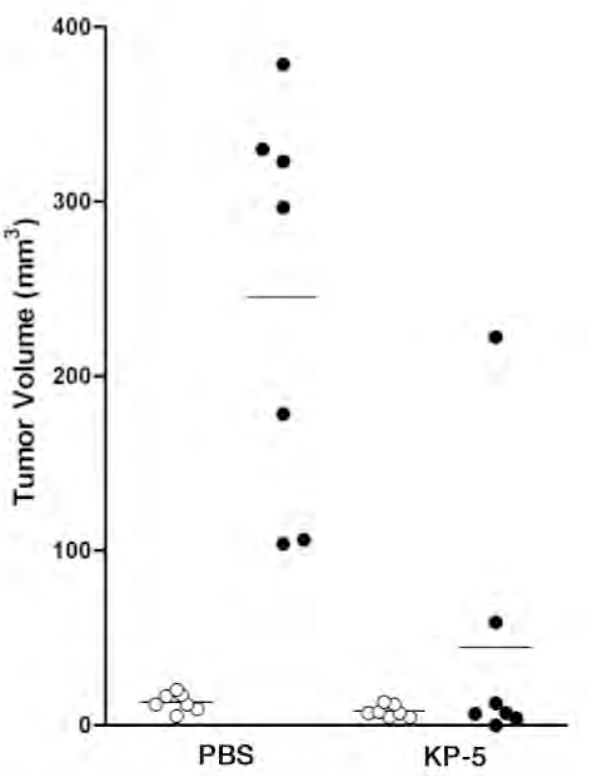

Figure 14.

We also looked at the survival of the PC-3 tumor bearing mice treated with KP-5. The Kaplan-Meier survival plot below (Figure 15) shows that about 70% of the mice in the KP-5-treated group were still alive after 20 weeks (140 days), whereas only about 30% of the control mice were alive at this time. Thus the survival of the KP-5 treated mice was 2.33 times that of the control mice.

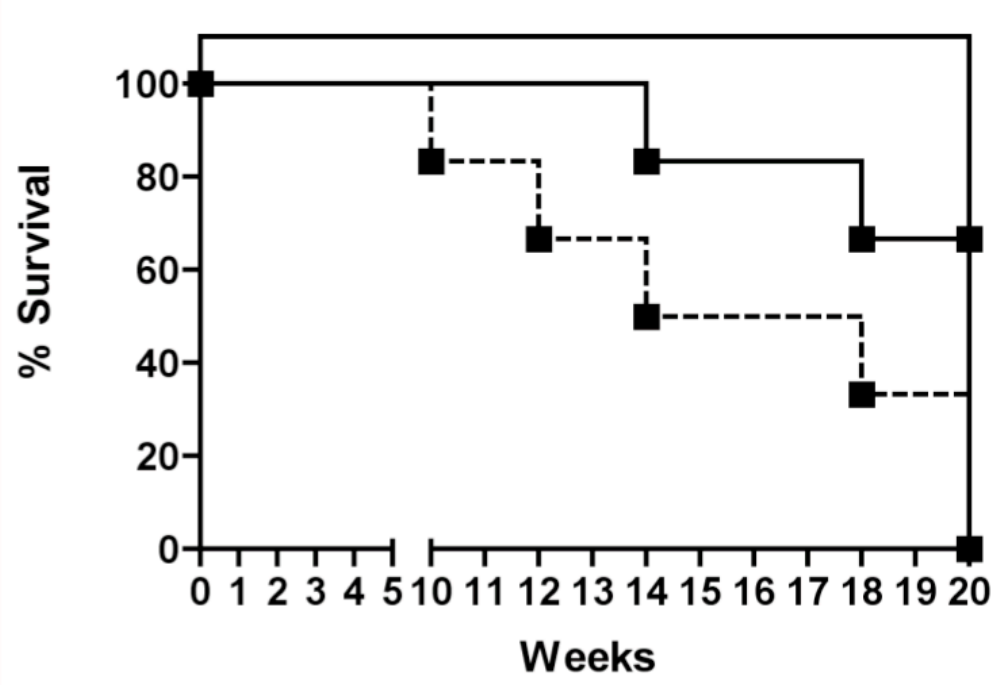

Figure 15.

Conclusion. As described above, the data for the treatment of PC-3 human tumor xenografts in nude mice with KP-5 was presented in Ellerby *et al.*, 2003, and was done under the aegis of DAMD17-01-1-0029. The results were very impressive, and the next step in this research is the encapsulation of KP-5 in a targeted nanospherical particle applied to TRAMP model of prostate cancer.

Task 5

Specific Aim 5: Determine the *in vivo* pharmacokinetics of HKPs in the TRAMP C model of prostate cancer.

Rationale. While working on the problem of why HKP-1 had failed in our study on human breast carcinoma xenografts, the team we had assembled learned that it was

possible that the active (or more active) fraction in our peptide preparations might be the dimer of HKP-1. Thus, in the process of debugging our problem with HKP-1, we began an investigation of the properties of both HP-3 and HKP-3, the dimers of HP-1 and HKP-1, respectively. We performed a successful *in vitro* study in cell culture demonstrating that the dimer HKP (HKP-3) was significantly more effective than the monomer (HKP-1) (Figure 16). This work was performed under DAMD17-01-1-0029, and was critical to any advancement.

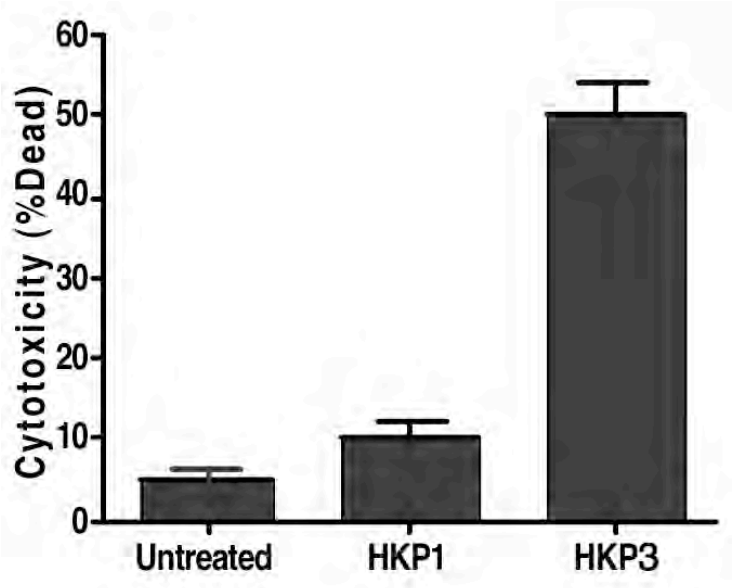

Figure 16.

Indeed, based on these results we then performed a successful study of HKP-3 in human breast carcinoma xenografts (Figure 17). In this study we compared the HKP-3 therapy alone, with the drug Abraxane, which is the drug paclitaxel encapsulated in an albumen nanoparticle. This allowed us to see if our approach would be complementary and synergetic, in that HKP-3 is anti-angiogenic, and Abraxane inhibits microtubule formation in cancerous cells thus preventing their division. We chose to evaluate the dimer HKP, HKP-3, in the MDA-MB-435 xenograft model of human breast cancer because we did not want to change two variables while investigating the properties of this new HKP. The MDA-MB-435 xenograft breast tumor model was the most familiar to our

laboratory. The next logical step would have been to evaluate HKP-3 in a model of PC-3 xenografts, and then in the TRAMP model, and future funding will facilitate this work.

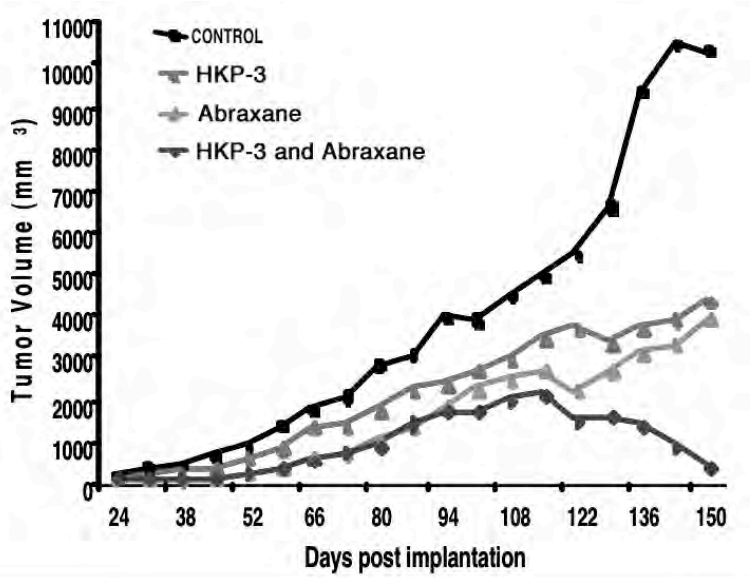

Figure 17. HKP Dimer (HKP-3) treatment of nude mice bearing human tumors. Data are shown for MDA-MB-435-derived breast carcinomas. HKP-3 treated tumors are smaller than control [CARAC-GG-D(KLAK LAK)2] treated tumor volumes at 19 weeks (*t* test, *P*=0.027). At nineteen weeks of treatment, tumor volume was significantly decreased between control group (10,298 mm3 ± 2,570) and HKP-3 (4,372 mm3 ± 2,470; p* < 0.05 vs control) or Abraxane™ (3,909 mm3 ± 506; p** < 0.01 vs control). The combination of Abraxane™ and HKP-3 reduced the tumor volume to 411 mm3 ± 386; (p** < 0.01 vs, Abraxane™ and HKP-3 monotherapy).

The combination of Abraxane with the vascular targeting antiangiogenic dimeric HKP peptide HKP-3 against the MDA-MB-435 xenograft breast tumor showed a significant reduction in tumor volume compared to monotherapy of either agent alone. MDA- MB-435 human tumor xenografts were established at an average tumor volume of 100 mm3, mice were randomized into groups of 12-13 animals and treated with HKP, Abraxane, or HKP and Abraxane. HKP-3 was delivered i.v. (250 *m*g) once a week, for a total of 16 weeks. The therapy was then terminated and yet the tumor volumes in the multidrug group continued to regress in volume. Abraxane was administered i.v., daily for 5 days at 10 mg/kg/day only for the first week of treatment. The Abraxane dose used was substantially below its MTD (30mg/kg/day, qdx5) to prevent the tumor from complete

regression so effect of HKP could be noted. HKP's are not as toxic as paclitaxel so this represents a real advance toward a less toxic therapy**.**

These results led us to ask the important question of why the dimer HKP-3 was more effective than the monomer HKP-1. In this process, we discovered that the dimer targeting peptide, HP-3, not only bound to the receptor (aminopeptidase N) involved in the internalization of HKPs into cells, but also inhibited the enzymatic activity of this enzyme via binding to a separate site on aminopeptidase N. The inhibition of aminopeptidase N enzymatic activity is well known to have an anti-angiogenic activity in its own right, and so this discovery explained why HP-3 was more effective, in that HP-3 functioned with a dual purpose – to internalize HKP-3 (thus killing endothelial cells and inhibiting angiogenesis), and at the same time, to inhibit aminopeptidase N (thus inhibiting angiogenesis).

Clearly, the next generation of HKPs would have been based on the targeting moiety HP-3, and the design and evaluation of such peptides is the next logical step in this research. The discovery of HP-3, and work on its properties form the basis of our substitution of work in Specific Aim 5. We made this decision not to perform detailed pharmacokinetics because research had not progressed to the extent that this made any sense, and because the study of HP-3 was very compelling, and as it turned out very productive. However, we did perform some basic preliminary toxicity studies (LD_{50}) and we discuss this work at the end of our discussion concerning the properties of HP-3.

Introduction to the Inhibition of Aminopeptidase N by HP-3 Work.

The inhibition of angiogenesis is an important target of cancer therapy because the survival, proliferation and metastasis of tumor cells require angiogenesis to supply tumor cells with oxygen and nutrition (Folkman *et al.*, 1971, Folkman *et al.*, 1995). Amino-peptidase N (APN/CD13, EC 3.4.11.2) is a type II transmembrane protein and a M1 class metalloprotease containing a Zn^{2+} binding motif, HEXXH (Bauvois *et al.*, 2006). APN is expressed in endothelial cells and is involved in angiogenesis including the neovascularization associated with tumor growth. The dysregulated expression of APN is also observed in various cancer cells, and affects tumor cell functions such as

proliferation, migration and invasion (Bauvois *et al.*, 2006). Therefore, APN plays a key role in tumor metastasis, and is a potential target for cancer therapeutic reagents.

A number of molecules, either purified from natural products, or synthesized as chemical compounds, have been reported as APN inhibitors, and show promise as anti-cancer drugs through the suppression of neovascularization (Bauvois *et al.*, 2006). In addition, APN is the target of certain drugs that have been developed to induce selective cell death in the endothelial cells that form tumor blood vessels. Indeed, the peptide CNGRC was previously identified as a tumor homing peptide (Arap *et el.*, 1998). Here we show that a dimer of the homing sequence CNGRC (HP-3) acts as a strong APN inhibitor. HP-3 inhibits purified APN activity, inhibits APN activity in living cells, and suppresses the migration, invasion, and proliferation of cells expressing APN. We also show that HP-3 inhibits tube formation in endothelial cells and the formation of capillary vessels on the chicken chorioallantoic membrane. Together, these results demonstrate the potential of HP-3, and molecules based on it, as new drugs for cancer therapy, through the inhibition of aminopeptidase N, and thereby of angiogenesis.

Methods for the Inhibition of Aminopeptidase N by HP-3.

Materials. Rat APN/CD13 purified from renal brush-border membranes was purchased from Calbiochem (La Jolla, CA). All HKP related peptides (Figure 18) were synthesized by AnaSpec (San Jose, CA) and dissolved in phosphate buffered saline (PBS). Bestatin, L-Alanine 4-methyl-coumaryl-7-amide (Ala-MCA) was purchased from Sigma (St. Lois, MO). WST-8 was purchased from Dojindo Laboratories (Kumamoto, Japan) as a cell counting kit-8. Recombinant human fibroblast growth factor-basic (bFGF) was purchased from Chemicon (Temecula, CA). All other chemicals also were purchased from Sigma or Calbiochem.

Cell Culture. Human Kaposi's sarcoma-derived cell line, KS1767, was maintained in Dulbecco's modified Eagle's medium (DMEM) supplemented 10% fetal calf serum (FCS) and penicillin/streptomycin, and cultured at 37˚C under an atmosphere of 5% CO_2. Human dermal microvascular endothelial cells (HMVEC/CADMEC^{TM}), the growth medium and other reagents for the cells were purchased from Cell Applications (San Diego, CA) and maintained following the manufacture's protocol.

Measurement of APN Activity. The APN activity was measured using a fluorogenic substrate, Ala-MCA on a 96-well black plate. APN was diluted in PBS (final conc. 1 x 10^{-3} U/ml) and was incubated with bestatin (10 μM) or NGR peptides (10-200 μM) in 0.01% BSA in PBS for 10 min on ice and 5 min at 37˚C, and then Ala-MCA (0.1 mM) warmed at 37˚C was added to the mixture. The enzymatic reaction was continued on a fluorescence plate reader (Molecular Devices, Sunnyvale, CA) at 37˚C for 15 min and then fluorescence intensity was immediately measured at the excitation and emission wavelength of 360 and 460 nm, respectively for fluorescent substrate. APN activity was also measured in intact cells. The cells were seeded on a 96-well black plate (clear bottom) and cultured overnight. After washing the cells with PBS, the cells were incubated with or without APN inhibitors for 15 min at 37˚C. The activity was then measured following the method describe above.

Cell Viability Assay. Cell proliferation and cytotoxicity assays were performed using the reagent WST-8, which estimates the intracellular dehydrogenase activity (following the manufacture's protocol). In brief, the cells were inoculated and cultured in 100 μl culture medium on a 96-well plate and then the viability was measured by adding 10 μl WST-8 to each well and cultured at 37˚C for 1h after treatment with or without HKP related peptides.

Chemomigration Assay. The migration activity of KS1767 cells was carried out using transwell cell culture inserts (8 μm polycarbonate membrane, Nunc, Rochester, NY). The inserts were placed into the wells of a 24-well plate. The cells were suspended in the inserts in serum free-DMEM supplemented with bFGF (50 ng/ml), with or without NGR peptides or bestatin, and cultured for 12 hours at 37˚C. The cells on the upper side of filters were scraped off using cotton swaps. The migrated cells on the lower surface of the filters were fixed by 80% ethanol and their nuclei were stained with propidium iodide (Sigma) and counted manually under a fluorescence microscope.

Cell Invasion Assay. The invasive activity of KS1767 cells was carried out using transwell cell culture inserts with their upper surfaces coated by Matrigel (10 μl/insert). The inserts were put into the wells of a 24-well plate. The cells were suspended in the inserts in serum free-DMEM supplied with bFGF (50 ng/ml) with or without NGR peptides, and cultured for 12 hours at 37˚C. The cells on the upper side of filters were

scraped off using cotton swaps. The invaded cells on lower surface of the filters were fixed by 80% ethanol and stained their nuclear with propidium iodide and counted by manually under a fluorescence microscope.

Tube Formation Assay. *In vitro* tube formation of endothelial cells was carried out using HMVEC cells. The cells inoculated on the surface of the Matrigel (BD Biosciences, Bedford, MA) in a 24-well plate were treated for 24 h with Bestatin or NGR peptides under the presence of bFGF. The tubular structures that formed were observed under a microscope and photographs taken.

CAM Assay. *In vivo* angiogenesis was assessed by the shell-free chicken chorioallantoic membrane (CAM) assay (Ho *et al.*, 2004). Fertilized eggs (Petaluma farms, Petaluma, CA) were kept in a humidified incubator at 37˚C for 3 days, then the shells were cracked and the eggs cultured on Ø100-mm dishes at 37˚C with 5% CO_2 in air and saturated humidity for another 3 days. Methylcellulose disks were prepared from 1% methyl cellulose (Sigma) with NGR peptides or bestatin in PBS on the plastic film, and dried under laminar flow. The disks were put on the eggs and blood vessels under the disk were observed under a microscope after 48 hours and pictures were taken.

Statistical Analysis. All data are expressed as means ± SD. The Student's *t*-test was used to establish which groups differed from the control group. A *p* value of less than 0.05 was considered statistically significant.

Results for the Inhibition of Aminopeptidase N by HP-3.

HP-3 Inhibits Purified APN. Previously, we showed that HKP1 bound to APN, was thereby internalized into targeted endothelial cells, where HKP1 disrupted mitochondrial membranes, reducing or inhibiting angiogenesis *in vitro* and *in vivo* (Ellerby *et al.*, 1999). It was logical then to question whether or not HKP1, and related peptides (Figure 18), such as HP-3, could inhibit the enzymatic activity of APN.

Purified rat APN was incubated with Bestatin, a classic APN inhibitor, and five peptides related to HKPs (Figure 18), and the proteolytic activity of APN was measured using a synthetic fluorogenic peptide as a substrate. The concentrations of these peptides were adjusted by the amounts of NGR targeting sequence, that is, a mole of the dimers corresponded to two moles of the monomers.

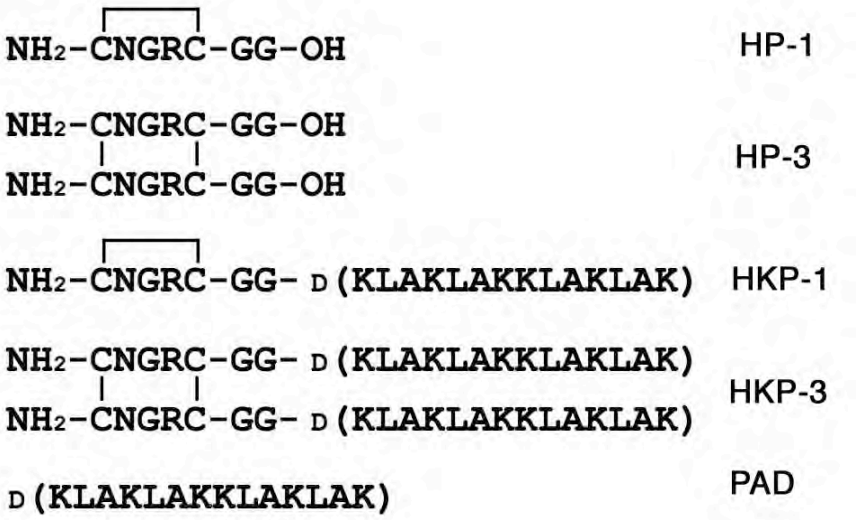

Figure 18. The Structure of HP-3 and Related Peptides. NGR monomer (HP-1) and HKP1 have a single disulfide bond between Cys^1 and Cys^5. NGR dimer (HP-3) and HKP-3 consist of two molecules of HP-1 or HKP1, which are linked by two disulfide bonds Cys^1-Cys^1 and Cys^5-Cys^5, respectively. All pro-apoptotic domains (PAD) are composed of D-amino acids.

Bestatin showed the strongest inhibition as previously reported. Surprisingly, among all HKP related peptides tested, only HP-3 strongly inhibited the APN activity in a dose dependent manner. HKP1 and HKP-3showed only weak inhibition at high concentrations, while HP-1 and pro-apoptotic domain (PAD) did not inhibit APN activity (Figure 19). From the inhibition curve, the IC_{50} value of HP-3 for APN was 35 μM (Figure 20A). HP-3 showed APN inhibition more than twice that of HP-1. And although the IC_{50} values for bestatin inhibition of APN vary in the literature, here we calculated an IC_{50} value of 3.5 μM for bestatin.

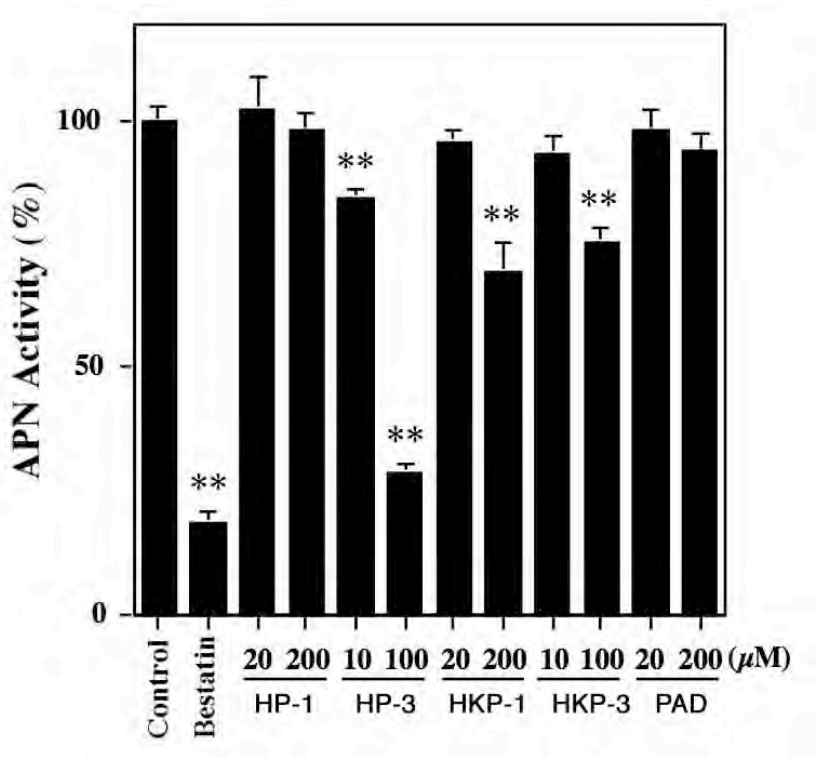

Figure 19. Inhibition of APN by HP-3 and Related Peptides. Purified rat APN was incubated with bestatin, HP-3, and related peptides, and then APN activity was measured using a fluorogenic substrate, Ala-MCA. Activities are shown as the percentage of control (PBS). The results show mean ± SD of five independent experiments. $^{**}p < 0.01$ versus control.

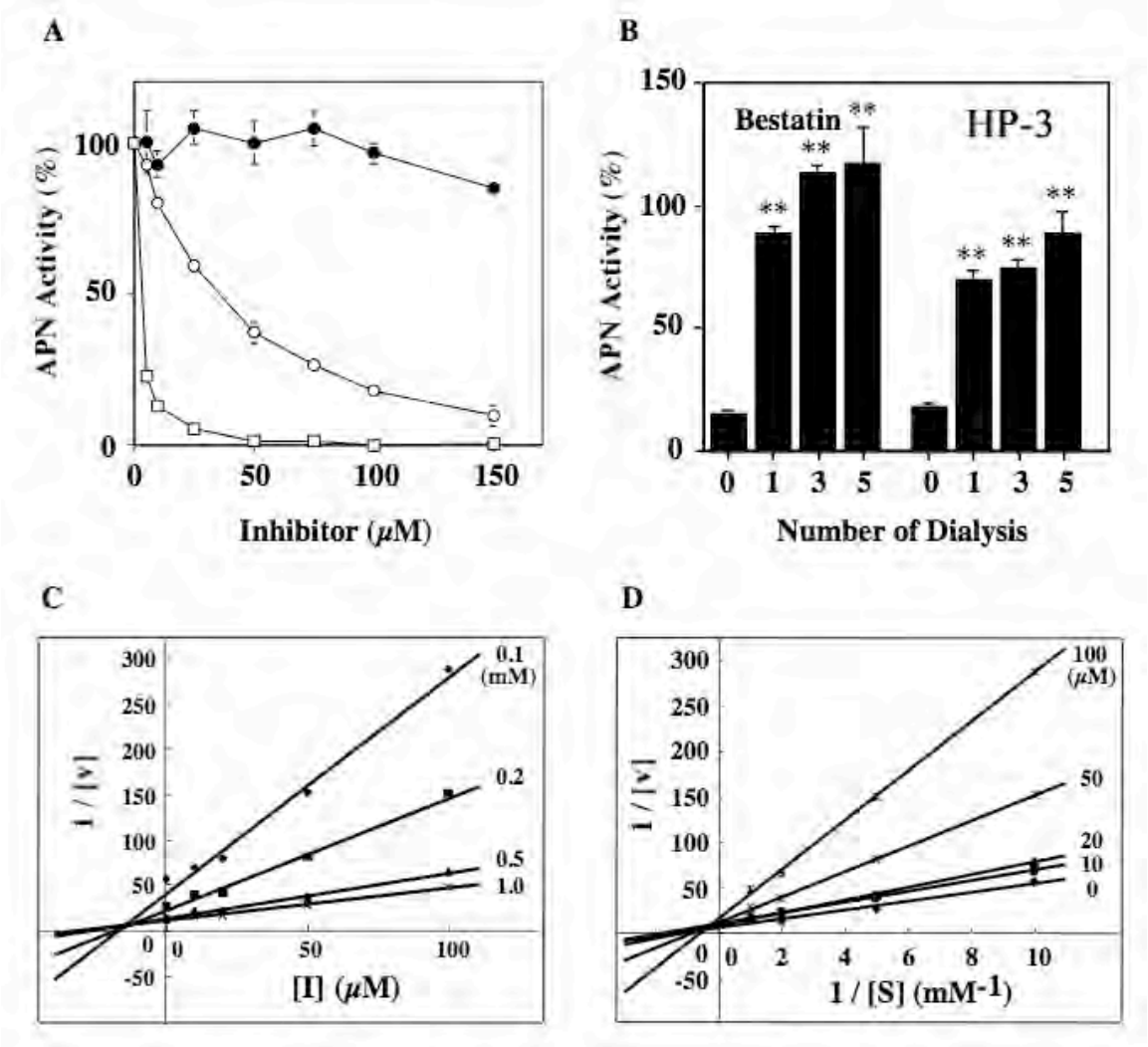

Figure 20. The Effects of HP-3 on APN Activity. Purified rat APN was used for the analysis of the dose dependence, the reversibility, and the kinetic of the enzyme inhibition. (A) Purified rat APN activity was measured after incubation with various concentrations of HP-1 (●), HP-3 (❍), and bestatin (□). From the inhibition curve, the IC_{50} value of HP-3 was 35 μM and bestatin was 3.5 μM. (B) Reversibility was estimated by measuring the residual enzyme activities after filtration through an YM-30 unit. The activities were recovered by filtration cycles. (C, D) The kinetics was determined by Dixon plot (C) and Lineweaver-Burk plot (D). These results show that APN inhibition by HP-3 was reversible and competitive with a Ki value of 14.4 μM. The results show mean ± SD of three independent experiments. $^{**}p < 0.01$ versus control.

Mechanism of APN Inhibition by HP-3. In order to further investigate the inhibition of APN by HP-3, rat APN was incubated with or without bestatin or HP-3 at 4˚C and residual enzymatic activity was measured as an initial value. Each reaction solution was then put on a Microcon YM-30 filter unit (Millipore, Bedford, MA) and centrifuged for 10 min at 14,000 x g. The activities were measured for the retained solution on the filter unit after resuspension in the PBS to the volume before centrifugation. The reactions were further applied to the filter unit and repeated centrifuge and measurement of the activity. The APN activity was then recovered by a cycle of filter dialysis (Figure 20B), thus demonstrating that the inhibition of APN by HP-3 was reversible. Kinetic analysis of the inhibition of HP-3 using a Dixon plot, showed the Ki value to be 14.4 μM (Figure 20C). Analysis by a Lineweaver-Burk plot, showed no effect on the V_{max}^{-1} value of APN, demonstrating that HP-3 is a competitive inhibitor for APN (Figure 20D). Thus, we determined that HP-3 is a reversible and non-classical competitive inhibitor of APN.

HP-3 Inhibits APN in Living Cells. The inhibition of APN activity was also measured in living cultured cells, using the Kaposi's sarcoma cell line, KS1767. We confirmed the expression of human APN by the KS1767 cells using western blot and RT-PCR (data not shown). The KS1767 cells were incubated with bestatin and HKP-related peptides, and the APN activity was measured using the synthesized substrate. HP-3 also inhibited APN in culture in a concentration dependent manner, but the inhibition levels were lower than that found with purified rat APN (50% on the KS 1767 cells at 100 μM) (Figure 21).

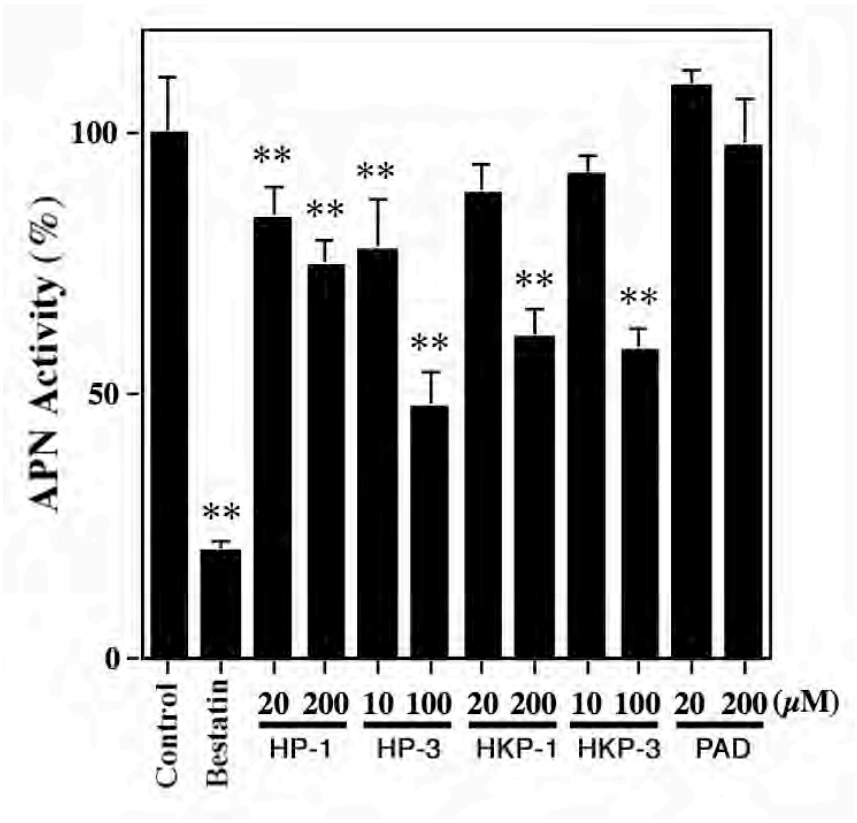

Figure 21. Inhibition of APN Activity in Living Cells. APN positive human Kaposi's sarcoma cell line, KS1767, was used for measuring the inhibition of APN activity, which was measured using the fluorogenic substrate, Ala-MCA. Activities are shown as the percentage of control reaction. The results show the mean ± SD of five independent experiments. $^{**}p < 0.01$ versus control.

Bestatin inhibited APN in living cells as strongly as that found with purified rat APN. HKP1 and HKP-3also inhibited APN activity in cultured cells, although they only weakly inhibited purified rat APN. HP-3 and bestatin also inhibited mouse APN activity in HEK 293T cells stably expressing mouse APN (data not shown).

HP-3 Inhibits Proliferation, Migration and Invasion of Kaposi's Sarcoma Cells. Beyond the inhibition of APN enzymatic activity by HP-3, we investigated the inhibition of proliferation, migration and invasion of KS1767 cells.

We began by considering the effect of the NGR peptides, proliferation. KS1767 cells were seeded low density (10-20% of confluence) and cultured with HP-1, HP-3 or bestatin for 3 days, and then the cell number were estimated by intracellular

dehydrogenase activities using WST-8. Surprisingly, the results were contrary to the enzyme inhibition. While bestatin had no statistically significant effects on proliferation, both HP-1 and HP-3 demonstrated a dramatic effect on proliferation (Figure 22A).

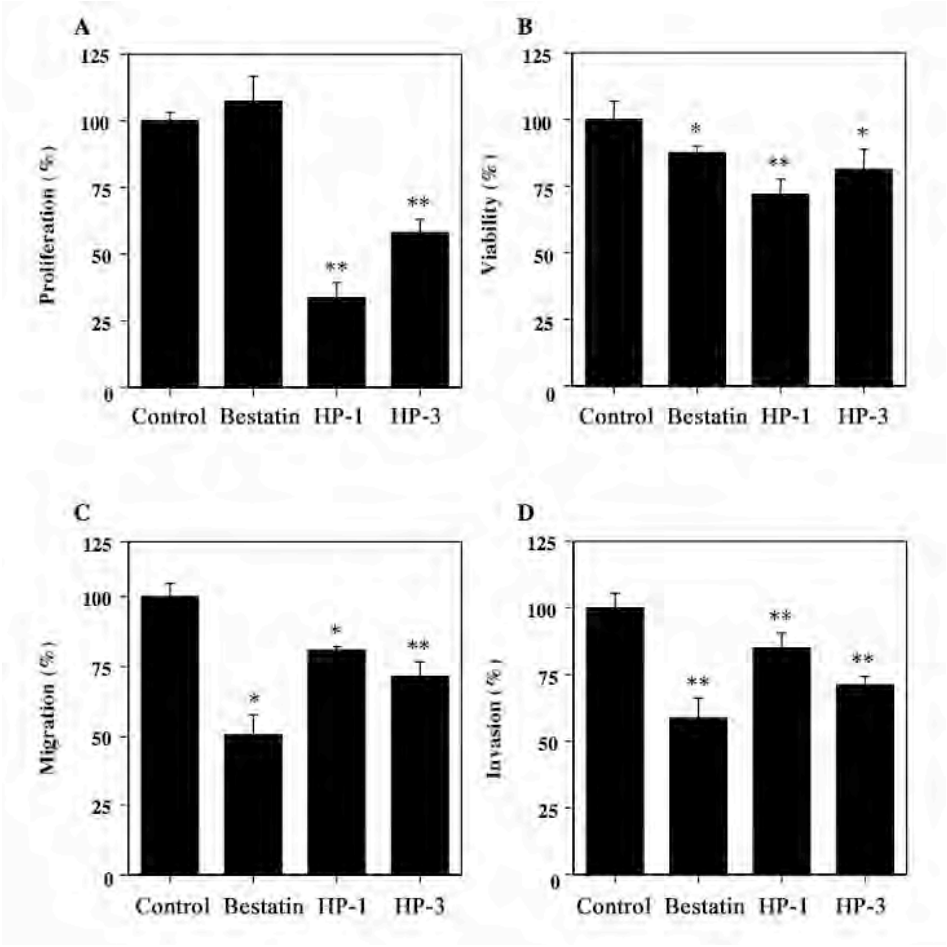

Figure 22. HP-3 Inhibits Proliferation, Migration and Invasion. Inhibition of APN acitvity in the Kaposi's sarcoma (KS) cell line inhibits various cellular activities by bestatin (10 μM), HP-1 (200 μM), and HP-3 (100 μM). Cell proliferation and viability were measured using WST-8. Cell proliferation was arrested by HP-3 and HP-1, but not by bestatin (A). The peptides also affected viability of cells (B). KS cells were put on culture inserts (8.0 μm pore size) with bFGF and Matrigel was used to coat cell inserts for the invasion assay. Migrated and invaded cells were counted under fluorescence microscopy after ethanol fixing and PI staining. The inhibitors suppressed the migration (C) and invasion (D) of the KS1767 cells. The results show mean ± SD of three independent experiments at least. *$p < 0.05$, **$p < 0.01$ versus control.

We also estimated the cytotoxicity of these inhibitors in cell viability assays. The KS1767 cells were seeded and cultured by the confluent state. The cells were exposed to the inhibitors for 24 hours, and then cell viability was assessed by WST-8 (Figure 22B). Both HP-3, and especially HP-1, reduced viability of KS1767 cells.

We next evaluated the possible effect of the NGR peptides on migration and invasion of KS1767 cells. KS1767 cells demonstrated clear migration and invasion activity in the presence of bFGF. KS1767 cells were incubated with or without the NGR peptides or bestatin and then the cells were evaluated in invasion and migration assays (Figure 22C and 22D). The HP-3 showed strong inhibition of both migration (reduced to 72%) and invasion (reduced to 71.1%). The bestatin was the strongest among these APN inhibitors, limiting migration to 50.4% and invasion to 58.5% respectively. These results were congruent with the enzymatic inhibition behavior of these inhibitors.

HP-3 Inhibits Tube formation and Angiogenesis. To determine whether NGR peptides would affect angiogenesis, we tested the effect of the peptides *in vitro* and *in vivo*. First, we evaluated the effects of the NGR peptides during the differentiation of HMVEC into capillary-like structures. HMVECs form cord-like structures on Matrigel in the presence of bFGF. NGR peptides (200 μM HP-1 or 100 μM HP-3) or bestatin (10 μM) disturbed the network formation (Figure 23).

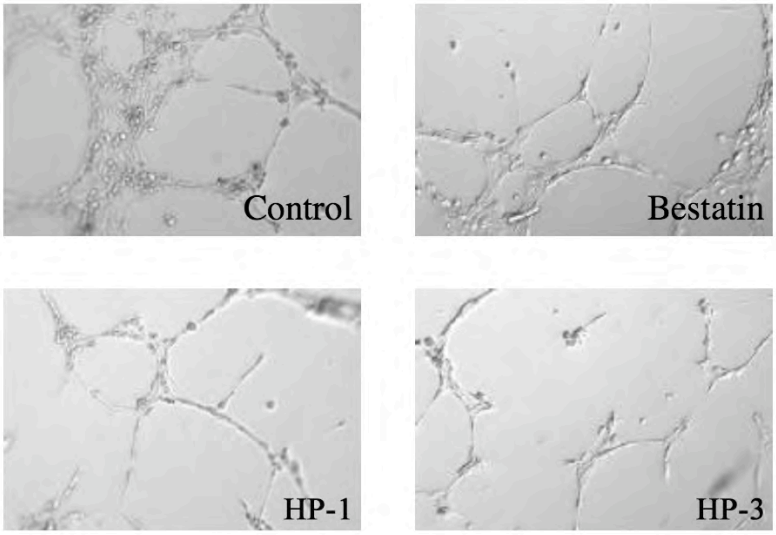

Figure 23. HP-3 Inhibits Tube formation. Human dermal endothelial cells were cultured with bFGF and control (PBS); bestatin (10 μM), HP-1 (200 μM), and HP-3 (100 μM) on Matrigel. APN inhibitors disturbed HMVEC cord formation.

Cytotoxicities of HMVEC by these inhibitors were not observed, as confirmed by the WST-8 assay (Data not shown). We next estimated the effect of the inhibitors on angiogenesis using the chicken chorioallantoic membrane (CAM) assay. The results clearly demonstrate that the NGR peptides and bestatin inhibited the development of capillary vessels (Figure 24).

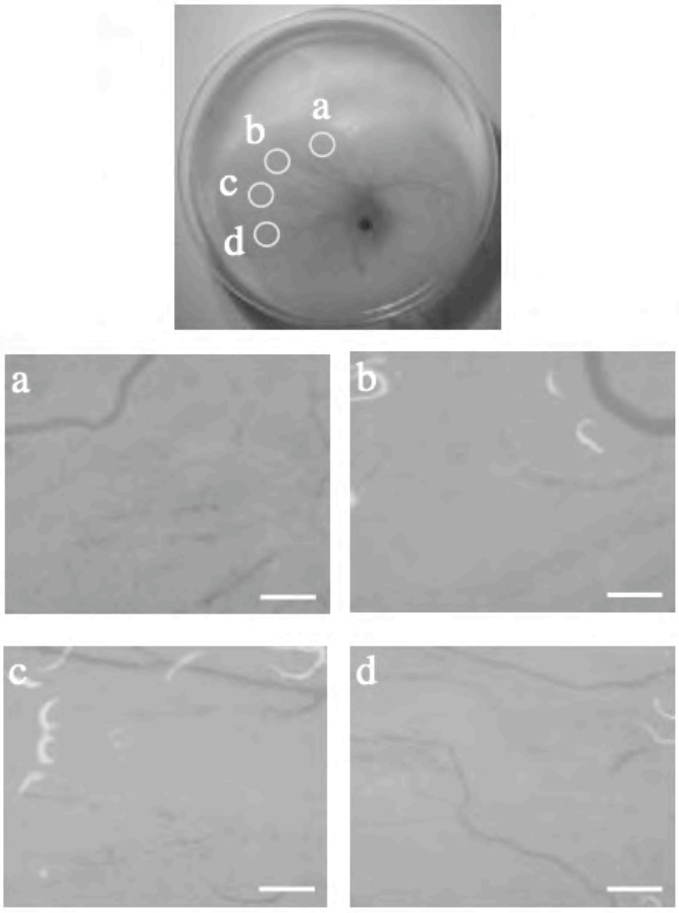

Figure 24. HP-3 Inhibits CAM Angiogenesis. Fertilized eggs were used for shell-free CAM assays. Whole eggs were cultured in 10-cm dishes (Top). Methylcellulose disks containing PBS (a), bestatin (b), HP-1 (c), and HP-3 (d) were placed on the CAM. Angiogenesis on the CAM was prevented under the disks containing APN inhibitors. (a-d) the original magnifications were x 3. Scale bars = 0.5 mm.

Conclusion for the Inhibition of Aminopeptidase N by HP-3.

Here we demonstrated the promise of the peptide HP-3 as a potential therapeutic anti-cancer drug, or as the structural basis for such a drug. Previously, the peptide CNGRC was found to target the endothelial cells that form tumor blood vessels (Arap *et al*., 1998), while not targeting the endothelial cells that form normal blood vessels (Curnis *et al*., 2002). Subsequent to this discovery, we (and others) developed CNGRC as a targeting moiety for cancer treatment (Ellerby *et al*., 1999, Curnis *et al*., 2000), cancer

cell imaging (Zhang *et al*., 2005) and also cardiac angiogenesis imaging (Buehler *et al*., 2006) utilizing the specificity of APN binding on endothelial cells and tumor cells.

Indeed central to our recent work has been the development of HKPs, of which HKP1 was the first prototype (Ellerby *et al.*, 1999). These small, dual-purpose molecules specifically hunt and attack the blood supply of tumors, through the elimination of the endothelial cells that form tumor blood vessels. We (and others) have also applied our technology to arthritis (Gerlag *et al.*, 2001), organ reduction (Arap *et al.*, 2002), and obesity (Kolonin *et al.*, 2006).

One of the strengths of our approach has been the fact that various "targeting" domains can be combined with various "killing" domains, such that we have really invented a new pharmacology, and not just a single drug. In the process of drug development, it was natural for us to begin to investigate, not just the binding and internalization properties of our drugs, but also the potential that we might be inhibiting the enzymatic activity of APN synergistically. This led us to the present study.

Various APN inhibitors have been reported and these are also known to suppress angiogenesis (Bauvois *et al*., 2006), even though the mechanism and relationship between the inhibition of APN and the suppression of angiogenesis is still unknown. We found here that the HP-3 peptide inhibits APN activity in a reversible and competitive manner. The "gold standard" aminopeptidase N inhibitor bestatin inhibits APN with similar pharmacodynamics.

In agreement with the crystal structure of bacterial zinc-aminopeptidase, shows that bestatin binds to the active site pocket of APN (Addlagatta *et al*., 2006; Ito *et al*., 2006; Kyrieleis *et al*., 2005; Di Matteo *et al*., 2006). In contrast, CNGRC peptides have been predicted to bind to $W^N/_D$DLWLN (Pasqualini *et al*., 2002) and not in the active site pocket (Kyrieleis *et al*., 2005) — the HEXXH sequence, the Zn^{2+} binding motif of the active site of metalloproteases, such as APN (Pasqualini *et al*., 2002) — responsible for enzymatic activity. However, $W^N/_D$DLWLN and HEXXH are in close approximation to each other, and we deduce this is the reason why the HP-3 inhibits APN activity stronger than HP-1. The conformation of the monomer peptide is dependent on the loop structure formed by the disulfide bond joining the Cys residues of CNGRC (Ellerby *et al*., 1999), and this structure is very important for binding to APN (Di Matteo *et al*., 2006; Colombo

et al., 2002; Majhen *et al*., 2006). The loop of HP-1 may not be large enough to disturb the binding of the substrates to enzymatic binding site of APN. On the other hand, HP-3 is linked by two disulfide bonds between two HP-1 on Cys^1 and Cys^5, respectively. Although we do not know the exact structure of HP-3 at this time, it is possible that the more open structure disturbs the access of substrates to APN.

In this work we showed that HP-3 inhibited the enzymatic activity of purified APN. HP-3 also inhibited the APN on living cells, but somewhat less than with the purified enzyme. However HP-3 also had an effect on KS1767 cell proliferation, migration, and invasion.

The inhibitions by the NGR peptides, except for proliferation, seem to depend on the inhibition of APN activity, because these are in proportion to the degree of the inhibition of the enzyme activities by inhibitors. On the other hand, other mechanisms would seem to exist for the inhibition of proliferation because HP-1 shows stronger inhibition than bestatin and HP-3. Furthermore, although bestatin inhibited proliferation only weakly, it strongly inhibited purified APN activity.

Even though the mechanisms of inhibition of Kaposi's sarcoma cell proliferation by HP-1 are unclear, the combination of both NGR peptides may show synergistic effects to angiogenesis and the tumor cell activities. Because the KS1767 cells have both properties of endothelial cells (Samaniego *et al*., 1998) and neoplastic, the peptides would be expected to inhibit the metastasis of sarcoma and other APN-positive tumor cells.

Indeed, the other APN inhibitors, curcumin and BE15, inhibits APN-positive tumor cell invasion (Shim *et al*., 2003; Saitoh *et al*., 2006). The peptides also inhibit angiogenesis in proportion to the degree of the APN inhibition. The inhibitions of tube formation of HMVEC by the peptides show the possibility of the inhibition of forming the capillary vessels around the tumor cells. Furthermore, the peptides inhibit formation of the capillary vessels on CAM assay. Therefore we have shown the inhibition of *in vivo* angiogenesis during chicken embryo development, providing further evidence that the peptides would be expected to suppress tumor angiogenesis.

The inhibition of tumor angiogenesis is a major strategy in cancer therapy (Folkman *et al*., 1971; Folkman *et al*., 2005). The NGR monomer and dimer peptides

target the endothelial cells undergoing tumor neovascularization and suppress angiogenesis through the inhibition of APN activity but not through the induction of endothelial cell death. As a result, the peptides are expected to reduce the tumor volume and metastasis without the side effects associated with potentially more toxic related peptides/drugs.

In conclusion, HP-3 inhibits APN activity and affects angiogenesis, and may offer the possibility that it will reduce the expansion of tumor volume, metastasis, and tumor angiogenesis *in vivo*. From these results it is clear that further development of HP-3 as a stand alone therapeutic or as the basis for a therapeutic is warranted, and may lead to new drug candidates for cancer therapy.

Results for the *In Vivo* Toxicity studies.

While we could not perform a complete pharmacokinetic analysis, we did perform basic pharmacokinetic/toxicity experiments on HKP-1, HKP-2, and HKP-3. Specifically, we determined the LD_{50} for these peptides in nude mice. Previously, for HKP-1 and HKP-2 the dose of 250 μg was determined by performing a pilot test on only 2 mice per group for HKP-1, with the doses of 1000 μg and 250 μg. All the mice died at the dose of 1000 μg and since they survived at 250 μg that was the dose that was originally used (Ellerby *et al.*, 1999). We determined in our laboratory by using 10 mice per group that the LD_{50} for HKP-1, HKP-2 and HKP-3 was approximately 500 μg. Furthermore, we performed a preliminary gross histology examination of 10 mice given 2 injections of HKP-1, spaced one week apart. No observable gross pathology was evident in the kidneys, liver, heart, and lungs of the mice.

Key Research Accomplishments

- Determined that HKP-2 inhibited metastasis in the TRAMP model of prostate cancer, when given as either an IP or IV injection (see **Task 1**).

- Determined that HKP-2 demonstrated a trend toward increased survival in the TRAMP model of prostate cancer (see **Task 1**).

- Determined that a single weekly injection (rather than 2x week) was optimal for HKP-2 in the TRAMP model of prostate cancer (see **Task 1**).

- Designed 6 new peptides (see **Task 2**).

- Determined that the therapeutic indices of HKP-1 and HP-1 for PC-3 prostate carcinoma cells were similar to that of other cell types (see **Task 3**).

- Determined that the therapeutic indices of HKP-2 for PC-3 prostate carcinoma cells were similar to that of other cell types (see **Task 3**).

- Determined the therapeutic indices of HP-3 and HKP-3 (the dimer peptides) for PC-3 prostate carcinoma cells (and other cells). We found that the therapeutic index of HKP-3 was significantly better than that of HKP-1 (factor of 5) and somewhat better even than HKP-2 (see **Task 3**).

- Determined that the therapeutic indices of KP-4 and HKP-4 for PC-3 prostate carcinoma (and that of other cell types) were far superior to HKP-1 and HKP-2 (see **Task 3**).

- Determined that the therapeutic indices of KP-5 for PC-3 prostate carcinoma cells were similar to that of other cell types, showing a preference of cancer cells over normal cells by a factor or 2-4 (see **Task 3**).

- Determined that the therapeutic indices of KP-6 and HKP-6 for PC-3 prostate carcinoma cells (and other cell types) (see **Task 3**).

- Determined that KP-5 inhibited tumor growth as measured by tumor volume in a PC-3 prostate carcinoma xenograft model (by a factor of 5-fold in volume) (see **Task 4**).

- Determined that KP-5 incresed survival in a PC-3 prostate carcinoma xenograft model (see **Task 4**).

- While debugging our problem with peptide, we determined that the dimeric HKP-3 was more effective than the monomeric HKP-1 in *in vito* cytotoxicity assays (see **Task 5**).

- While debugging our problem with peptide, determined that the therapeutic effect of HKP-3 was similar to that of Abraxane, and that both together has a synergetic effect in the 435 xenograft model of human breast carcinoma (see **Task 5**).

- Determined that HP-3 (the dimeric targeting peptide) inhibited purified amino-peptidase N in *in vitro* assays (see **Task 5**).

- Determined that HP-3 (the dimeric targeting peptide) inhibited amino-peptidase N in *in vitro* cell culture assays (see **Task 5**).

- Determined that HP-3 (the dimeric targeting peptide) inhibited cell proliferation *in vitro* assays (see **Task 5**).

- Determined that HP-3 (the dimeric targeting peptide) inhibited migration in *in vitro* assays (see **Task 5**).

- Determined that HP-3 (the dimeric targeting peptide) inhibited invasion in *in vitro* assays (see **Task 5**).

- Determined that HP-3 (the dimeric targeting peptide) inhibited tube formation in *in vitro* assays (see **Task 5**).

- Determined that HP-3 (the dimeric targeting peptide) inhibited angiogenesis in the CAM *in vitro* assay (see **Task 5**).

- Determined that HKP-1, HKP-2 and HKP-3 all had approximately the same LD_{50} (500μg) in preliminary pharmacokinetic/toxicology studies (see **Task 5**).

- Determined that HKP-1 did not induce any gross pathological changes in the heart, liver, lung, and kidney of nude mice in preliminary pharmacokinetic /toxicology studies (see **Task 5**).

Reportable Outcomes

Papers, manuscripts, abstracts, presentations

- Ellerby HM, Lee S, Ellerby LM, Chen S, Kiyota T, del Rio G, Sugihara G, Sun Y, Bredesen DE, Arap W, Pasqualini R. An artificially designed pore-forming protein with anti-tumor effects. *J Biol Chem* 278: 35311-6, 2003.

- Satoshi Fujimura, Rebeccah R. Riley, Sylvia F. Chen, Lisa M. Ellerby, and H. Michael Ellerby. A Dimer of the Tumor-Targeting Peptide CNGRC Inhibits Aminopeptidase N. Submitted 2008.

- Satoshi Fujimura, Rebeccah R. Riley, Sylvia F. Chen, Lisa M. Ellerby, and H. Michael Ellerby. Hunter-Killer Peptide Inhibits Metastasis in the TRAMP Model of Prostate Cancer. In Preparation 2008.

- **A *de novo* Designed Protein with Anti-Tumor Effects.** H. Michael Ellerby, Sannamu Lee, Rebecca Andrusiak, Lisa M. Ellerby, Sylvia F. Chen, Taira Kiyota, Gabriel del Rio, Gohsuke Sugihara, Yan Sun, Dale Bredesen, Wadih Arap, Renata Pasqualini. Buck Institute, Novato, CA; Fukuoka University, Fukuoka, Japan; The Burnham Institute, La Jolla, CA; University of Texas, M.D. Anderson Cancer Center, Houston, TX. Presentation at 94th AACR Annual Meeting, April 2003.

- **Abraxane (ABI-007) Acts Synergistically with the Antiangiogenic Agents Avastin and Novel CD-13 Targeted Pro-Apoptotic Peptides (HKP).** Rebeccah Riley, Satoshi Fujimora, Sophia Ran, Vuong Trieu, Neil Desai, Patrick Soon-Shiong, Cristina Sandoval, Leigh Plesniak, Dale E. Bredesen, Sylvia Chen, Lisa M. Ellerby, H. Michael Ellerby, Sophia Ran, Neil Desai, Cristina Sandoval, Dale E. Bredesen. Presentation at 96th AACR Annual Meeting, Anaheim, CA, April 2005.

Patents and licenses applied for and/or issued

- Patent Number for "SGP (KP-5) as an Anti-tumor Agent." 2007 US 10/846,479. Application available form Buck Institute.
- Patent Number for "The Anti-Angiogenic Effects of a Dimer of a Hunter-Killer Peptide". (HKP-3) 2005 Intl. PCT/US 2005/010951. Application available form Buck Institute.

Degrees obtained that are supported by this award
None.

Development of cell lines, tissue or serum repositories
None.

Informatics such as databases and animal models, etc
None

Funding applied for based on work supported by this award
None.

Employment or research opportunities applied for and/or received on experiences/training supported by this award
None.

Conclusion

As described in Ellerby *et al*. 1999, we designed short peptides, Hunter Killer Peptides (HKP), composed of two functional domains, one a tumor blood vessel 'homing' motif and the other a programmed cell death-inducing sequence, and synthesized them by simple chemistry. The 'homing' domain was designed to guide the peptide to targeted cells and allow internalization. The pro-apoptotic domain was designed to be non-toxic outside cells, but toxic when internalized into targeted cells by the disruption of mitochondrial membranes. We demonstrated in Ellerby *et al*. 1999, that HKPs show strong anti-cancer activity in mice (xenografts of human breast carcinomas and melanomas). We also reported in Arap *et al.*, 2002, that HKPs delayed the development of the cancers in prostate cancer-prone transgenic mice (TRAMP mice).

In the work described in this report, performed under DAMD17-01-1-0029, we worked on a comprehensive development program for Hunter-Killer Peptides. The scope of this program allowed us to adapt to potential problems, and indeed we encountered a problem with our original HKP-1, as described in the body of this report. However, in the process of working on this problem we were led to invent a new targeting peptide (HP-3), the dimeric form of HP-1, and determine that it acted through a dual mechanism: the binding to aminopeptidase N (facilitating the internalization of HKPs), and through a separate binding site, the potent inhibition of aminopeptidase N enzymatic activity, both *in vitro* and in cell culture models of angiogenesis. Thus HP-3 synergistically acts through two separate anti-angiogenic mechanisms. The manuscript describing this work is included in the Appendix (Fujimura *et al.*, 2008).

In addition to this peptide we also designed and evaluated other peptides both *in vitro*, and in the case of KP-5 *in vivo* in the PC-3 xenograft model of prostate cancer. Although we were unable to determine with certainly the nature of the problem we were experiencing with HKP-1, in the process of working on the problem, we determined that a hunter-killer peptide based on HP-3, HKP-3, was more effective than HKP-1 in *in vitro* assays. Based on this we completed a test evaluation of HKP-3 in the 435-breast carcinoma xenograft model, and determined that it was as about effective as Abraxane in increasing survival, and when taken together as a combined therapy HKP-3 and Abraxane were even more effective. Although this work was not performed in a prostate

model, this work was completed as part of the process of investigating the problem we had with HP-1 and the results clearly advanced our research and since this form of our therapy is a general anti-angiogenic therapy has immediate application to prostate cancer as well. The unique properties of another of our new peptides, KP-5, led us to evaluate its efficacy in a mouse model of prostate cancer. KP-5 demonstrated the ability to directly lyse tumor cells themselves, without being proteolytically degraded before this could occur. Thus we did not need to target KP-5, as it could be directly injected into tumors. This fact precluded us from using the TRAMP model, as no single primary tumor arises in this model. Thus we evaluated KP-5 in the PC-3 prostate xenograft model in nude mice. Our results indicate that KP-5 limits tumor growth and extends survival as well This work was published as the cover article in Ellerby *et al.*, 2003.

As we were working on the problem associated with HKP-1, we proceeded to evaluate HKP-2 in the TRAMP model. We chose HKP-2 for these experiments because the targeting part of the peptide is not based on CNGRC, but rather is an RGD-based peptide. We considered two separate concentrations and two methods of drug delivery (IV and IP). The results indicated that HKP-2 could inhibit metastasis and also the data showed a trend toward an increase in survival, although this latter effect was clearly not as strong as with HKP-2 in the xenograft models that it was tested in previously. This may reflect a difference in the kinetics between the TRAMP and xenograft models. This work forms the basis of a manuscript in preparation.

"So What Section." The real power of our approach lies in the fact that we are not restricted to a particular peptide, or formulation. Indeed, in this work on the comprehensive development program of our peptides, the built-in flexibility of our basic designs allowed us to work around any problems encountered, to work toward a natural evolution of our therapy to become as effective as possible. The most significant, and practical results of this work were the discovery of a completely novel targeting peptide HP-3, that then could form the basis of a new therapeutic HKP-3 (and future therapeutics), the successful application of HKP-2 to the TRAMP model of prostate cancer, the successful application of KP-5 to the PC-3 xenograft model of prostate cancer, and that our approach can compete with and act synergistically with other anticancer agents such as Abraxane. Based on these critical discoveries we can now

proceed to design and evaluate the next generation of our peptides. Such designs include third generation formulations such as nanospherical particles, coated with tethered HP-3 as a targeting strategy, and encapsulating KP-5. Such designs should decrease nonspecific toxicity associated with killer domains, and allow for many thousands of drug molecules to be internalized all at once with a single receptor interaction. Summarizing the work, we have designed new and successful HKPs, and have successfully evaluated their therapeutic potency in prostate xenografts and in the TRAMP model of prostate cancer. Future work involves the continued development optimization our novel class of anticancer therapeutics, with the ultimate goal of creating a practical therapeutic product for the treatment of prostate cancer.

References

Addlagatta, A., Gay, L., and Matthews, B. W. Structure of aminopeptidase N from Escherichia coli suggests a compartmentalized, gated active site. Proc Natl Acad Sci U S A, 103: 13339-13344, 2006.

Arap W, Pasqualini R, & Ruoslahti E. Cancer treatment by targeted drug delivery to tumor vasculature in a mouse model. *Science* **279**:377-380 (1998).

Arap W, Haedicke W, Bernasconi M, Kain R, Rajotte D, Krajewski S, Ellerby HM, Bredesen DE, Pasqualini R, Ruoslahti E (2002). Targeting the prostate for destruction through a vascular address. *PNAS* 99(3):1527-31.

Bauvois, B. and Dauzonne, D. Aminopeptidase-N/CD13 (EC 3.4.11.2) inhibitors: chemistry, biological evaluations, and therapeutic prospects. Med Res Rev, 26: 88-130, 2006.

Buehler, A., van Zandvoort, M. A., Stelt, B. J., Hackeng, T. M., Schrans-Stassen, B. H., Bennaghmouch, A., Hofstra, L., Cleutjens, J. P., Duijvestijn, A., Smeets, M. B., de Kleijn, D. P., Post, M. J., and de Muinck, E. D. cNGR: a novel homing sequence for CD13/APN targeted molecular imaging of murine cardiac angiogenesis in vivo. Arterioscler Thromb Vasc Biol, 26: 2681-2687, 2006.

Colombo, G., Curnis, F., De Mori, G. M., Gasparri, A., Longoni, C., Sacchi, A., Longhi, R., and Corti, A. Structure-activity relationships of linear and cyclic peptides containing the NGR tumor-homing motif. J Biol Chem, 277: 47891-47897, 2002.

Curnis, F., Sacchi, A., Borgna, L., Magni, F., Gasparri, A., and Corti, A. Enhancement of tumor necrosis factor alpha antitumor immunotherapeutic properties by targeted delivery to aminopeptidase N (CD13). Nat Biotechnol, 18: 1185-1190, 2000.

Curnis, F., Arrigoni, G., Sacchi, A., Fischetti, L., Arap, W., Pasqualini, R., and Corti, A. Differential binding of drugs containing the NGR motif to CD13 isoforms in tumor vessels, epithelia, and myeloid cells. Cancer Res, 62: 867-874, 2002.

del Rio G, Castro-Obregon S, Rao R, Ellerby HM, Bredesen DE (2001). APAP, a sequence- pattern recognition approach identifies substance P as a potential apoptotic peptide. *FEBS Lett.* 494(3):213-9.

Di Matteo, P., Curnis, F., Longhi, R., Colombo, G., Sacchi, A., Crippa, L., Protti, M. P., Ponzoni, M., Toma, S., and Corti, A. Immunogenic and structural properties of the Asn-Gly-Arg (NGR) tumor neovasculature-homing motif. Mol Immunol, 43: 1509-1518, 2006.

Ellerby HM, Martin SJ, Ellerby LM, Naiem SS, Rabizadeh S, Salvesen GS, Casiano CA, Cashman NR, Green DR, Bredesen DE. Establishment of a cell-free system of neuronal apoptosis: comparison of premitochondrial, mitochondrial, and postmitochondrial phases. *J Neurosci* 17: 6165-78, 1997

Ellerby HM, Arap W, Ellerby LM, Kain R, Andrusiak R, Del Rio G, Krajewski S, Lombardo CR, Rao R, Ruoslahti E, Bredesen DE, Pasqualini R (1999). Anti-cancer activity of targeted pro-apoptopic peptides. *Nature Medicine* 5(9):1032-1038.

Ellerby HM, Lee S, Andrusiak R, Ellerby LM, Chen S, Kiyota T, del Rio G, Sugihara G, Arap W, Bredesen DE & Pasqualini R (2003). An artificially designed pore-forming protein with anti-tumor effects. *J. Biol. Chem.* 278, 35311-35316.

Folkman, J. Tumor angiogenesis: therapeutic implications. N Engl J Med, 285: 1182-1186, 1971.

Folkman, J. Seminars in Medicine of the Beth Israel Hospital, Boston. Clinical applications of research on angiogenesis. N Engl J Med, 333: 1757-1763, 1995.

Fujimura S, Riley R, Chen S, Ellerby L, and Ellerby, HM. "A Dimer of the Tumor-Targeting Peptide CNGRC Inhibits Aminopeptidase N." in review, 2008.

Furuya T, Kiyota T, Lee S, Inoue T, Sugihara G, Logvinova A, Goldsmith P, Ellerby HM. Nanotubules formed by highly hydrophobic amphiphilic alpha-helical peptides and natural phospholipids. *Biophys J* 84: 1950-9, 2003

Gerlag, D. M., Borges, E., Tak, P. P., Ellerby, H. M., Bredesen, D. E., Pasqualini, R., Ruoslahti, E., and Firestein, G. S. Suppression of murine collagen-induced arthritis by targeted apoptosis of synovial neovasculature. Arthritis Res, 3: 357-361, 2001.

Gingrich, J. R. Barrios, R. J., Morton, R. A., Boyce, B. F., DeMayo, F. J., Finegold, M. J., Angelopoulou, R., Rosen, J. M. & Greenberg, N. M. (1996) Cancer Res. 56,4096-4102.

Ho, P. Y., Liang, Y. C., Ho, Y. S., Chen, C. T., and Lee, W. S. Inhibition of human vascular endothelial cells proliferation by terbinafine. Int J Cancer, 111: 51-59, 2004.

Hsu, C. S., Ross, B. D., Chrisp, C. E., Derrowm S. Z., Charles, L. G., Pienta, K. J., Greenberg, N. M., Zeng, Z. & Sandor, M. G. (1998) 1. Urol. 160, 1500-1505.

Ishii *et al.* Biol Pharm Bull. 24(3):226-30 (2001).

Ito, K., Nakajima, Y., Onohara, Y., Takeo, M., Nakashima, K., Matsubara, F., Ito, T., and Yoshimoto, T. Crystal structure of aminopeptidase N (proteobacteria alanyl aminopeptidase) from Escherichia coli and conformational change of methionine 260 involved in substrate recognition. J Biol Chem, 281: 33664-33676, 2006

Javadpour M, Juban M, Lo W, Bishop S, Alberty J, Cowell S, Becker C, & McLaughlin M. De novo antimicrobial peptides with low mammalian cell toxicity. *J. Med. Chem.* **39**,

3107-3113 (1996).

Kolonin, M. G., Saha, P. K., Chan, L., Pasqualini, R., and Arap, W. Reversal of obesity by targeted ablation of adipose tissue. Nat Med, 10: 625-632, 2004.

Kyrieleis, O. J., Goettig, P., Kiefersauer, R., Huber, R., and Brandstetter, H. Crystal structures of the tricorn interacting factor F3 from Thermoplasma acidophilum, a zinc aminopeptidase in three different conformations. J Mol Biol, 349: 787-800, 2005.

Lee S, Ellerby HM, Kiyota T, Sugihara G: DeNovo Design and Synthesis of Small Globular Protein Forming a Pore in Lipid Bilayers. In: *Controlled Drug Delivery: Designing Technologies for the Future*, pp 139-148. Ed by K Park and RJ Mrsny. Washington, DC, American Chemical Society, 2000

Lee S, Furuya T, Kiyota T, Takami N, Murata K, Niidome Y, Bredesen DE, Ellerby HM, Sugihara G. De novo-designed peptide transforms Golgi-specific lipids into Golgi- like nanotubules. *J Biol Chem* 276: 41224-8, 2001

Majhen, D., Gabrilovac, J., Eloit, M., Richardson, J., and Ambriovic-Ristov, A. Disulfide bond formation in NGR fiber-modified adenovirus is essential for retargeting to aminopeptidase N. Biochem Biophys Res Commun, 348: 278-287, 2006.

Matsumoto E, Kiyota T, Lee S, Sugihara G, Yamashita S, Meno H, Aso Y, Sakamoto H, Ellerby HM. Study on the packing geometry, stoichiometry, and membrane interaction of three analogs related to a pore-forming small globular protein. *Biopolymers* 56: 96-108, 2000.

Pasqualini, R., Koivunen, E., Kain, R., Lahdenranta, J., Sakamoto, M., Stryhn, A., Ashmun, R. A., Shapiro, L. H., Arap, W., and Ruoslahti, E. Aminopeptidase N is a receptor for tumor-homing peptides and a target for inhibiting angiogenesis. Cancer Res, 60: 722-727, 2000.

Rabizadeh S, Ye X, Sperandio S, Wang JJ, Ellerby HM, Ellerby LM, Giza C, Andrusiak RL, Frankowski H, Yaron Y, Moayeri NN, Rovelli G, Evans CJ, Butcher LL, Nolan GP, Assa-Munt N, Bredesen DE. Neurotrophin dependence domain: a domain required for the mediation of apoptosis by the p75 neurotrophin receptor. *J Mol Neurosci* 15: 215-29, 2000

Saido-Sakanaka, H., Ishibashi, J., Sagisaka, A., Momotani, E. & Yamakawa, M. Synthesis and characterization of bactericidal oligopeptides designed on the basis of an insect anti-bacterial peptide. *Biochem J* 338 (Pt 1), 29-33 (1999).

Saitoh, Y., Koizumi, K., Minami, T., Sekine, K., Sakurai, H., and Saiki, I. A derivative of aminopeptidase inhibitor (BE15) has a dual inhibitory effect of invasion and motility on tumor and endothelial cells. Biol Pharm Bull, 29: 709-712, 2006.

Samaniego, F., Markham, P. D., Gendelman, R., Watanabe, Y., Kao, V., Kowalski, K., Sonnabend, J. A., Pintus, A., Gallo, R. C., and Ensoli, B. Vascular endothelial growth factor and basic fibroblast growth factor present in Kaposi's sarcoma (KS) are induced by inflammatory cytokines and synergize to promote vascular permeability and KS lesion development. Am J Pathol, 152: 1433-1443, 1998.

Shim, J. S., Kim, J. H., Cho, H. Y., Yum, Y. N., Kim, S. H., Park, H. J., Shim, B. S., Choi, S. H., and Kwon, H. J. Irreversible inhibition of CD13/aminopeptidase N by the antiangiogenic agent curcumin. Chem Biol, 10: 695-704, 2003.

Zheng Duo-Qi J. Biol. Chem., 275(32), 24565-24574 (2000).

Zhang, Z., Harada, H., Tanabe, K., Hatta, H., Hiraoka, M., and Nishimoto, S. Aminopeptidase N/CD13 targeting fluorescent probes: synthesis and application to tumor cell imaging. Peptides, 26: 2182-2187, 2005.

List of Personnel

(5/1/02-4/30/05)

H. Michael Ellerby, PhD

Dale E. Bredesen, MD

Rammohan Rao, PhD

Sylvia Chen, PhD

Rebeccah Riley, BS

Satoshi Fujimura, PhD

ISSN 0021-9258 (print)
ISSN 1083-351x (electronic)
JBCHA3 278(37) 34733–35856 (2003)

The Online Version of This Issue Contains Supplemental Material

The Journal of Biological Chemistry

SEPTEMBER 12, 2003 VOLUME 278 NUMBER 37

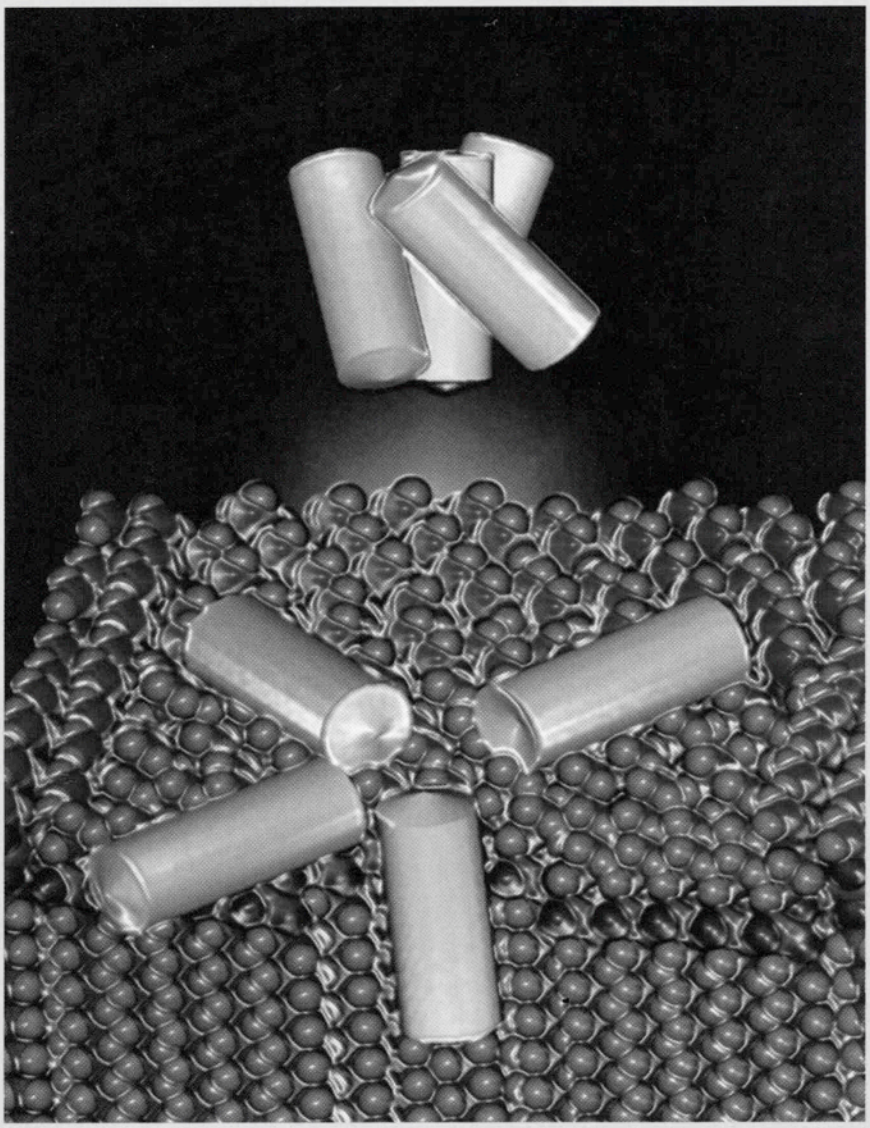

PUBLISHED BY THE AMERICAN SOCIETY FOR
BIOCHEMISTRY AND MOLECULAR BIOLOGY

Founded by Christian A Herter and Sustained in Part by the Christian A Herter Memorial Fund

THE JOURNAL OF BIOLOGICAL CHEMISTRY
Vol. 278, No. 37, Issue of September 12, pp. 35311–35316, 2003

Printed in U.S.A.

An Artificially Designed Pore-forming Protein with Anti-tumor Effects*

Received for publication, January 16, 2003, and in revised form, May 7, 2003
Published, JBC Papers in Press, May 14, 2003, DOI 10.1074/jbc.M300474200

H. Michael Ellerby‡§, Sannamu Lee¶, Lisa M. Ellerby‡, Sylvia Chen‡, Taira Kiyota¶, Gabriel del Rio‡, Gohsuke Sugihara¶, Yan Sun‖, Dale E. Bredesen‡, Wadih Arap‖, and Renata Pasqualini‖**

From the ‡Program on Cancer and Aging, The Buck Institute, Novato, California 94945, the ¶Department of Chemistry, Faculty of Science, Fukuoka University, Jonan-ku, Fukuoka 814-80, Japan, and ‖The University of Texas M. D. Anderson Cancer Center, Houston, Texas 77030

Protein engineering is an emerging area that has expanded our understanding of protein folding and laid the groundwork for the creation of unprecedented structures with unique functions. We previously designed the first native-like pore-forming protein, small globular protein (SGP). We show here that this artificially engineered protein has membrane-disrupting properties and anti-tumor activity in several cancer animal models. We propose and validate a mechanism for the selectivity of SGP toward cell membranes in tumors. SGP is the prototype for a new class of artificial proteins designed for therapeutic applications.

The tendency of amphipathic peptides to assemble in aqueous solution and of the β-turn to form a loop has been successfully employed to design coiled-coil proteins (1–3), various helix bundle proteins (4–9), and β-structural proteins (10, 11). *De novo* design of proteins with biological function, such as heme-binding, catalysis, or the formation of a membrane pore or channel, is perhaps the most challenging goal of peptide chemistry (12–19). Much has been done recently in terms of designing membrane proteins that are correctly incorporated into membranes. However, relatively few attempts have been made to design proteins capable of disrupting membranes and subsequently causing cell death *in vivo* (19, 20).

Small globular protein (SGP)[1] is a 69-amino acid, 4-helix bundle protein, composed of 3 amphipathic helices, which consist of Leu and Lys residues and surround a single hydrophobic helix consisting of Ala residues, which create a pocket-like structure (Fig. 1, *A* and *B*) (21, 22). SGP is monomeric in solution and denatures in a highly cooperative manner, characteristic of native globular-like proteins. SGP was conceived and designed based on the structure of the colicin family of bacteriocins (23–26). Although most naturally occurring, pore-forming proteins maintain their tertiary structure when disrupting membranes, the colicins undergo a spontaneous transition from a native folded state in solution to an open umbrella-like state in membranes. SGP was designed to mimic this membrane insertion mechanism, which was confirmed in synthetic bilayers, where SGP formed a uniform size pore (14pS) (21). It is still unknown whether or not SGP oligomerizes to form a channel.

Given that SGP forms pores in synthetic membranes, we asked whether it could disrupt biological membranes at the cellular level and whether it could be used successfully *in vivo* as an anti-tumor agent. We also investigated whether SGP would show any selectivity toward tumor cell lines *in vitro* and *in vivo*.

EXPERIMENTAL PROCEDURES

Reagents—SGP, SGP-L, and SGP-E were synthesized according to the Fmoc procedure starting from Fmoc-Leu-PEG (polyethylene glycol) resin using a Miligen automatic peptide synthesizer (Model 9050) to monitor the de-protection of the Fmoc group by UV absorbance (21). After cleavage from the resin by trifluoroacetic acid, the crude peptide obtained was purified by HPLC chromatography with an ODS column, 20 × 250 mm, with a gradient system of water/acetonitrile containing 0.1% trifluoroacetic acid. Amino acid analysis was performed after hydrolysis in 5.7 M HCl in a sealed tube at 110 °C for 24 h. Analytical data obtained were as follows: Gly, 6.2 (6); Ala, 9.5 (10); Leu, 26.5 (25); Asp, 3.0 (3); Pro, 2.9 (3); Tyr, 3.1 (3); Lys, 18.9 (18). Molecular weight was determined by fast atom bombardment mass spectroscopy using a JEOL JMX-HX100: base peak, 7555.1; calculated for $C_{367}H_{639}O_{77}N_{91}H^+$, 7554.8. Peptide concentrations were determined from the UV absorbance of Trp and three Tyr residues at 280 nm in buffer (e = 8000). Gel filtration HPLC chromatography was performed using Tris buffer (10 mM Tris, 150 mM NaCl, pH 5.0 or pH 7.4) on COSMOSIL 5DIOL-300 (Nakalai Tesk, Kyoto, Japan).

Computer Model—The computer-generated model of SGP was made with the program Insight II (Molecular Simulations Inc., San Diego, CA) running on an Octane SSE work station (Silicon Graphics, Cupertino, CA).

Cell Culture—All cell lines were obtained commercially. The Kaposi's sarcoma-derived cell line KS1767 and the breast carcinoma cell line MDA-MB-435 have been described previously (27–29) and were cultured in 10% fetal bovine serum/Dulbecco's modified Eagle's medium, containing antibiotics.

Quantification of Cell Death—Cell viability was determined by morphology (29, 30). For viability assays, KS1767 cells were incubated with the concentrations of SGP, SGP-L, SGP-E, or control peptides indicated in the figures and in Table I. Briefly, at the given time points, cell culture medium was aspirated from adherent cells. Cells were then gently washed once with PBS at 37 °C. A 20-fold dilution of the dye mixture (100 μg/ml acridine orange and 100 μg/ml ethidium bromide) in PBS was then gently pipetted on the cells and viewed on an inverted microscope (Nikon TE 300). Cells with nuclei exhibiting margination and condensation of chromatin and/or nuclear fragmentation (early/mid

* This work was supported by Grants CA84262 (to H. M. E.) and CA69381 (to D. E. B.) from the National Institutes of Health/National Cancer Institute, Grants PC001502 (to H. M. E.) and DAMD17-98-1-8581 (to D. E. B.) from the United States Army Medical Research and Materiel Command, American Biosciences Inc. (to H. M. E. and D. E. B.), and grants from the Gilson-Longenbaugh Foundation (to W. A. and R. P.). The costs of publication of this article were defrayed in part by the payment of page charges. This article must therefore be hereby marked "*advertisement*" in accordance with 18 U.S.C. Section 1734 solely to indicate this fact.

§ To whom correspondence may be addressed. E-mail: mellerby@buckinstitute.org.

** To whom correspondence may be addressed. E-mail: rpasqual@notes.mdacc.tmc.edu.

[1] The abbreviations used are: SGP, small globular protein; Fmoc, *N*-(9-fluorenyl)methoxycarbonyl; HPLC, high pressure liquid chromatography; PBS, phosphate-buffered saline.

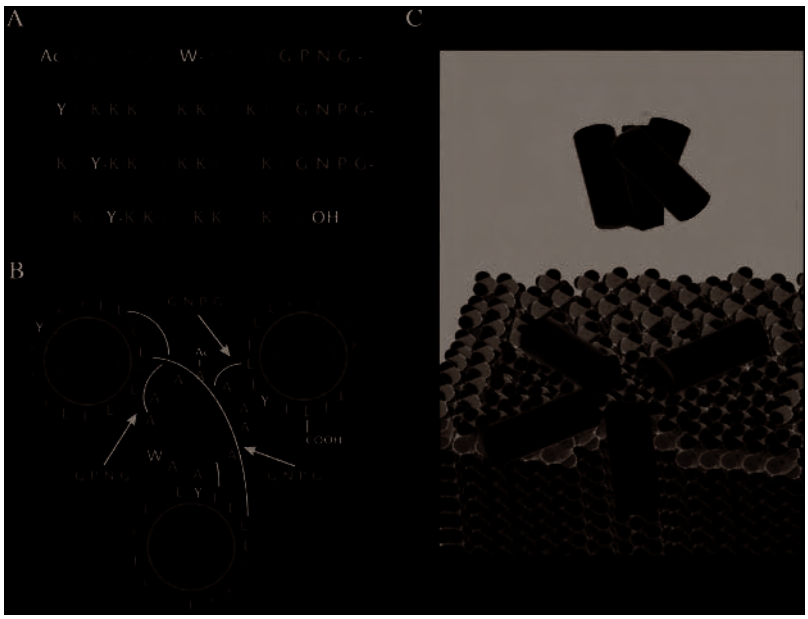

FIG. 1. **SGP representations and mechanism.** *A*, amino acid sequence of SGP. Hydrophobic leucine and alanine residues are shown in *red*, and positively charged lysine residues are in *green*. Loop residues (glycine, proline, and asparagine) are shown in *blue*, and tyrosine and tryptophan residues are in *black*. *B*, helical wheel diagram of SGP. *C*, the putative mechanism of SGP. (Note *red* and *green* colors reversed in *B*). In the aqueous phase SGP folds into a globular protein (*upper*), but in lipid membranes it adopts an inverted umbrella-like structure forming a pore (*lower*).

apoptosis-acridine orange positive) or with compromised plasma membranes (late apoptosis-ethidium bromide positive) were scored as not viable; 500 cells per time point were scored in each experiment. Percent viability was calculated relative to untreated cells.

Human Tumor Xenografts—MDA-MB-435-, KS1767-, PC-3-, and H358-derived human tumor xenografts were established in 2-month-old female or male (according to the tumor type), nude/nude Balb/c mice (Jackson Labs, Bar Harbor, ME) by administering 10^6 tumor cells per mouse in a 200 μl volume of serum-free Dulbecco's modified Eagle's medium into the mammary fat pad or on the flank (29). The mice were anesthetized with Avertin as described (29). SGP was administered directly into the center of the tumor mass at a concentration of 100 μM or 1 mM given slowly in 5 μl increments, for a total volume of 40 μl. Measurements of tumors were taken by caliper under anesthesia and used to calculate tumor volume (29). Animal experimentation was reviewed and approved by the Institutional Animal Care and Use Committee.

Histology—MDA-MB-435-derived breast carcinoma and KS1767-derived Kaposi sarcoma xenografts and organs were removed, fixed in Bouin solution, embedded in paraffin for preparation of tissue sections, and stained with hematoxylin and eosin (29).

Skin Toxicity—2-month-old female nude mice (Jackson Labs) were anesthetized with Avertin. 10 μl of 100 μM SGP or PBS was injected into the skin. The injected areas were monitored for 2 weeks.

Cytotoxicity Assays—Cell viability was determined by morphology (29, 30). KS1767 cells were incubated with SGP at 1 mM in the presence or absence of matrigel or polymeric fibronectin (sFN). The fibronectin polymer was produced as described (31). Briefly, cell culture medium was aspirated from adherent cells. Cells were then coated with matrigel (gently pipetted on each well to completely coat the entire cell layer), or the fibronectin polymer, and incubated at 37 °C for 10 min. SGP was added and the cells were viewed on an inverted microscope (Nikon TE 300). KS1767 cells were also exposed to doxorubicin (20 μg/well) or SGP in the presence or absense of matrigel for 24 h. Cell viability (%) was evaluated after no treatment (medium or matrigel alone), incubation with SGP or doxorubicin. Cell death was evaluated morphologically (29, 30), and cell viability was compared relative to untreated controls (no matrigel) or absence of SGP.

RESULTS

SGP Effects on Cultured Cells—To evaluate the effects of SGP on cell membranes we treated multiple human cell lines of different origins (Table I). These lines included the Kaposi's sarcoma-derived cell line KS1767, the breast carcinoma-derived cell line MDA-MD-435, and the microvessel endothelial cell line dermal microvessel endothelial cells (27–29). Treatment of KS1767 cells with >10 μM SGP led to rapid non-necrotic, non-apoptotic cell death, characterized by 100% loss of viability within 60 s (Fig. 2*A*), as determined by Trypan Blue

TABLE I
Comparison of LC_{50} data for SGP, SGP-L, and SGP-E on a variety of cultured human cell types, including primary cultures of vascular endothelial cells

Cell Applications Dermal Microvessel Endothelial Cells (CADMEC), Human Umbilical Cord Vascular Endothelial Cells (HUVEC) and Pulmonary Artery Endothelial Cells (HPAEC), tumor cell lines (PC3 human prostate cancer cells, KS1767 Kaposi's sarcoma cells, H358 human lung carcinoma cells), and 293 human kidney cells. This table illustrates the fact that the altering the structure of SGP can diminish its cell death inducing ability. The dash marks (—) indicate no data obtained.

Cell Line	LC_{50} at 30 min		
	SGP	SPG-L	SPG-E
		μM	
KS 1767	5	60	30
	4	60	30
PC3	2.5	—	—
H358	6	—	—
CADMEC	5	60	30
HUVEC	7	—	—
HPAEC	5	—	—
293	5	—	—

positivity. Such a rapid response suggests that the plasma membrane has been disrupted. Lowering the concentration of SGP to between 5 and 10 μM led to induction of necrosis (scored morphologically), resulting in almost 100% loss of KS1767 cell viability over 60 min (Fig. 2*B*). SGP levels below 5 μM led to the induction of apoptosis over a 24-hour period (Fig. 2*C*), which was confirmed by a caspase-3 activation assay. KS1767 cells were unaffected by a 24 h incubation in 100 μM of a control peptide (Fig. 2*D*). However, the classic morphological signs of apoptosis, such as nuclear condensation (Fig. 2*E*, *short arrow*) and plasma membrane blebbing (Fig. 2*E*, *long arrow*), were apparent in KS1767 cells after a 24-hour treatment with 3 μM SGP. Similar results were obtained using different cell lines, including several types of malignant cells (solid tumors and leukemic cell lines) and non-neoplastic cells (including endothelial cells and fibroblasts isolated from multiple organs and cells of glial origin, Table I). As negative controls, we used altered forms of SGP (SGP-L and SGP-E). In SGP-L, the central all alanine helix was replaced by an all leucine helix. In SGP-E, lysines have been replaced by glutamic acids, and we had previously determined that the ability of such analogs to

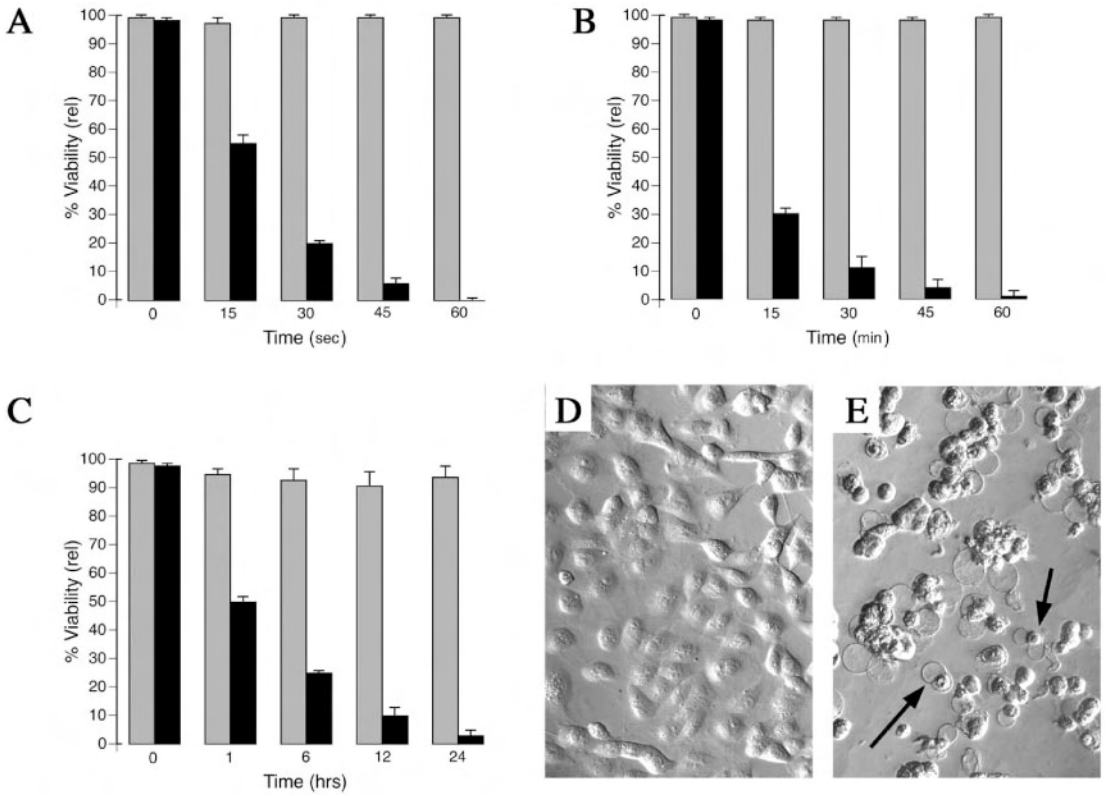

FIG. 2. **SGP treatment of cultured tumor cells.** *A*, human Kaposi's sarcoma-derived KS1767 cells treated with 10 μM SGP undergo extremely rapid non-necrotic, non-apoptotic cell death within 60 s (*black bars*), whereas those treated with 100 μM of negative control peptide DLSLARLATARLAI are unaffected (*scheme bars*) ($p < 0.04$). *B*, necrosis is observed in KS1767 cells treated with 10 μM SGP within 60 min (*black bars*), whereas those treated with 100 μM of negative control peptide are unaffected after 60 min (*gray bars*) ($p < 0.03$). *C*, apoptosis is observed after treatment with 3 μM SGP over 24 h, whereas cells treated with 100 μM of negative control peptide are unaffected after 24 h (*gray bars*) ($p < 0.05$). Hoffman contrast microscopy of KS1767 cells treated with 100 μM of negative control peptide (*D*) for 24 h or 3 μM SGP for 24 h (*E*). Cells with nuclei exhibiting margination and condensation of chromatin and/or nuclear fragmentation (early/mid apoptosis-acridine orange positive) or with compromised plasma membranes (late apoptosis-ethidium bromide positive) were scored as not viable (500 cells per time point were scored in each experiment). Percent viability was calculated relative to untreated cells under all experimental conditions. Classic morphological characteristics of cell death including condensed nuclei (*short arrows*) and plasma membrane blebbing (*long arrows*) are evident. Results were reproduced in more than three independent experiments.

disrupt synthetic membranes is diminished (22). SGP-L and SGP-E were substantially less toxic to mammalian cultured cells (Table I). The LC_{50} was increased by at least 10-fold in all cell types tested with SGP-L and SGP-E when these inactive versions of the protein were tested. These observations clearly show that the integrity of the SGP helices is required for SGP membrane disrupting activity. Taken together, these data demonstrate that SGP is a potent membrane-disrupting agent, but also that it is not cell-selective and it will affect tumor-derived cells as well as normal cells at similar concentrations (~3 μM).

SGP Has Anti-tumor Activity in Vivo—Given the potent membrane-disrupting activity of SGP, we proceeded to evaluate SGP anti-tumor activity in nude mice bearing human tumor xenografts. We hypothesized that direct administration of SGP might reduce tumor volume and retard metastasis. In the first set of experiments, tumors were allowed to form after injection of a breast carcinoma cell line (MDA-MD-435) and then treated with local injections of SGP. We observed that tumor volume was significantly smaller in SGP-treated mice than in the PBS-treated control mice (Fig. 3*A*). Starting tumor volumes ranged from about 100 mm^3 to large sizes of about 600 mm^3. Tumor-bearing mice were given four weekly treatments of PBS, or 100 μM or 1 mM SGP (40 μl/treatment given in 5 μl increments). After a 4-week period without treatment, the tumor volumes were measured at 8 weeks. The average tumor volume at the end of the experiment in the SGP-treated groups was 5× less than the average volume seen in the PBS-treated group (Fig. 3*A*). There was no difference between the average

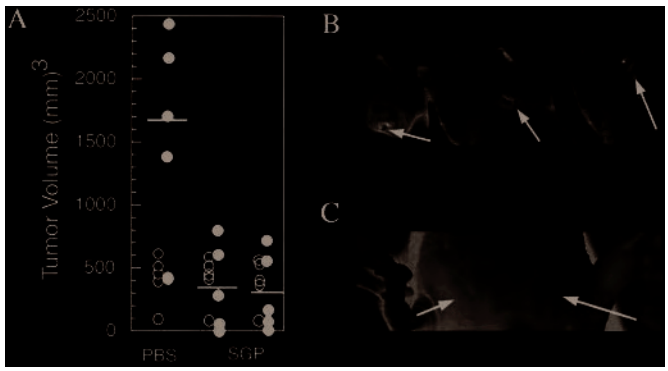

FIG. 3. **SGP treatment of nude mice bearing human breast cancer-derived xenografts.** Data are shown for human MDA-MB-435-derived breast carcinomas. Mice had tumor volumes ranging from 100 mm^3 to 600 mm^3 and were divided in similar groups based on matched tumor volumes at the start of the experiment (*open circles*). *A*, SGP-treated tumors are smaller than controls (PBS-treated or SGP-treated tumor volumes at the end of the experiment are represented as *closed circles*). Differences in tumor volumes at 8 weeks are shown (*t* test, $p < 0.05$). A total of 10 mice received SGP. *B*, representative pictures of tumors after 4 weekly treatments with SGP at 40 μl/week, $n = 5$ for each experimental group. The volume of the PBS-treated tumor is 400 mm^3 (*left*), whereas 100 μM SGP (*middle*) and 1 mM SGP (*right*) treated tumors have flattened and virtually disappeared. These three tumors began at volumes of 100 mm^3. *C*, lack of skin toxicity of SGP. Subcutaneous injection (40 μl) of 100 μM SGP (*left injection sight*, *arrow*) and of PBS (*right injection site*, *arrow*) demonstrates that SGP is relatively non-toxic to normal skin. Results represented in *C* were reproduced in eight independent experiments.

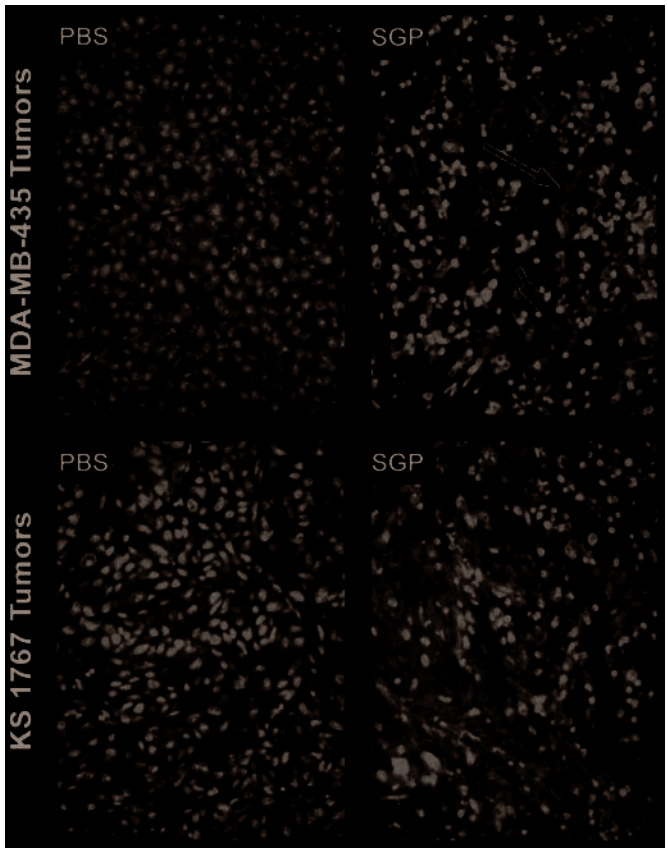

FIG. 4. **SGP-treated tumors undergo widespread cell death.** Histopathological tissue sections of human tumor xenografts harvested at 8 weeks after treatment initiation are shown. Tissue sections from human MDA-MB-435-derived breast carcinoma xeno-grafts from nude mice treated with PBS-treated tumor tissue but with 100 μM SGP, show extensive apoptosis with many evident condensed nuclei (*short arrows*) and an intact extra-cellular matrix (*long arrows*); $n = 7$ for each experimental group. Tissue sections from human KS1767-derived Kaposi's sarcoma xenografts in nude mice had a similar outcome, a representative image of a PBS-treated tumor, and a tumor treated with SGP are shown.

tumor volumes of the 2 SGP treatment groups. Mice treated with SGP remained tumor-free for up to 4 months after tumor implantation, before being euthanized for histological evaluation. These observations indicate that both primary tumor growth (Fig. 4) and metastases were inhibited. Surgical examination of the tumor sites revealed no sign of tumor cells. Similar results were obtained when xenografts were produced by injection of prostate (Fig. 5*A*) and lung carcinoma (Fig. 5, *B* and *C*) cell lines. By successfully treating a large number of mice and testing the effects of SGP on several different tumor xenograft models (including carcinomas, sarcomas, and melanomas), we firmly established the therapeutic properties of SGP. Our data also show that that the anti-tumor effects of SGP are not limited to a specific tumor type. We also determined whether SGP produced adverse side effects such as necrosis when injected under normal skin. Strikingly, in all mice tested, SGP did not produce any surface effect when injected intradermally or sub-cutaneously (Fig. 3*C*) when compared with mice that did not receive the active form of SGP.

Histopathological analysis of SGP-treated MDA-MD-435 human breast carcinoma xenografts showed widespread cell death (Fig. 4, *upper right panel*), as compared with PBS-treated tumors (Fig. 4, *upper left panel*). Many condensed nuclei were apparent (Fig. 4, *upper left panel*, *short arrows*), and there was no effect on the extracellular matrix (Fig. 4*B*, *long arrows*). Apoptosis was confirmed by a caspase-3 activation assay (data not shown). It is noteworthy that whereas 100 μM SGP induced almost immediate cell death *in vitro* that was apparently neither apoptotic nor necrotic, 100 μM SGP induced apoptosis *in vivo*. Work is underway to evaluate lower concentrations. SGP-treated human KS1767 Kaposi's sarcoma-derived xenografts showed similar effects (Fig. 4, *left* and *right panels*). Histological analysis of the major organs of SGP-treated mice showed no overt pathology, confirming that SGP treatments do not affect sites other than the injected tumor area (data not shown). Thus, SGP has anti-tumor specific effects, without showing any tumor cell-specific effects.

Mechanism of SGP Action and Selectivity toward Cell Membranes—To determine the mechanisms responsible for selective anti-tumor activity of SGP *in vivo*, we designed a matrigel

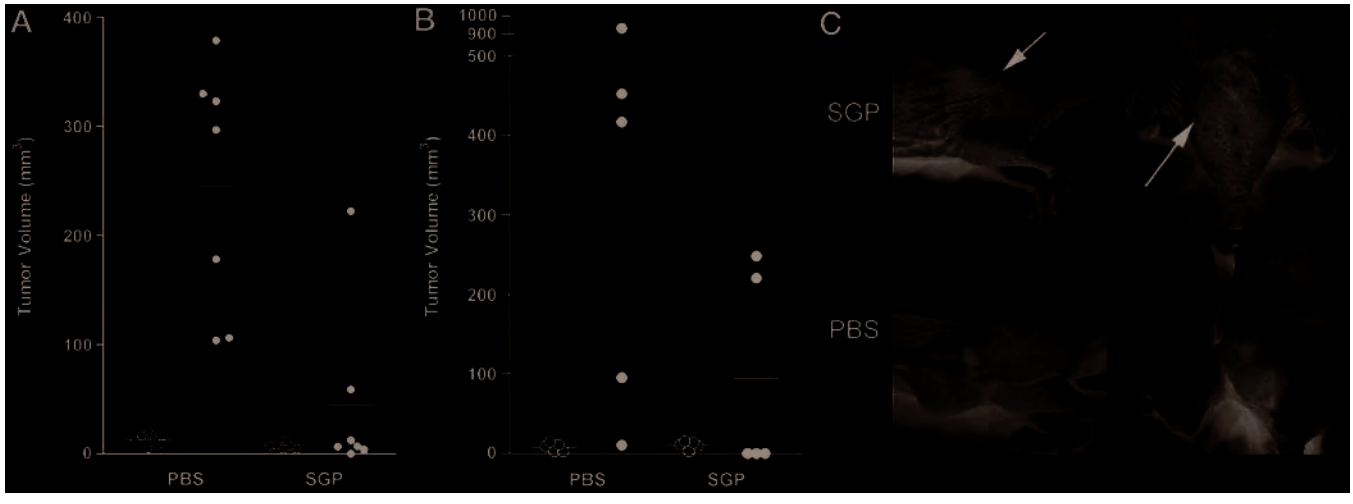

FIG. 5. **SGP treatment of nude mice bearing human prostate and lung cancer xenografts.** Data are shown for human PC3-derived prostate carcinoma and H358 lung carcinoma. Tumor cells were implanted on the flank at the start of the experiments. Mice were divided in similar groups based on matched tumor volumes at the start of the experiment (*open circles*). *A*, SGP-treated PC-3 tumors are smaller than control PBS-treated tumors. Differences in tumor volumes at 10 weeks are shown (t test, $p < 0.05$). *B*, SGP-treated H358 tumors are smaller than control PBS-treated tumors. Differences in tumor volumes at 9 weeks are shown (t test, $p < 0.05$). *C*, representative pictures of tumors after 6 weekly treatments at 40 μl/week (see "Experimental Procedures"); $n = 7$ for each experimental group. SGP-treated tumors, as indicated, have disappeared. A, SGP-treated tumors are smaller than controls (PBS-treated or SGP-treated tumor volumes at the end of the experiment are represented as closed circles).

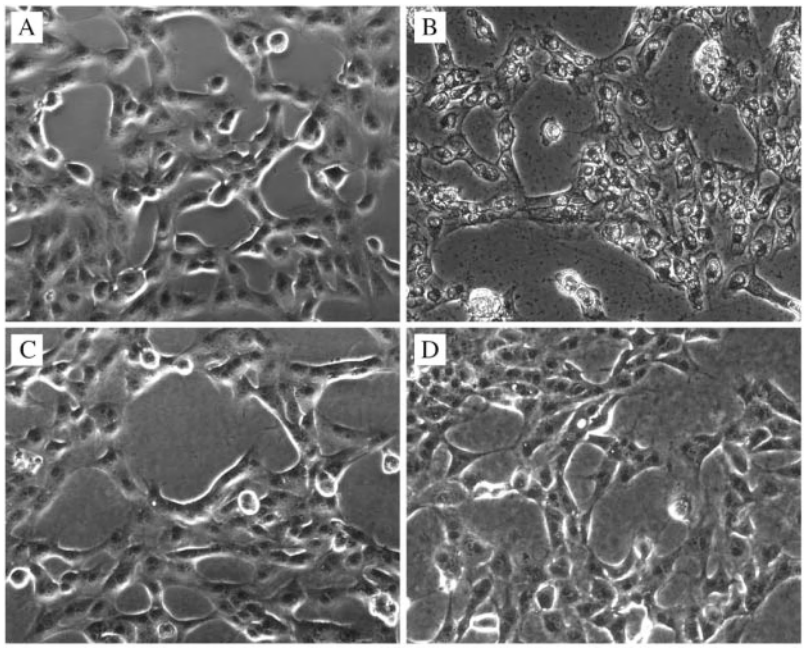

FIG. 6. **SGP treatment of cultured tumor cells in the presence or absence of matrigel or polymeric fibronectin.** Treatment of KS1767 cells with 1 mM SGP decreases cell viability and leads to condensed nuclei and plasma cell membrane blebbing (*B*), whereas cells treated with 1 mM of SGP in the presence of matrigel remain unaffected after 60 min (*D*). KS1767 cells without (*A*) or with a layer of matrigel (*C*) remained healthy for as long as 48 h. Results were reproduced in four independent experiments.

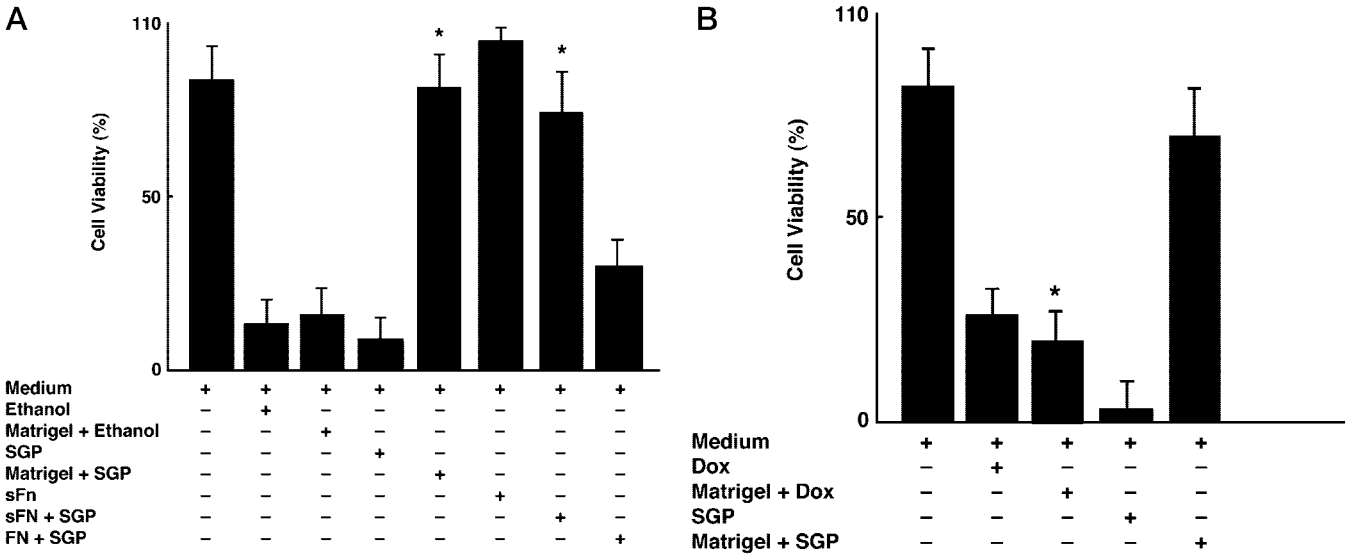

FIG. 7. **Cytotoxic assay *in vitro* and effects of matrigel.** *A*, KS1767 cells were exposed to doxorubicin or SGP in the presence or absence of matrigel for 24 h. Cell viability (%) was evaluated at 24 h after no treatment (medium or matrigel alone), or incubation with SGP or doxorubicin (20 μg/well), as indicated. In contrast to SGP, doxorubidin decreased cell viability (*, $p < 0.01$) in the presence of matrigel. Shown are S.E. obtained from triplicate wells. Results were reproduced in four independent experiments. *B*, KS1767 cells were exposed to SGP in the presence or absence of polymeric fibronectin. In contrast to cells exposed to ethanol, cells treated with 1 mM of SGP in the presence of polymeric fibronectin (sFN) remain unaffected (*, $p < 0.01$). Cell viability (%) was evaluated morphologically. Shown are S.E. obtained from triplicate wells. Results were reproduced in three independent experiments.

assay (to mimic extracellular matrix). In the absence of matrigel, SGP led to severe disruption of cell membranes, resulting in almost 100% loss of viability over 10 min (Fig. 6*B*). In contrast, in the presence of matrigel, KS1767 cells were unaffected by incubation with 1 mM SGP (Fig. 6*D*). This loss of membrane disrupting ability in the presence of a thin matrigel layer could account for the lack of SGP toxicity seen *in vivo*. Ethanol, as shown in Fig. 7*A*, or cytotoxic drugs such as doxorubicin (Fig. 7*B*) damaged the cell layer under similar conditions, regardless of the presence of matrigel, which fails to provide protection from the other toxic agents because these other agents more readily diffuse through the matrix. When matrigel was replaced by polymeric fibronectin (sFN) (31), another form of matrix, SGP was also ineffective and did not interfere with cell viability (Fig. 7*A*), whereas ethanol induced massive cell death. Fibronectin alone did not prevent SGP activity and was used as a control.

The observations in this model are consistent with the lack of skin toxicity seen with SGP. We propose that the discrepancy between *in vitro* and *in vivo* SGP effects (anti-tumor cell activity *versus* selective anti-tumor activity) results from the potent membrane-disrupting activity of SGP, which is inactivated in the presence of extracellular matrix and connective tissue.

DISCUSSION

SGP represents a novel class of anti-cancer proteins whose therapeutic effects can be optimized by amino acid substitution and by altering helical domain length and hydrophobicity (32).

Although SGP is a nonspecific membrane-disrupting agent, it is selective in the sense that the disruption is limited *in vivo*. Unlike detergents, which solubilize membranes, SGP physically disrupts membrane architecture, leading to cell lysis. This explains the lack of SGP toxicity when the protein is injected sub-cutaneously or intradermally. Recently published data (22) also suggest that the lipid membrane-disruption properties of SGP are responsible for the anti-tumor activity of the agent.

We report one of the first examples of a pore-forming peptide or protein, natural or synthetic, being applied successfully to treat established human tumor xenografts. It is important to emphasize that SGP is not a bacterial toxin, although such agents (or their natural or recombinant form) have been extensively explored as anti-cancer therapies (33, 34). Several pore-forming peptides and proteins have been shown to have moderate efficacy in killing tumor cells *in vitro*, yet very limited anti-tumor effects were seen *in vivo*. The anti-bacterial peptides magainin (and synthetic derivatives) (35), cecropin (and synthetic derivatives) (36), granulysin (37), and NK-lysin (38) are toxic to tumor cells in culture. The pore-forming protein verotoxin 1 (a colicin) has also been shown to have a toxic effect on tumor cells *in vitro* (39). Magainin, cecropin, and verotoxin 1 also had limited efficacy *in vivo* in mice bearing murine tumors (35, 36, 39).

Cytotoxic agents developed within the past few decades have been based on naturally existing compounds, synthetic peptides, or protein fragments representing active membrane-disrupting domains. In contrast to such compounds, SGP is a protein that was artificially created to perform a pre-determined biological function. Moreover, therapeutically significant cell membrane disrupting activity was observed *in vivo*.

SGP activity appears to be restricted to the presence of lipid bilayers *in vitro*, whereas *in vivo* its activity appears to be limited to tumors *in vivo* due to the protective effect of extracellular matrix components. *In vitro*, SGP shows no selectivity toward normal or malignant cells under the experimental conditions tested. We show here that SGP is potentially a valid anti-cancer agent; applications include Kaposi's sarcoma, malignant melanoma of the skin, or palliation for unresectable or metastatic tumors in anatomical sites difficult to treat with other modalities. Moreover, SGP variants in which residues critical for helical structure are altered are inactive, suggesting that the structure of the protein is intrinsically linked to its ability to damage cell membranes. Although the *de novo* design of proteins with biological function is in its early stages, novel therapeutic strategies may emerge from the activity of designed proteins such as SGP.

Acknowledgments—We thank Drs. Marco Arap, William A. Cramer, and David Greenberg for comments and critical reading of the manuscript.

REFERENCES

1. DeGrado, W. F., Wasserman, Z. R., and Lear, J. D. (1989) *Science* **243,** 622–628
2. Betz, S. F., Liebman, P. A., and DeGrado, W. F. (1997) *Biochemistry* **36,** 2450–2458
3. Bryson, J. W., Desjarlais, J. R., Handel, T. M., and DeGrado, W. F. (1998) *Prot. Sci.* **7,** 1404–1414
4. Walsh, S. T., Cheng, H., Bryson, J. W., Roder, H., and DeGrado, W. F. (1999) *Proc. Natl. Acad. Sci. U. S. A.* **96,** 5486–5491
5. Hecht, M. H., Richardson, J. S., Richardson, D. C., and Ogden, R. C. (1990) *Science* **249,** 884–891
6. Dekker, N., Cox, M., Boelens, R., Verrijzer, C. P., van der Vliet, P. C., and Kaptein, R. (1993) *Nature* **362,** 852–855
7. Zhou, N. E., Kay, C. M., and Hodges, R. S. (1992) *J. Biol. Chem.* **267,** 2664–2670
8. Kamtekar, S., Schiffer, J. M., Xiong, H., Babik, J. M., and Hecht, M. H. (1993) *Science* **262,** 1680–1685
9. Monera, O. D., Zhou, N. E., Lavigne, P., Kay, C. M., and Hodges, R. S. (1996) *J. Biol. Chem.* **271,** 3995–4001
10. Quinn, T. P., Tweedy, N. B., Williams, R. W., Richardson, J. S., and Richardson, D. C. (1994) *Proc. Natl. Acad. Sci. U. S. A.* **91,** 8747–8751
11. Hecht, M. H. (1994) *Proc. Natl. Acad. Sci. U. S. A.* **91,** 8729–8730
12. Tuchscherer, G., Scheibler, L., Dumy, P., and Mutter, M. (1998) *Biopolymers* **47,** 63–73
13. Handel, T. M., Williams, S. A., and DeGrado, W. F. (1993) *Science* **261,** 879–885
14. Lazar, G. A., Desjarlais, J. R., and Handel, T. M. (1997) *Prot. Sci.* **6,** 1167–1178
15. Rojas, N. R., Kamtekar, S., Simons, C. T., McLean, J. E., Vogel, K. M., Spiro, T. G., Farid, R. S., and Hecht, M. H. (1997) *Prot. Sci.* **6,** 2512–2524
16. Farinas, E., and Regan, L. (1998) *Prot. Sci.* **7,** 1939–1946
17. Tommos, C., Skalicky, J. J., Pilloud, D. L., Wand, A. J., and Dutton, P. L. (1999) *Biochem.* **38,** 9495–9507
18. Corey, M. J., and Corey, E. (1996) *Proc. Natl. Acad. Sci. U. S. A.* **93,** 11428–11434
19. Bayley, H. (1999) *Curr. Opin. Biotechnol.* **10,** 94–103
20. Mingarro, I., von Heijne, G., and Whitley, P. (1997) *Trends Biotechnol.* **15,** 432–437
21. Lee, S., Kiyota, T., Kunitake, T., Matsumoto, E., Yamashita, S., Anzai, K., and Sugihara, G. (1997) *Biochem.* **36,** 3782–3791
22. Matsumoto, E., Kiyota, T., Lee, S., Sugihara, G., Yamashita, S., Meno, H., Aso, Y., Sakamoto, H., and Ellerby, H. M. (2001) *Biopolymers* **56,** 96–108
23. Konisky, J. (1982) *Ann. Rev. Microbiol.* **36,** 125–144
24. van der Goot, F. G., Gonzalez-Manas, J. M., Lakey, J. H., and Pattus, F. (1991) *Nature* **354,** 408–410
25. Zakharov S. D., Lindeberg M., Griko Y., Salamon Z., Tollin G., Prendergast F. G., and Cramer, W. A. (1998) *Proc. Natl. Acad. Sci., U. S. A.* **95,** 4282–4287
26. Mel, S. F., and Stroud, R. M. (1993) *Biochem.* **32,** 2082–2089
27. Herndier, B. G., Werner, A., Arnstein, P., Abbey, N. W., Demartis, F., Cohen, R. L., Shuman, M. A., and Levy, J. A. (1994) *Aids* **8,** 575–581
28. Reisbach, G., Gebhart, E., and Cailleau, R. (1982) *Anticancer Res.* **2,** 257–260
29. Ellerby, H. M., Arap, W., Ellerby, L. M., Kain, R., Andrusiak, R., Rio, G. D., Krajewski, S., Lombardo, C. R., Rao, R., Ruoslahti, E., Bredesen, D. E., and Pasqualini, R. (1999) *Nat. Med.* **5,** 1032–1038
30. Ellerby, H. M., Martin, S. J., Ellerby, L. M., Naiem, S. S., Rabizadeh, S., Salvesen, G. S., Casiano, C. A., Cashman, N. R., Green, D. R., and Bredesen, D. E. (1997) *J. Neurosci.* **17,** 6165–6178
31. Pasqualini, R., Bourdoulous, S., Koivunen, E., Woods, V. L., Jr., and Ruoslahti, E. (1996) *Nature Med.* **2,** 1197–1203
32. Dathe, M., Wieprecht, T., Nikolenko, H., Handel, L., Maloy, W. L., MacDonald, D. L., Beyermann, M., and Bienert, M. (1997) *FEBS Lett.* **403,** 208–212
33. Pastan, I., Chaudhary, V., and FitzGerald D. J. (1992) *Ann. Rev. Biochem.* **61,** 331–354
34. Brothman, A. (1997) in *Encyclopedia of Cancer* (Bertino, J., ed) 2nd Ed., pp. 1303–1313, Academic Press, New York
35. Ohsaki, Y., Gazdar, A. F., Chen, H. C., and Johnson, B. E. (1992) *Cancer Res.* **52,** 3534–3538
36. Moore, A. J., Devine, D. A., and Bibby, M. C. (1994) *Peptide Res.* **7,** 265–269
37. Gamen, S., Hanson, D. A., Kaspar, A., Naval, J., Krensky, A. M., and Anel, A. (1998) *J. Immunol.* **161,** 1758–1764
38. Andersson, M., Gunne, H., Agerberth, B., Boman, A., Bergman, T., Sillard, R., Jornvall, H., Mutt, V., Olsson, B., Wigzell H., Dagerlind, A., Bowman, H. G., and Gudmundsson, G. H. (1995) *EMBO J.* **14,** 1615–1625
39. Farkas-Himsley, H., Hill, R., Rosen, B., Arab, S., and Lingwood, C. A. (1995) *Proc. Natl. Acad. Sci. U. S. A.* **92,** 6996–7000

A Dimer of the Tumor-Targeting Peptide CNGRC Inhibits Aminopeptidase N

Satoshi Fujimura,[1] Rebeccah R. Riley,[1] Sylvia F. Chen,[1]

Lisa M. Ellerby,[1] and H. Michael Ellerby[1,2]

[1]Buck Institute for Age Research, 8001 Redwood Blvd., Novato, CA 94945, USA and

[2]College of Pharmacy, Touro University, 1310 Johnson Lane, Mare Island, Vallejo, CA 94592, USA

Running title: Dimer of CNGRC peptide as an APN inhibitor

Keywords: CNGRC, NGR, Aminopeptidase N, APN, CD13, Tumor homing, Tumor targeting, Angiogenesis inhibitor, Tumor angiogenesis

Grant support: DAMD17-01-1-0029.

Requests for reprints: Dr. H. Michael Ellerby, College of Pharmacy, Touro University, 1310 Johnson Lane, Mare Island, Vallejo, CA 94592. Phone: 707-638-5907; E-mail: mellerby@touro.edu.

Abstract

Aminopeptidase N (APN/CD13) is expressed on endothelial cells and is involved in angiogenesis including the neovascularization during tumor growth, thus APN inhibitors represent potential anti-cancer drugs through the suppression of angiogenesis. Previously, Asn-Gly-Arg (NGR) was identified as an APN binding sequence and was used as a tumor homing peptide. Here we show that a dimer (NGRd) composed of two monomers linked through disulfide bonds is a potent APN inhibitor. Indeed, NGRd, inhibits purified APN activity, inhibits APN activity in living cells, and suppresses the migration, invasion, and proliferation of cells expressing APN. We also show that NGRd inhibits tube formation in endothelial cells and the formation of capillary vessels on the chicken chorioallantoic membrane. Together, these results demonstrate the potential of NGRd in the development of new drugs for cancer therapy, through the inhibition of angiogenesis.

Introduction

The inhibition of angiogenesis is one of the targets of cancer therapy because the survival, proliferation and metastasis of tumor cells require neovascularization to supply oxygen and nutrition(1, 2). Aminopeptidase N (APN/CD13, EC 3.4.11.2) is a type II transmembrane protein and a M1 class matalloprotease containing a Zn^{2+} binding motif, HEXXH (3). APN is expressed in endothelial cells and is involved in angiogenesis including the neovascularization associated with tumor growth. The dysregulated expression of APN is also observed in various cancer cells, and affects tumor cell functions such as proliferation, migration and invasion (3). Therefore, APN plays a key role in tumor metastasis, and is a potential target for cancer therapeutic reagents.

A number of molecules, either purified from natural products or synthesized as chemical compounds, have been reported as APN inhibitors and show promise as anti-cancer drugs through the suppression of neovascularization (3). In addition, APN is the target of certain drugs that induce cell death in the endothelial cells that form tumor blood vessels. Previously, the peptide CNGRC was identified as a tumor homing peptide (4). This

peptide binds to APN selectively expressed on the endothelial cells that form tumor vasculature (5), but not on normal endothelial cells or myeloid cells (6). Taking advantage of this property, this sequence was combined with a peptide that is harmless to the outside of all cells, but deadly to cells that internalize the composite peptide (7). The first prototype in a series of such peptides, denoted in this work as Hunter-Killer Peptide 1 (HKP1), combined CNGRC as a targeting domain, and $_{D}$(KLAKLAKKLAKLAK) as a pro-apoptotic domain; composed of D-amino acids to avoid enzymatic degradation (7). HKP1 binds to APN on the cell surface, via the targeting domain, CNGRC, and then is internalized into the cytosol through APN, where it induces apoptosis though mitochondrial membrane disruption via the pro-apoptotic domain $_{D}$(KLAKLAKKLAKLAK). HKP1 and related peptides were found to suppress tumor volume, and to increase survival through the inhibition of tumor blood vessel neovascularization (7).

In this work, we show that a dimer of the homing sequence CNGRC (NGRd) acts as a strong APN inhibitor. NGRd inhibits purified APN activity, inhibits APN activity in living cells, and suppresses the migration, invasion, and proliferation of cells expressing

APN. We also show that NGRd inhibits tube formation in endothelial cells and the formation of capillary vessels on the chicken chorioallantoic membrane. Together, these results demonstrate the potential of NGRd, and molecules based on it, as new drugs for cancer therapy, through the inhibition of aminopeptidase N, and thereby of angiogenesis.

Materials and Methods

Materials. Rat APN/CD13 purified from renal brush-border membranes was purchased from Calbiochem (La Jolla, CA). All HKP related peptides (Figure 1) were synthesized by AnaSpec (San Jose, CA) and dissolved in phosphate buffered saline (PBS). Bestatin, L-Alanine 4-methyl-coumaryl-7-amide (Ala-MCA) was purchased from Sigma (St. Lois, MO). WST-8 was purchased from Dojindo Laboratories (Kumamoto, Japan) as a cell counting kit-8. Recombinant human fibroblast growth factor-basic (bFGF) was purchased from Chemicon (Temecula, CA). All other chemicals also were purchased from Sigma or Calbiochem.

Cell Culture. Human Kaposi's sarcoma-derived cell line, KS1767, was maintained in Dulbecco's modified Eagle's medium (DMEM) supplemented 10% fetal calf serum (FCS) and penicillin/streptomycin, and cultured at 37˚C under an atmosphere of 5% CO_2. Human dermal microvascular endothelial cells (HMVEC/CADMEC™), the growth medium and other reagents for the cells were purchased from Cell Applications (San Diego, CA) and maintained following the manufacture's protocol.

Measurement of APN Activity. The APN activity was measured using a fluorogenic substrate, Ala-MCA on a 96-well black plate. APN was diluted in PBS (final conc. 1 x 10^{-3} U/ml) and was incubated with bestatin (10 μM) or NGR peptides (10-200 μM) in 0.01% BSA in PBS for 10 min on ice and 5 min at 37˚C, and then Ala-MCA (0.1 mM) warmed at 37˚C was added to the mixture. The enzymatic reaction was continued on a fluorescence plate reader (Molecular Devices, Sunnyvale, CA) at 37˚C for 15 min and then fluorescence intensity was immediately measured at the excitation and emission wavelength of 360 and 460 nm, respectively for fluorescent substrate. APN activity was also measured in intact cells. The cells were seeded on a 96-well black plate (clear bottom) and

cultured overnight. After washing the cells with PBS, the cells were incubated with or without APN inhibitors for 15 min at 37°C. The activity was then measured following the method describe above.

Cell Viability Assay. Cell proliferation and cytotoxicity assays were performed using the reagent WST-8, which estimates the intracellular dehydrogenase activity (following the manufacture's protocol). In brief, the cells were inoculated and cultured in 100 μl culture medium on a 96-well plate and then the viability was measured by adding 10 μl WST-8 to each well and cultured at 37°C for 1h after treatment with or without HKP related peptides.

Chemomigration Assay. The migration activity of KS1767 cells was carried out using transwell cell culture inserts (8 μm polycarbonate membrane, Nunc, Rochester, NY). The inserts were placed into the wells of a 24-well plate. The cells were suspended in the inserts in serum free-DMEM supplemented with bFGF (50 ng/ml), with or without NGR peptides or bestatin, and cultured for 12 hours at 37°C. The cells on the upper side of filters were scraped off using cotton swaps. The migrated cells on the lower surface of the filters

were fixed by 80% ethanol and their nuclei were stained with propidium iodide (Sigma) and counted manually under a fluorescence microscope.

Cell Invasion Assay. The invasive activity of KS1767 cells was carried out using transwell cell culture inserts with their upper surfaces coated by Matrigel (10 μl/insert). The inserts were put into the wells of a 24-well plate. The cells were suspended in the inserts in serum free-DMEM supplied with bFGF (50 ng/ml) with or without NGR peptides, and cultured for 12 hours at 37˚C. The cells on the upper side of filters were scraped off using cotton swaps. The invaded cells on lower surface of the filters were fixed by 80% ethanol and stained their nuclear with propidium iodide and counted by manually under a fluorescence microscope.

Tube Formation Assay. *In vitro* tube formation of endothelial cells was carried out using HMVEC cells. The cells inoculated on the surface of the Matrigel (BD Biosciences, Bedford, MA) in a 24-well plate were treated for 24 h with Bestatin or NGR peptides under the presence of bFGF. The tubular structures that formed were observed under a microscope and photographs taken.

CAM Assay. *In vivo* angiogenesis was assessed by the shell-free chicken chorioallantoic membrane (CAM) assay (8). Fertilized eggs (Petaluma farms, Petaluma, CA) were kept in a humidified incubator at 37˚C for 3 days, then the shells were cracked and the eggs cultured on Ø100-mm dishes at 37˚C with 5% CO_2 in air and saturated humidity for another 3 days. Methylcellulose disks were prepared from 1% methyl cellulose (Sigma) with NGR peptides or bestatin in PBS on the plastic film, and dried under laminar flow. The disks were put on the eggs and blood vessels under the disk were observed under a microscope after 48 hours and pictures were taken.

Statistical Analysis. All data are expressed as means ± SD. The Student's *t*-test was used to establish which groups differed from the control group. A p value of less than 0.05 was considered statistically significant.

Results

NGRd Inhibits Purified APN. Previously, we showed that HKP1 bound to APN,

was thereby internalized into targeted endothelial cells, where HKP1 disrupted mitochondrial membranes, reducing or inhibiting angiogenesis *in vitro* and *in vivo* (7). It was logical then to question whether or not HKP1, and related peptides (Fig. 1), such as NGRd, could inhibit the enzymatic activity of APN.

Purified rat APN was incubated with Bestatin, a classic APN inhibitor, and five peptides related to HKPs (Fig. 1), and the proteolytic activity of APN was measured using a synthetic fluorogenic peptide as a substrate. The concentrations of these peptides were adjusted by the amounts of NGR targeting sequence, that is, a mole of the dimers corresponded to two moles of the monomers.

Bestatin showed the strongest inhibition as previously reported. Surprisingly, among all HKP related peptides tested, only NGRd strongly inhibited the APN activity in a dose dependent manner. HKP1 and HKP1d showed only weak inhibition at high concentrations, while NGRm and pro-apoptotic domain (PAD) did not inhibit APN activity (Fig. 2). From the inhibition curve, the IC_{50} value of NGRd for APN was 35 μM (Fig. 3A). NGRd showed APN inhibition more than twice that of NGRm. And although the IC_{50} values for

bestatin inhibition of APN vary in the literature, here we calculated an IC_{50} value of 3.5 μM for bestatin.

Mechanism of APN Inhibition by NGRd. In order to further investigate the inhibition of APN by NGRd, rat APN was incubated with or without bestatin or NGRd at 4˚C and residual enzymatic activity was measured as an initial value. Each reaction solution was then put on a Microcon YM-30 filter unit (Millipore, Bedford, MA) and centrifuged for 10 min at 14,000 x g. The activities were measured for the retained solution on the filter unit after resuspension in the PBS to the volume before centrifugation. The reactions were further applied to the filter unit and repeated centrifuge and measurement of the activity. The APN activity was then recovered by a cycle of filter dialysis (Fig. 3B), thus demonstrating that the inhibition of APN by NGRd was reversible. Kinetic analysis of the inhibition of NGRd using a Dixon plot, showed the Ki value to be 14.4 μM (Fig. 3C). Analysis by a Lineweaver-Burk plot, showed no effect on the V_{max}^{-1} value of APN, demonstrating that NGRd is a competitive inhibitor for APN (Fig. 3D). Thus, we determined that NGRd is a reversible and non-classical competitive inhibitor of APN.

NGRd Inhibits APN in Living Cells. The inhibition of APN activity was also measured in living cultured cells, using the Kaposi's sarcoma cell line, KS1767. We confirmed the expression of human APN by the KS1767 cells using western blot and RT-PCR (data not shown). The KS1767 cells were incubated with bestatin and HKP-related peptides, and the APN activity was measured using the synthesized substrate. NGRd also inhibited APN in culture in a concentration dependent manner, but the inhibition levels were lower than that found with purified rat APN (50% on the KS 1767 cells at 100 μM) (Fig. 4). Bestatin inhibited APN in living cells as strongly as that found with purified rat APN. HKP1 and HKP1d also inhibited APN activity in cultured cells, although they only weakly inhibited purified rat APN. NGRd and bestatin also inhibited mouse APN activity in HEK 293T cells stably expressing mouse APN (data not shown).

NGRd Inhibits Proliferation, Migration and Invasion of the Kaposi's Sarcoma Cells. Beyond the inhibition of APN enzymatic activity by NGRd, we investigated the inhibition of proliferation, migration and invasion of KS1767 cells.

We began by considering the effect of the NGR peptides, proliferation. KS1767

cells were seeded low density (10-20% of confluence) and cultured with NGRm, NGRd or bestatin for 3 days, and then the cell number were estimated by intracellular dehydrogenase activities using WST-8. Surprisingly, the results were contrary to the enzyme inhibition. While bestatin had no statistically significant effects on proliferation, both NGRm and NGRd demonstrated a dramatic effect on proliferation (Fig. 5A). We also estimated the cytotoxicity of these inhibitors in cell viability assays. The KS1767 cells were seeded and cultured by the confluent state. The cells were exposed to the inhibitors for 24 hours, and then cell viability was assessed by WST-8 (Fig. 5B). Both NGRd, and especially NGRm, reduced viability of KS1767 cells.

We next evaluated the possible effect of the NGR peptides on migration and invasion of KS1767 cells. KS1767 cells demonstrated clear migration and invasion activity in the presence of bFGF. KS1767 cells were incubated with or without the NGR peptides or bestatin and then the cells were evaluated in invasion and migration assays (Fig. 5C and 5D). The NGRd showed strong inhibition of both migration (reduced to 72%) and invasion (reduced to 71.1%). The bestatin was the strongest among these APN inhibitors, limiting

migration to 50.4% and invasion to 58.5% respectively. These results were congruent with the enzymatic inhibition behavior of these inhibitors.

NGRd Inhibits Tube formation and Angiogenesis. To determine whether NGR peptides would affect angiogenesis, we tested the effect of the peptides *in vitro* and *in vivo*. First, we evaluated the effects of the NGR peptides during the differentiation of HMVEC into capillary-like structures. HMVECs form cord-like structures on Matrigel in the presence of bFGF. NGR peptides (200 μM NGRm or 100 μM NGRd) or bestatin (10 μM) disturbed the network formation (Fig. 6). Cytotoxicities of HMVEC by these inhibitors were not observed, as confirmed by the WST-8 assay (Data not shown). We next estimated the effect of the inhibitors on angiogenesis using the chicken chorioallantoic membrane (CAM) assay. The results clearly demonstrate that the NGR peptides and bestatin inhibited the development of capillary vessels (Fig. 7).

Discussion

In this report, we demonstrate the promise of the peptide NGRd as a potential therapeutic anti-cancer drug, or as the structural basis for such a drug. Previously, the peptide CNGRC was found to target the endothelial cells that form tumor blood vessels(4), while not targeting the endothelial cells that form normal blood vessels (6). Subsequent to this discovery, we (and others) developed CNGRC as a targeting moiety for cancer treatment (7, 9), cancer cell imaging (10) and also cardiac angiogenesis imaging (11) utilizing the specificity of APN binding on endothelial cells and tumor cells.

Indeed central to our recent work has been the development of HKPs, of which HKP1 was the first prototype (7). These small, dual-purpose molecules specifically hunt and attack the blood supply of tumors, through the elimination of the endothelial cells that form tumor blood vessels. We (and others) have also applied our technology to arthritis (12), organ reduction (13), and obesity (14).

One of the strengths of our approach has been the fact that various "targeting" domains can be combined with various "killing" domains, such that we have really invented a new pharmacology, and not just a single drug. In the process of drug development,

it was natural for us to begin to investigate, not just the binding and internalization properties of our drugs, but also the potential that we might be inhibiting the enzymatic activity of APN synergistically. This led us to the present study.

Various APN inhibitors have been reported and these are also known to suppress angiogenesis (3), even though the mechanism and relationship between the inhibition of APN and the suppression of angiogenesis is still unknown. We found here that the NGRd peptide inhibits APN activity in a reversible and competitive manner. The "gold standard" aminopeptidase N inhibitor bestatin inhibits APN with similar pharmacodynamics.

In agreement with the crystal structure of bacterial zinc-aminopeptidase, shows that bestatin binds to the active site pocket of APN (15-17). In contrast, CNGRC peptides have been predicted to bind to $W^N/_D$DLWLN (5) and not in the active site pocket (17) — the HEXXH sequence, the Zn^{2+} binding motif of the active site of metalloproteases, such as APN (5) — responsible for enzymatic activity. However, $W^N/_D$DLWLN and HEXXH are in close approximation to each other, and we deduce this is the reason why the NGRd inhibits APN activity stronger than NGRm. The conformation of the monomer peptide is dependent

on the loop structure formed by the disulfide bond joining the Cys residues of CNGRC (7), and this structure is very important for binding to APN (18-20). The loop of NGRm may not be large enough to disturb the binding of the substrates to enzymatic binding site of APN. On the other hand, NGRd is linked by two disulfide bonds between two NGRm on Cys^1 and Cys^5, respectively. Although we do not know the exact structure of NGRd at this time, it is possible that the more open structure disturbs the access of substrates to APN.

In this work we showed that NGRd inhibited the enzymatic activity of purified APN. NGRd also inhibited the APN on living cells, but somewhat less than with the purified enzyme. However NGRd also had an effect on KS1767 cell proliferation, migration, and invasion.

The inhibitions by the NGR peptides, except for proliferation, seem to depend on the inhibition of APN activity, because these are in proportion to the degree of the inhibition of the enzyme activities by inhibitors. On the other hand, other mechanisms would seem to exist for the inhibition of proliferation because NGRm shows stronger inhibition than bestatin and NGRd. Furthermore, although bestatin inhibited proliferation only weakly,

it strongly inhibited purified APN activity.

Even though the mechanisms of inhibition of Kaposi's sarcoma cell proliferation by NGRm are unclear, the combination of both NGR peptides may show synergistic effects to angiogenesis and the tumor cell activities. Because the KS1767 cells have both properties of endothelial cells (21) and neoplastic, the peptides would be expected to inhibit the metastasis of sarcoma and other APN-positive tumor cells.

Indeed, the other APN inhibitors, curcumin and BE15, inhibits APN-positive tumor cell invasion (22, 23). The peptides also inhibit angiogenesis in proportion to the degree of the APN inhibition. The inhibitions of tube formation of HMVEC by the peptides show the possibility of the inhibition of forming the capillary vessels around the tumor cells. Furthermore, the peptides inhibit formation of the capillary vessels on CAM assay. Therefore we have shown the inhibition of *in vivo* angiogenesis during chicken embryo development, providing further evidence that the peptides would be expected to suppress tumor angiogenesis.

The inhibition of tumor angiogenesis is a major strategy in cancer therapy (1, 2).

The NGR monomer and dimer peptides target the endothelial cells undergoing tumor neovascularization and suppress angiogenesis through the inhibition of APN activity but not through the induction of endothelial cell death. As a result, the peptides are expected to reduce the tumor volume and metastasis without the side effects associated with potentially more toxic related peptides/drugs.

In conclusion, NGRd inhibits APN activity and affects angiogenesis, and may offer the possibility that it will reduce the expansion of tumor volume, metastasis, and tumor angiogenesis *in vivo*. From these results it is clear that further development of NGRd as a stand alone therapeutic or as the basis for a therapeutic is warranted, and may lead to new drug candidates for cancer therapy.

References

1. Folkman, J. Tumor angiogenesis: therapeutic implications. N Engl J Med, 285: 1182-1186, 1971.

2. Folkman, J. Seminars in Medicine of the Beth Israel Hospital, Boston. Clinical applications of research on angiogenesis. N Engl J Med, 333: 1757-1763, 1995.

3. Bauvois, B. and Dauzonne, D. Aminopeptidase-N/CD13 (EC 3.4.11.2) inhibitors: chemistry, biological evaluations, and therapeutic prospects. Med Res Rev, 26: 88-130, 2006.

4. Arap, W., Pasqualini, R., and Ruoslahti, E. Cancer treatment by targeted drug delivery to tumor vasculature in a mouse model. Science, 279: 377-380, 1998.

5. Pasqualini, R., Koivunen, E., Kain, R., Lahdenranta, J., Sakamoto, M., Stryhn, A., Ashmun, R. A., Shapiro, L. H., Arap, W., and Ruoslahti, E. Aminopeptidase N is a receptor for tumor-homing peptides and a target for inhibiting angiogenesis. Cancer Res, 60: 722-727, 2000.

6. Curnis, F., Arrigoni, G., Sacchi, A., Fischetti, L., Arap, W., Pasqualini, R., and Corti, A. Differential binding of drugs containing the NGR motif to CD13 isoforms in tumor vessels, epithelia, and myeloid cells. Cancer Res, 62: 867-874, 2002.

7. Ellerby, H. M., Arap, W., Ellerby, L. M., Kain, R., Andrusiak, R., Rio, G. D., Krajewski, S., Lombardo, C. R., Rao, R., Ruoslahti, E., Bredesen, D. E., and Pasqualini, R. Anti-cancer activity of targeted pro-apoptotic peptides. Nat Med, 5: 1032-1038, 1999.

8. Ho, P. Y., Liang, Y. C., Ho, Y. S., Chen, C. T., and Lee, W. S. Inhibition of human vascular endothelial cells proliferation by terbinafine. Int J Cancer, 111: 51-59, 2004.

9. Curnis, F., Sacchi, A., Borgna, L., Magni, F., Gasparri, A., and Corti, A. Enhancement of tumor necrosis factor alpha antitumor immunotherapeutic properties by targeted delivery to aminopeptidase N (CD13). Nat Biotechnol, 18: 1185-1190, 2000.

10. Zhang, Z., Harada, H., Tanabe, K., Hatta, H., Hiraoka, M., and Nishimoto, S. Amin-

Aminopeptidase N/CD13 targeting fluorescent probes: synthesis and application to tumor cell imaging. Peptides, 26: 2182-2187, 2005.

11. Buehler, A., van Zandvoort, M. A., Stelt, B. J., Hackeng, T. M., Schrans-Stassen, B. H., Bennaghmouch, A., Hofstra, L., Cleutjens, J. P., Duijvestijn, A., Smeets, M. B., de Kleijn, D. P., Post, M. J., and de Muinck, E. D. cNGR: a novel homing sequence for CD13/APN targeted molecular imaging of murine cardiac angiogenesis in vivo. Arterioscler Thromb Vasc Biol, 26: 2681-2687, 2006.

12. Gerlag, D. M., Borges, E., Tak, P. P., Ellerby, H. M., Bredesen, D. E., Pasqualini, R., Ruoslahti, E., and Firestein, G. S. Suppression of murine collagen-induced arthritis by targeted apoptosis of synovial neovasculature. Arthritis Res, 3: 357-361, 2001.

13. Arap, W., Haedicke, W., Bernasconi, M., Kain, R., Rajotte, D., Krajewski, S., Ellerby, H. M., Bredesen, D. E., Pasqualini, R., and Ruoslahti, E. Targeting the prostate for destruction through a vascular address. Proc Natl Acad Sci U S A, 99: 1527-1531, 2002.

14. Kolonin, M. G., Saha, P. K., Chan, L., Pasqualini, R., and Arap, W. Reversal of obesity by targeted ablation of adipose tissue. Nat Med, 10: 625-632, 2004.

15. Addlagatta, A., Gay, L., and Matthews, B. W. Structure of aminopeptidase N from Escherichia coli suggests a compartmentalized, gated active site. Proc Natl Acad Sci U S A, 103: 13339-13344, 2006.

16. Ito, K., Nakajima, Y., Onohara, Y., Takeo, M., Nakashima, K., Matsubara, F., Ito, T., and Yoshimoto, T. Crystal structure of aminopeptidase N (proteobacteria alanyl aminopeptidase) from Escherichia coli and conformational change of methionine 260 involved in substrate recognition. J Biol Chem, 281: 33664-33676, 2006.

17. Kyrieleis, O. J., Goettig, P., Kiefersauer, R., Huber, R., and Brandstetter, H. Crystal structures of the tricorn interacting factor F3 from Thermoplasma acidophilum, a zinc aminopeptidase in three different conformations. J Mol Biol, 349: 787-800, 2005.

18. Di Matteo, P., Curnis, F., Longhi, R., Colombo, G., Sacchi, A., Crippa, L., Protti, M. P., Ponzoni, M., Toma, S., and Corti, A. Immunogenic and structural properties of

the Asn-Gly-Arg (NGR) tumor neovasculature-homing motif. Mol Immunol, 43: 1509-1518, 2006.

19. Colombo, G., Curnis, F., De Mori, G. M., Gasparri, A., Longoni, C., Sacchi, A., Longhi, R., and Corti, A. Structure-activity relationships of linear and cyclic peptides containing the NGR tumor-homing motif. J Biol Chem, 277: 47891-47897, 2002.

20. Majhen, D., Gabrilovac, J., Eloit, M., Richardson, J., and Ambriovic-Ristov, A. Disulfide bond formation in NGR fiber-modified adenovirus is essential for retargeting to aminopeptidase N. Biochem Biophys Res Commun, 348: 278-287, 2006.

21. Samaniego, F., Markham, P. D., Gendelman, R., Watanabe, Y., Kao, V., Kowalski, K., Sonnabend, J. A., Pintus, A., Gallo, R. C., and Ensoli, B. Vascular endothelial growth factor and basic fibroblast growth factor present in Kaposi's sarcoma (KS) are induced by inflammatory cytokines and synergize to promote vascular permeability and KS lesion development. Am J Pathol, 152: 1433-1443, 1998.

22. Shim, J. S., Kim, J. H., Cho, H. Y., Yum, Y. N., Kim, S. H., Park, H. J., Shim, B. S.,

Choi, S. H., and Kwon, H. J. Irreversible inhibition of CD13/aminopeptidase N by the antiangiogenic agent curcumin. Chem Biol, 10: 695-704, 2003.

23. Saitoh, Y., Koizumi, K., Minami, T., Sekine, K., Sakurai, H., and Saiki, I. A derivative of aminopeptidase inhibitor (BE15) has a dual inhibitory effect of invasion and motility on tumor and endothelial cells. Biol Pharm Bull, 29: 709-712, 2006.

Figures

Figure 1. The Structure of NGRd and Related Peptides. NGR monomer (NGRm) and HKP1 have a single disulfide bond between Cys^1 and Cys^5. NGR dimer (NGRd) and HKP1d consist of two molecules of NGRm or HKP1, which are linked by two disulfide bonds Cys^1-Cys^1 and Cys^5-Cys^5, respectively. All pro-apoptotic domains (PAD) are composed of D-amino acids.

Figure 2. Inhibition of APN by NGRd and Related Peptides. Purified rat APN was incubated with bestatin, NGRd, and related peptides, and then APN activity was measured using a fluorogenic substrate, Ala-MCA. Activities are shown as the percentage of control (PBS). The results show mean ± SD of five independent experiments. $^{**}p < 0.01$ versus control.

Figure 3. The Effects of NGRd on APN Activity. Purified rat APN was used for the analy-

sis of the dose dependence, the reversibility, and the kinetic of the enzyme inhibition. (A) Purified rat APN activity was measured after incubation with various concentrations of NGRm (●), NGRd (❍), and bestatin (□). From the inhibition curve, the IC_{50} value of NGRd was 35 μM and bestatin was 3.5 μM. (B) Reversibility was estimated by measuring the residual enzyme activities after filtration through an YM-30 unit. The activities were recovered by filtration cycles. (C, D) The kinetics was determined by Dixon plot (C) and Lineweaver-Burk plot (D). These results show that APN inhibition by NGRd was reversible and competitive with a Ki value of 14.4 μM. The results show mean ± SD of three independent experiments. $^{**}p < 0.01$ versus control.

Figure 4. Inhibition of APN Activity in Living Cells. APN positive human Kaposi's sarcoma cell line, KS1767, was used for measuring the inhibition of APN activity, which was measured using the fluorogenic substrate, Ala-MCA. Activities are shown as the percentage of control reaction. The results show the mean ± SD of five independent experiments. $^{**}p < 0.01$ versus control.

Figure 5. NGRd Inhibits Proliferation, Migration and Invasion. Inhibition of APN acitvity in the Kaposi's sarcoma (KS) cell line inhibits various cellular activities by bestatin (10 μM), NGRm (200 μM), and NGRd (100 μM). Cell proliferation and viability were measured using WST-8. Cell proliferation was arrested by NGRd and NGRm, but not by bestatin (A). The peptides also affected viability of cells (B). KS cells were put on culture inserts (8.0 μm pore size) with bFGF and Matrigel was used to coat cell inserts for the invasion assay. Migrated and invaded cells were counted under fluorescence microscopy after ethanol fixing and PI staining. The inhibitors suppressed the migration (C) and invasion (D) of the KS1767 cells. The results show mean ± SD of three independent experiments at least. $^{*}p < 0.05$, $^{**}p < 0.01$ versus control.

Figure 6. NGRd Inhibits Tube formation. Human dermal endothelial cells were cultured with bFGF and control (PBS); bestatin (10 μM), NGRm (200 μM), and NGRd (100 μM) on

Matrigel. APN inhibitors disturbed HMVEC cord formation.

Figure 7. NGRd Inhibits CAM Angiogenesis. Fertilized eggs were used for shell-free CAM assays. Whole eggs were cultured in 10-cm dishes (Top). Methylcellulose disks containing PBS (a), bestatin (b), NGRm (c), and NGRd (d) were placed on the CAM. Angiogenesis on the CAM was prevented under the disks containing APN inhibitors. (a-d) the original magnifications were x 3. Scale bars = 0.5 mm.

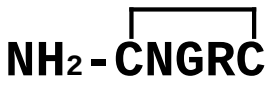

NGRm

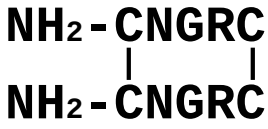

NGRd

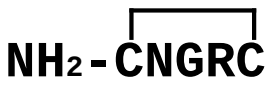

HKP1

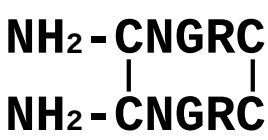

HKP1d

PAD

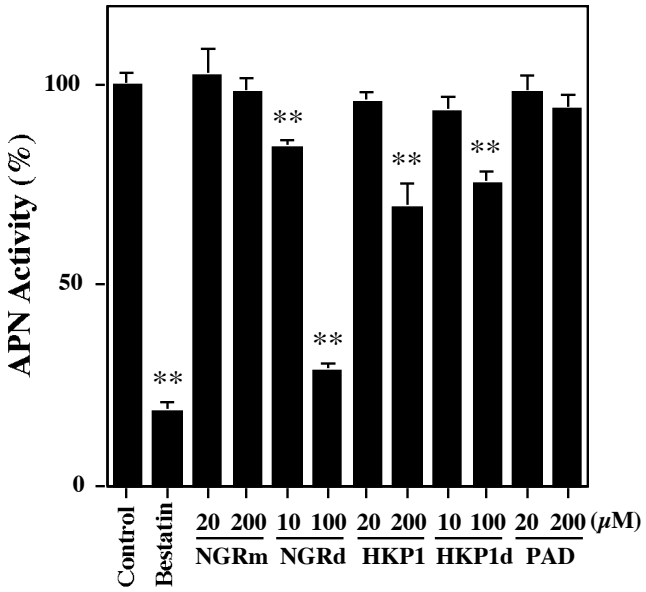
APN Activity (%)
100
50
0
**
**
**
**
**
Control
Bestatin
20 200
NGRm
10 100
NGRd
20 200
HKP1
10 100
HKP1d
20 200
PAD
(μM)

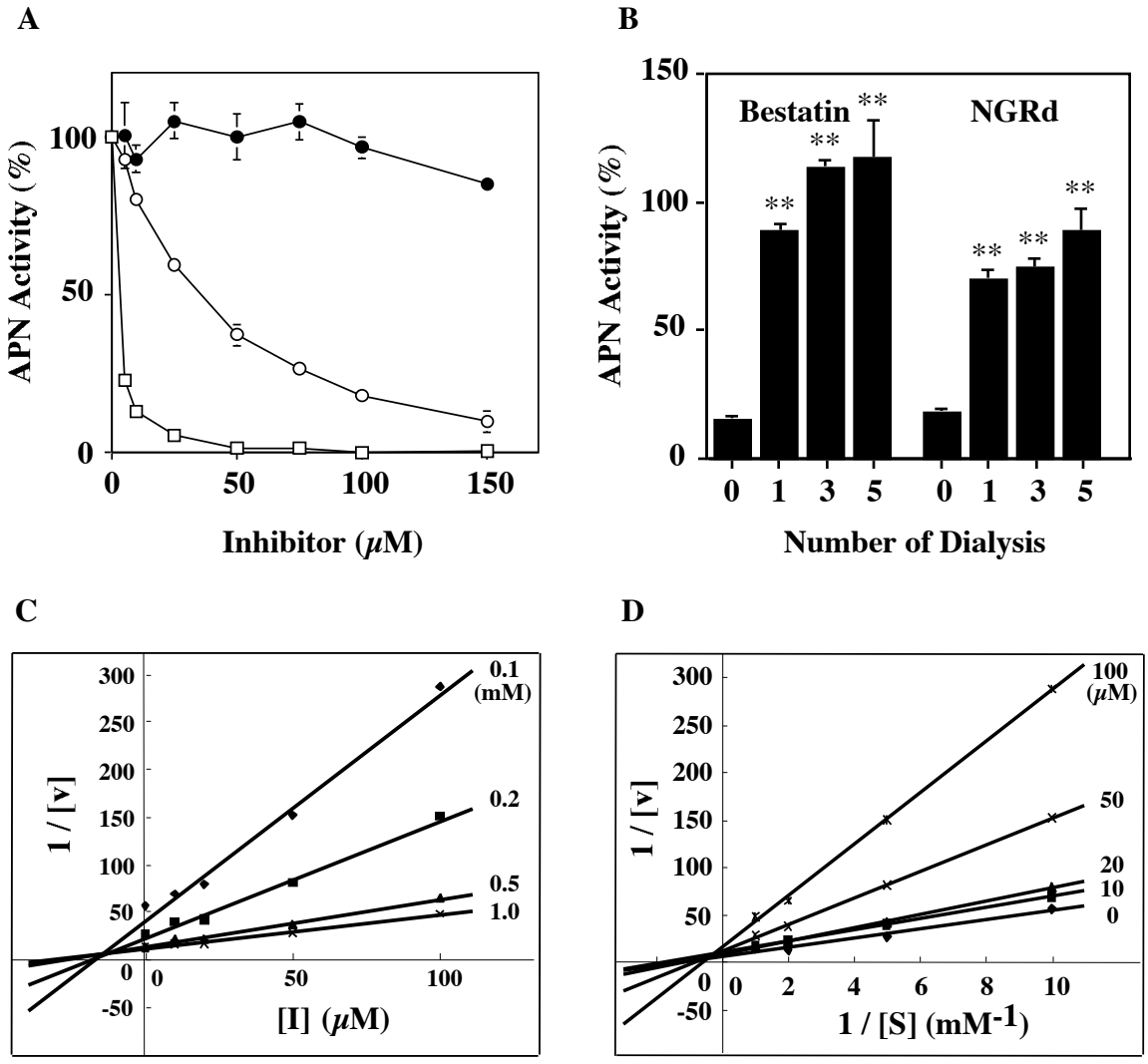
A
APN Activity (%)
100
50
0
0
50
100
150
Inhibitor (μM)
B
150
100
50
0
APN Activity (%)
Bestatin
NGRd
**
0 1 3 5 0 1 3 5
Number of Dialysis
C
1 / [v]
300
250
200
150
100
50
0
-50
0
50
100
[I] (μM)
0.1 (mM)
0.2
0.5
1.0
D
1 / [v]
300
250
200
150
100
50
0
-50
0 2 4 6 8 10
1 / [S] (mM-1)
100 (μM)
50
20
10
0

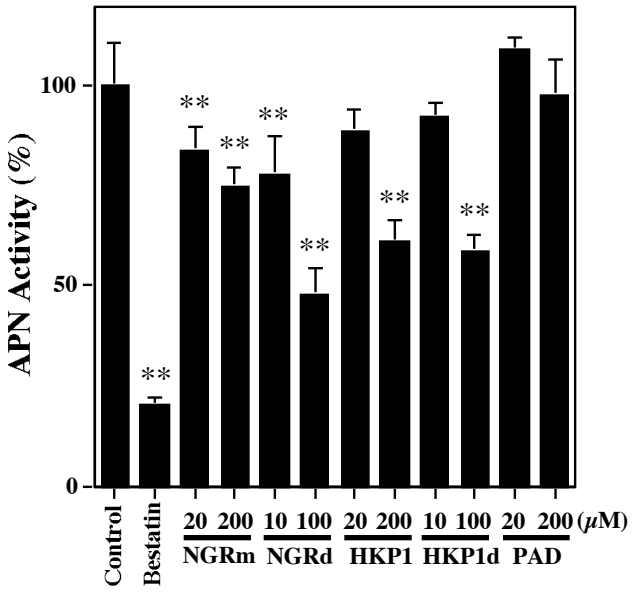
APN Activity (%)
100
50
0
**
Control
Bestatin
20 200
NGRm
10 100
NGRd
20 200
HKP1
10 100
HKP1d
20 200
PAD
(μM)

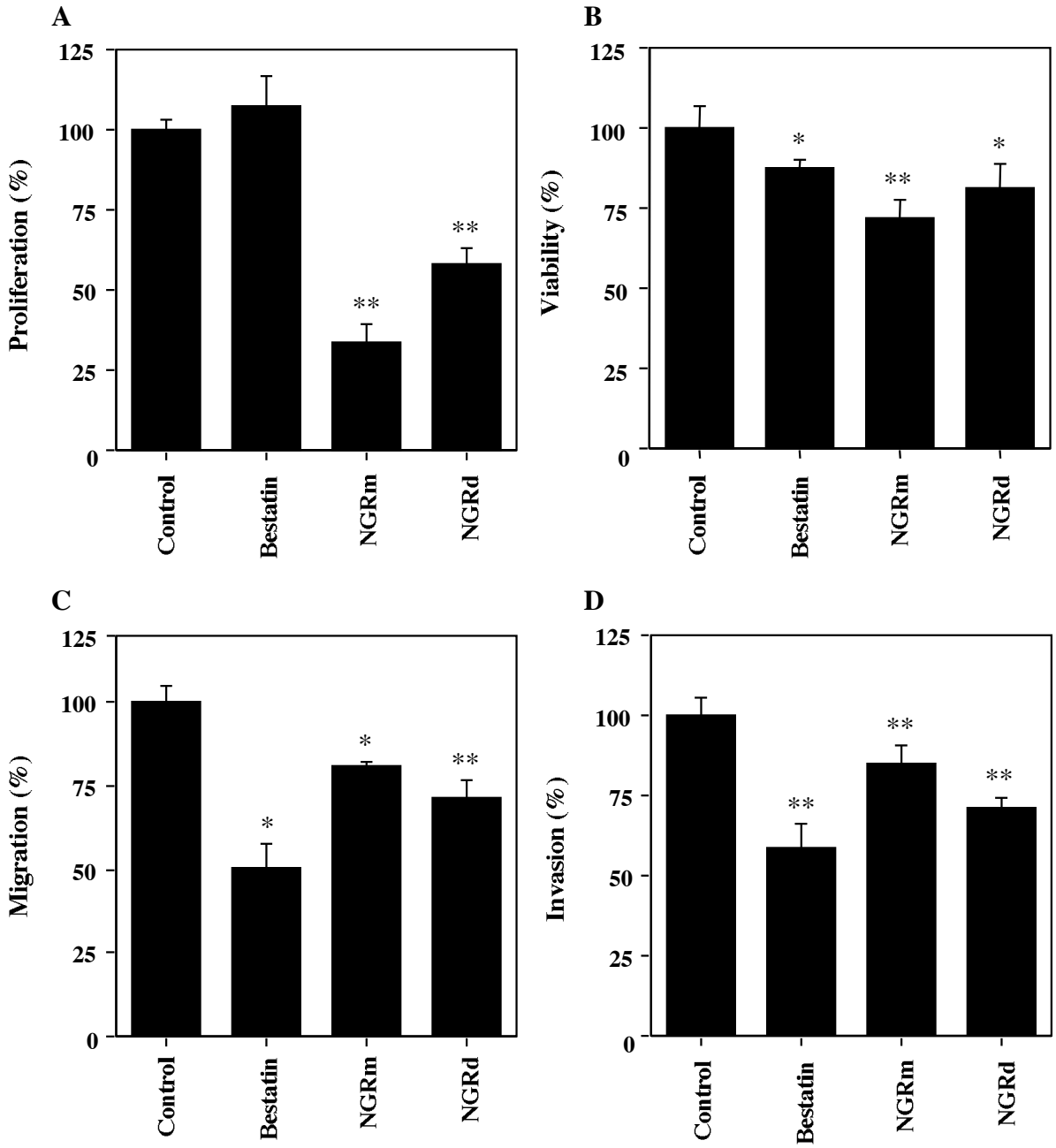
A
Proliferation (%)
125
100
75
50
25
0
**
**
Control
Bestatin
NGRm
NGRd
B
Viability (%)
125
100
75
50
25
0
*
**
*
Control
Bestatin
NGRm
NGRd
C
Migration (%)
125
100
75
50
25
0
*
*
**
Control
Bestatin
NGRm
NGRd
D
Invasion (%)
125
100
75
50
25
0
**
**
**
Control
Bestatin
NGRm
NGRd

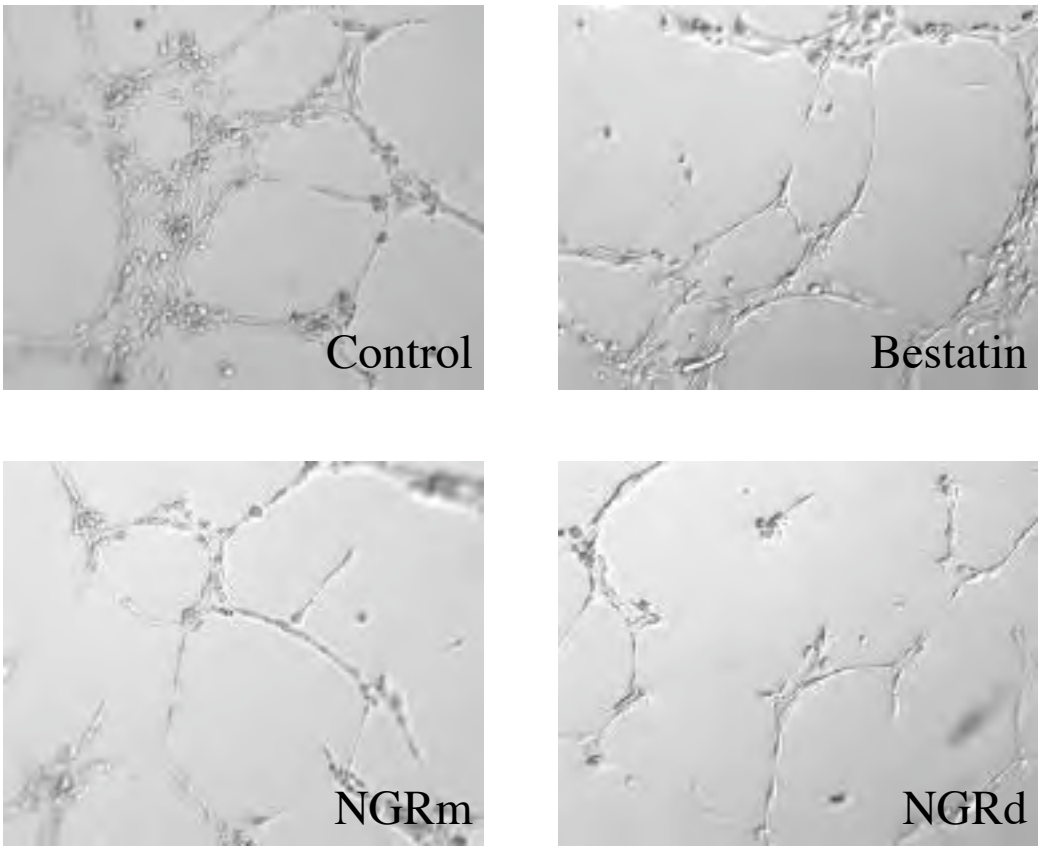
Control
Bestatin
NGRm
NGRd

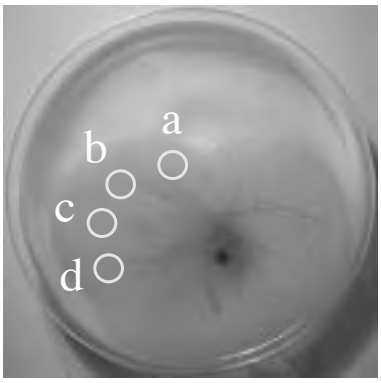
a
b
c
d

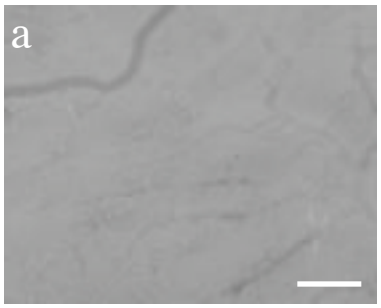
a

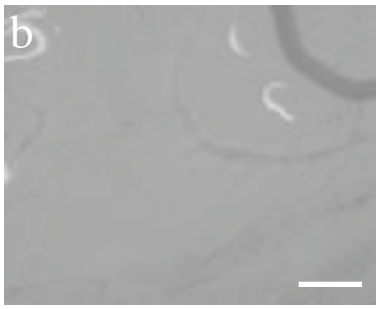
b

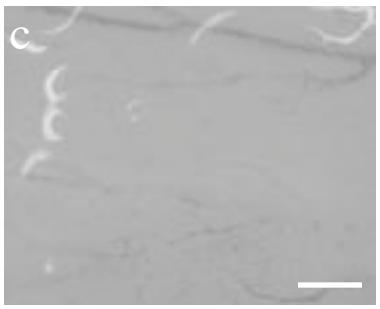
c

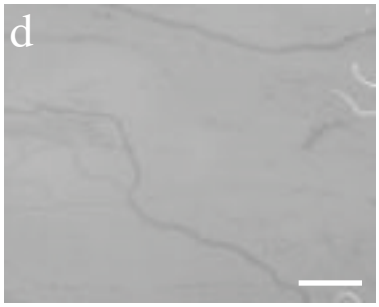
d